Aalto University
School of Engineering

Christian Karv

Shear and punching resistance of steel fibre reinforced concrete slabs

Thesis submitted for examination for the degree of Master of Science in Technology.

Espoo 31.1.2017
Supervisor: Professor Risto Kiviluoma
Advisors: DI Jürgen Mandl, M.Sc. Martti Matsinen

Aalto University
School of Engineering

Aalto University,
P.O. Box 12100, FI-00076 AALTO
www.aalto.fi

Abstract of master's thesis

Author Christian Karv

Title of thesis Shear and punching resistance of steel fibre reinforced concrete slabs

Degree programme Degree Programme in Structural Engineering and Building Technology

Major Structural Engineering **Code** Rak.thes

Thesis supervisor Professor Risto Kiviluoma

Thesis advisors DI Jürgen Mandl, M.Sc. Martti Matsinen

Date 31.1.2017 **Number of pages** 67 + 35 **Language** English

Steel fibre reinforced concrete (SFRC) is a composite material consisting of steel fibres and concrete. The commercial use of SFRC started in the late 1960s. However, although SFRC has shown great potential in structural applications, it is not widely used. In Europe, one explanation for its low usage could be the absence of SFRC in the Eurocodes, which comprise the harmonized European standards used as a basis for most structural designs in Europe today. Because SFRC has not yet been included in the Eurocodes, many countries have developed their own national guidelines or standards for this material. However, these guidelines/standards may differ significantly from each other, leading to possible over- or under-estimating the capacity of a structural member.

Therefore, the aim of this thesis is to show how the shear and punching capacity for SFRC slabs are determined according to six different national guidelines or standards and to analyse how the estimated capacity varies between these guidelines/standards. Furthermore, this thesis evaluates the feasibility of using numerical simulations provided in commercial finite element software package to determine the punching resistance for SFRC slabs. Finally, the numerical simulation results were used to form an alternative theoretical model for determining the punching resistance for SFRC slabs.

This thesis shows that there is a great range in estimated capacity between the examined national standards/guidelines. This fact clearly demonstrates that there is certainly a need for a common SFRC standard. With more test data and an international standard, it would become easier to ensure safe designs using this material.

Keywords steel fibre reinforced concrete, shear resistance, punching resistance, finite element method

Aalto-universitetet
Högskolan för
ingenjörsvetenskaper

Aalto-universitetet,
PB 12100, 00076 AALTO
www.aalto.fi

Sammandrag av diplomarbetet

Författare Christian Karv

Titel Skjuv- och genomstansningshållfasthet för stålfiberbetongarmerade plattor

Utbildningsprogram Utbildningsprogrammet för konstruktions- och byggnadsproduktionsteknik

Huvudämne Konstruktionsteknik **Kod för professuren** Rak.thes

Övervakare Professor Risto Kiviluoma

Handledare DI Jürgen Mandl, M.Sc. Martti Matsinen

Datum 31.1.2017 **Sidantal** 67+35 **Språk** Engelska

Stålfiberarmerad betong (SFRC) är ett kompositmaterial som består av stålfibrer och betong. Den kommersiella användningen av SFRC började i slutet av 1960-talet men trots att SFRC har visat stor potential även i bärande konstruktioner används det sällan idag. Inom Europa är en förklarning till dess låga användning att SFRC ännu inte är inkluderat i Eurokoderna, vilka används som grund för konstruktionsplanering inom Europa idag. Eftersom SFRC ännu inte har inkluderats i Eurokoderna har många europeiska länder utvecklat egna standarder eller rekommendationer för detta material. Dessa standarder/rekommendationer kan dock skilja sig signifikant från varandra vilket eventuellt kan leda till över- eller underdimensionering av konstruktioner.

Syftet med denna avhandling är att visa hur skjuv- och genomstansningshållfastheten för SFRC-plattor bestäms enligt sex olika nationella standarder/rekommendationer samt att analysera hur den estimerade kapaciteten enligt dessa standarder/rekommendationer skiljer sig från varandra. Dessutom används ett kommersiellt dataprogram till att numeriskt simulera genomstansnings-hållfastheten för SFRC-plattor. Slutligen, på basis av simuleringsresultaten, presenteras en alternativ beräkningsmodell för att bestämma genomstansningshållfastheten för SFRC-plattor.

Denna avhandling visar att skillnaderna mellan de undersökta nationella standarderna/rekommendationerna är signifikant, vilket tydligt visar att det finns ett behov för en gemensam standard för SFRC. Med mera testresultat och en internationell standard så skulle det vara enklare att planera säkra konstruktioner med detta material.

Nyckelord stålfiberarmerad betong, skjuvhållfasthet, genomstansningshållfasthet, finita elementmetoden

Preface

This Master's thesis has been conducted as part of the degree Master of Science (Technology) at the Aalto University School of Engineering.

I would like to express my warmest gratitude for their guidance and support to my instructors DI Jürgen Mandl, Severstal Metiz, M.Sc. Martti Matsinen, Piimat Oy, and to my supervisor Professor Risto Kiviluoma, Aalto University School of Engineering. I would also like to thank M.Sc. Teuvo Meriläinen, Sweco Rakennetekniikka Oy, and M.Sc. Hannu Nissinen, Sweco Rakennetekniikka Oy, for their helpful advice. I am very grateful to the company Sweco Rakennetekniikka Oy for letting me work on this Master's thesis at their office in Ilmala and for sponsoring my trip to the fibre concrete conference in Prague in September 2015.

For the financial support of this study I would like to thank Sweco Rakennetekniikka Oy, Bermanto Oy and Suomen Betonilattiayhdistys r.y (BLY). I would also like to thank the people at Červenka Consulting for great service.

Finally I would like to thank my friends and family for all their support during this time.

Espoo 31.1.2017

Christian Karv

Table of Contents

Symbols

Latin upper case letters

A_c	concrete area
A_{ct}^f	cross-sectional tension zone area in cracked concrete
A_{sl}	cross-sectional area bending reinforcement
A_{sw}	cross-sectional area of shear reinforcement
C	constant
$C_{Rd,c}$	constant
E_s	modulus of elasticity of reinforcement
F_{max}	load corresponding to the tensile strength of a specimen
L_x	span length in x-direction
L_y	span length in y-direction
N_{Ed}	normal force
P_p	punching shear resistance
$R_{e,3}$	equivalent flexural strength ratio
$R_{20,50}$	residual flexural strength
V_{Ed}	design shear force
V_R	punching capacity
V_{Rd}	design punching capacity
$V_{Rd,c}$	concrete design shear/punching resistance
$V_{Rd.c}^f$	fibre concrete design punching resistance
$V_{Rd,cf}$	fibre concrete design shear/punching resistance
$V_{Rk.cf.p.Karv1}$	fibre concrete characteristic punching resistance
$V_{Rk.cf.p.Karv2}$	fibre concrete characteristic punching resistance
$V_{Rd,F}$	design shear resistance provided by fibre concrete
$V_{Rd,f}$	design shear resistance provided by fibres
$V_{Rd,max}$	maximum punching resistance
$V_{Rd,s}$	design shear resistance provided by stirrups
F_j	load corresponding with $CMOD_j$ [mm] or δ_j

Latin lower case letters

a	constant
b	width
b_0	critical control perimeter (set at distance of $0.5d$)
b_f	flange width
b_w	width of cross section
d	effective depth
d_g	maximum aggregate size
d_{g0}	reference aggregate size
f_{cbk}	concrete characteristic flexural strength
f_{cd}	concrete design compression strength
f_{ck}	concrete characteristic compression strength
$f_{ctk(0.05)}$	concrete characteristic tensile strength
$f_{ctR,u}^f$	calculated residual tensile strength of SFRC
$f_{ct0,u}^f$	basic value of residual tensile strength

$f_{ft,R3}$	characteristic residual flexural tensile strength
f_{Fts}	coefficient
f_{Ftuk}	characteristic value of ultimate residual tensile strength for FRC
$f_{R,j}$	residual flexural tensile strength
$f_{r,j}$	residual flexural tensile strength
f_{yd}	steel design yield strength
h	slab total thickness
h_f	flange height
h_{sp}	distance between notch and top surface
k	slab thickness coefficient
k_{dg}	aggregate size coefficient
k_e	eccentricity coefficient
k_f	reduction factor
k_ψ	rotation coefficient
k_1	constant
l	span length
m_{Ed}	avarage design bending moment
m_{Rd}	avarage design flexural strength
n	coefficient
r_s	position where radial bending moment is zero
μ_1	critical control perimeter (set at distance of $2d$)
v_{fd}	calculated fibre contribution to punching
v_{min}	minimum punching resistance
w_u	maximum crack opening

Greek lower case letters

α_c^f	fibre concrete coefficient
γ_c	concrete partial factor
γ_f	fibre partial factor
γ_{ct}^f	steel fibre partial factor
δ_j	deflection
κ_F^f	reduction factor
κ_G^f	reduction factor
ρ	reinforcement ratio
σ_{cp}	normal force stress
σ_{swd}	shear reinforcement stress
τ_{fd}	fibre contribution to punching
ψ	slab rotation

Abbreviations

ACI	American Concrete Institute
ASTM	American Society for Testing and Materials
BY	Suomen Betoniyhdistys
CEB	Comité Euro-International du Béton
CMOD	crack mouth opening displacement
DAfStb	German Committee for Reinforced Concrete
EC2	Eurocode EN 1992-1-1
EN	European Standards
FEM	finite elementh method
fib	International Federation for Structural Concrete
FIN	Finnish guideline, BY 56
FRC	fibre reinforced concrete
GER	German standard DAfStb
LOP	limit of proportionality
LoA	level of approximation
MC2010	fib Model Code for Concrete Structures 2010
RC	reinforced concrete
RILEM	International Union of Laboratories and Experts in Construction Materials, Systems and Structures
SFRC	steel fibre reinforced concrete
SI	International System of Units (French: Système international d'unités)
SWE	Swedish standard SS 812310:2014
TR 34	Technical Report 34
UK3	Technical Report 34, third edition
UK4	Technical Report 34, Fourth edition

1 Introduction

As plain concrete is weak in tension (only about ten percent of its compressive strength), it must be reinforced to be able to be used in structural applications. Traditionally, reinforcing bars are put in the tension zone of the concrete to compensate for its poor tensile properties and in the compression zone for crack control. Recently, steel fibres, or a combination of steel fibres and reinforcing bars, have emerged as an alternative method for reinforcing concrete structures. Steel fibre reinforced concrete (SFRC) is a composite material consisting of concrete and steel fibres. By adding a sufficient amount of steel fibres into the concrete matrix the post-cracking properties of the hardened concrete will increase, as the evenly dispersed fibres are able to transfer stresses over the cracks, resulting in a reduced crack width of the concrete. [1]

Using SFRC in load-bearing structural applications is a relatively new practice. Although the most common application for SFRC is in ground-supported floors and shotcrete applications, it has shown good potential in demanding structural applications as well. Furthermore, using SFRF may in some cases enable the possibility to generate more cost-efficient solutions. In fact, SRFC structures have been realized in several European countries, including Germany, Austria, Belgium and Estonia. [2, 3]

In Europe, standardized methods to determine the material properties for all common building materials has been gathered in the Eurocodes. SFRC is yet to be included in the Eurocodes, partly explaining the relatively low usage of it. Nevertheless, over the last decades, much research has been conducted on SFRC. For instance, because of the absence of SFRC in the Eurocodes many nations have developed their own national guidelines for this material. However, since the guidelines may use different methods to determine the same property, the results may obviously be dissimilar, possibly leading to undesired higher costs.

The aim of this thesis is to compare national guidelines/standards in terms of their shear and punching capacity for SFRC slabs in order to determine the degree to which they differ from each other in their results. Following six are selected:

- BY 56 – Finland [4],
- SS 812310:2014 – Sweden [5],
- DAfStb – Germany [6],
- Technical Report 34 (TR 34) (third edition) – United Kingdom [7],
- Technical Report 34 (TR 34) (fourth edition) – United Kingdom [8] and
- MC2010 – fib Model Code for concrete structures 2010 [9].

These guidelines/standards have been chosen through discussion between the author and advisors involved in this project. The guidelines/standards will be tested using 18 structural cases, which differ in terms of the thickness of the slabs and amount of bending reinforcement. This will serve as the basis for an evaluation of whether the calculated

punching resistance is constant across the guidelines/standards or whether there are dissimilarities in their results. Thereafter, these values will be compared to results achieved through numerical simulation using a finite element software package. Finally, an alternative theoretical method will be presented for determining the punching capacity of the SFRC slab based on simulation results.

Since steel fibres are the most commercially common fibre type, this thesis will only focus on these. Other types of fibre, such as glass and polymer, will only be briefly discussed. Furthermore, this thesis will investigate only the shear and punching phenomenon for pile-supported SFRC slabs, as well as slabs with a maximum depth of 200 mm, both with and without traditional bending reinforcement. Other properties and structural parts will be left for further research. Moreover, the influence of eventual shear reinforcement on the shear and punching resistance is excluded. Further, although many approaches have been developed for determining certain characteristics of SFRC (e.g., [10, 11, 12, 13]), these theoretical models will not be discussed in this thesis.

The remainder of this thesis is divided into five chapters. Chapter 2 introduces fibre reinforced concrete. Chapter 3 discusses the theory behind the shear and punching phenomenon as well as presents and compares six different national guidelines or standards for determining the shear and punching resistance for SFRC slabs. Chapter 4 provides theory behind numerical simulations and presents the simulation results. Chapter 5 compares the results from the numerical simulation with the theoretical methods from the national guidelines/standard and presents an alternative theoretical method. Finally, Chapter 6 discusses the results and suggests further research.

2 Fibre reinforced concrete

2.1 History

The use of cementitious materials dates back to antiquity. In Yugoslavia archaeologists have found a hut with a floor made of cementitious materials from 5600 BC. This same kind of material has been found in numerous of old buildings, e.g. between the masonry blocks of the pyramids. The Greeks and Romans developed it further by mixing limestone with aggregate and pozzolana (volcanic ash). Thereby, they got a very durable material of which some buildings still stand. They had created what we today know as concrete. [14]

Figure 2.1 The Roman Pantheon dome, possibly the first lightweight concrete structure. Finished in 125 AD. [15]

Plain concrete is a brittle material that is weak in tension and therefore needs to be strengthened to be usable in structural applications. Adding some kind of fibre was one of the earliest ways of doing this. E.g., the hill of Aqar Quf near Bagdad, constructed approximately 3500 years ago, were built using sun-baked bricks reinforced with straws. [16]

Asbestos cement was the first widely used manufactured composite. It was developed in 1898 by Ludwig Hatschek (inventor of "the Hatschek process") and can be found widely around the world today. However, primarily due to the health hazards of asbestos, alternative fibre types were introduced in the 1960s and 1970s. [17]

In the late 1960s the commercial use of steel fibre reinforced concrete was introduced. However, it had already been used during World War II in the patching of bomb craters in airport runways. Glass fibres were introduced about the same time as steel fibres. Back then, the geometry of both glass and steel fibres were straight and smooth, which does not give as good mechanical bonding as today's fibres, which are often shaped with hooked or deformed ends. [16, 18]

Today, numerous of different types of fibres with different shape, material and mechanical properties are available. Even though steel fibre is the commercially most used fibre type, there are other strongly competitive alternatives, e.g., glass, polymer and synthetic fibres.

Furthermore, it is also possible to use mixtures of different fibre materials. Common fibre types and their properties are listed in Table 2.1. [16]

Table 2.1 Typical properties of fibres [16]

Fibre	*Diameter (μm)*	*Specific gravity*	*Modulus of elasticity (GPa)*	*Tensile strength (GPa)*	*Elongation at break (%)*
Steel	5–500	7.84	200	0.5–2.0	0.5–3.5
Glass	9–15	2.6	70–80	2–4	2–3.5
Asbestos					
Crocidolite	0.02–0.4	3.4	196	3.5	2.0–3.0
Chrysolite	0.02–0.4	2.6	164	3.1	2.0–3.0
Polypropylene	20–400	0.9–0.95	3.5–10	0.45–0.76	15–25
Aramid (kevlar)	10–12	1.44	63–120	2.3–3.5	2–4.5
Carbon (high strength)	8–9	1.6–1.7	230–380	2.5–4.0	0.5–1.5
Nylon	23–400	1.14	4.1–5.2	0.75–1.0	16.0–20.0
Cellulose	—	1.2	10	0.3–0.5	—
Acrylic	18	1.18	14–19.5	0.4–1.0	3
Polyethylene	25–1000	0.92–0.96	5	0.08–0.60	3–100
Wood fibre	—	1.5	71.0	0.9	—
Sisal	10–50	1.5	—	0.8	3.0
Cement matrix (for comparison)	—	1.5–2.5	10–45	0.003–0.007	0.02

2.2 Fibre reinforced concrete versus conventionally reinforced concrete

In traditional reinforced concrete, reinforcing bars are there to both increase the load bearing capacity of the structure (by transferring the loads over the macro-cracks that occur when a certain load is applied) and for crack control. Fibres, which are much more evenly distributed in the matrix, are able to pick up load and transfer stresses as soon as when non-visible micro-cracks occur (illustrated in Figure 2.2). When putting a sufficient amount of steel fibres into the matrix it significantly increases the toughness and durability of the concrete, making it more resistant to fatigue and dynamic loading (blast or seismic events). [16]

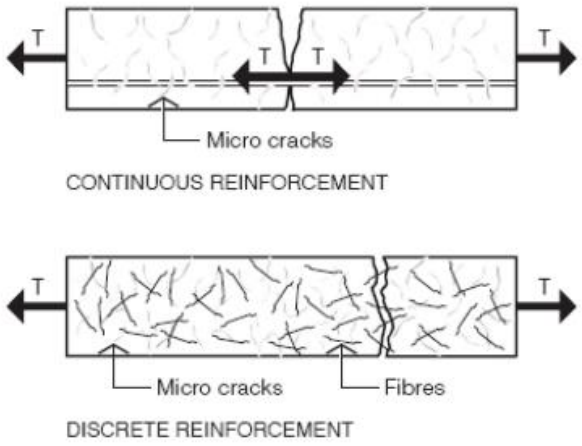

Figure 2.2 Reinforcement in a concrete matrix [19].

At first, steel fibres were used only in non-structural applications (such as ground floors) for crack control. Nowadays, due to the improved properties of fibres, steel fibres are increasingly used in more demanding structural applications, such as load-bearing slabs and foundations. Depending on the situation it is sometimes possible to replace conventional reinforcing bars, either partially or completely, with steel fibres. But, by using mixes of both fibres and bars it can be possible to achieve better results than when using only either one. [16]

The benefits with FRC are significant in especially ground-supported floors. First of all, using FRC, areas up to 3 000 m^2 can be casted in one session without the need to saw cut the floor (a conventionally casted floor is typically saw cut in a 6 m × 6 m or 8 m × 8 m pattern [3]). If there is no conventional reinforcement to be placed, a whole work phase can be eliminated, which may save a significant amount of both time and money. For instance when the Rocca Al Mare (Figure 2.13) building in Tallinn was built, the construction time was reduced by 9 weeks due to the use of SFRC in the elevated slabs [20]. Moreover, if there are no reinforcing bars, it is easier for the workers to move at the jobsite, and therefore, work safety is better. Also, FRC slabs are often thinner in design. One reason for this is that the concrete cover may be neglected in FRC applications, since there is no risk for corrosion damage in FRC structures. While single steel fibres may also corrode, this only happens if they are exposed on the surface and this has merely an aesthetic impact. Furthermore, if a steel fibre corrodes the corrosion will neither spread to other fibres nor make the concrete crack. [21, 22] Lastly, as a result of the development of standards, guidelines and overall knowhow about FRC, nowadays it is possible to design thinner and more complex concrete structures than before. [20] However, due to the absence of internationally accepted design methods, the usage of FRC is relatively low. [22]

2.3 Properties of steel fibre reinforced concrete

2.3.1 Steel fibre characteristics

There are numerous different types of steel fibres. They are often round but can also be flat or have a roughened surface. EN 14889-1 defines steel fibres as: *"straight or deformed pieces of cold-drawn steel wire, straight or deformed cut sheet fibres, melt extracted fibres,*

shaved cold drawn wire fibres and fibres milled from steel blocks, which are suitable for homogeneous mixing into concrete or mortar" [23]. The length of a fibre ranges between 12…60 mm and the diameter of a round fibre is typically between 0.25…1.0 mm. Examples of steel fibre shapes is shown in Figure 2.3. As illustrated in the figure, the ends of a fibre are often bent or deformed to make the fibre anchor better into the concrete. [16]

The fibre content is usually expressed in the unit "kg/m^3" and in Finland the fibre dosage for normal structural concrete ranges between 25 and 50 kg/m^3 [4]. Steel fibres are generally made of carbon steel or an alloy, such as stainless steel. Stainless steel is used in e.g. refractory applications or marine structures where corrosion-resistant fibres are needed. [16] The tensile strength ranges between 600…2500 MPa and the modulus of elasticity is approximately 210 000 MPa. [19]

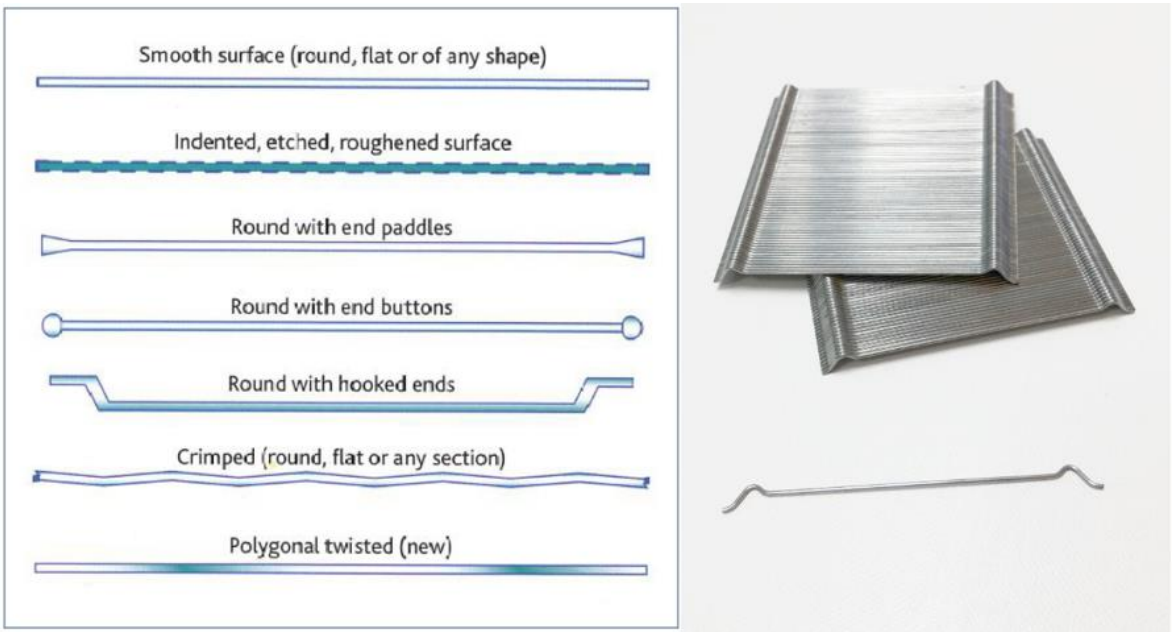

Figure 2.3. Left: common types of steel fibres. [19] Right: new steel fibre type (photo by author).

The aim when designing steel fibres is not to make a fibre that will be anchored as strongly as possible. Instead, the challenge is to design a fibre that, instead of failure in yielding, is pulled out of the concrete. Straight fibres are nowadays seldom used because they are too easily pulled out of the concrete. Hence, fibres almost always have bent ends. To be able to pull out the fibres, they have to be deformed, which, on the other hand, requires energy. The optimal fibre is pulled out of the concrete just before it starts to yield. To clarify, if the fibre yields instead of being pulled out, the structure behaves in a brittle manner, which is not favourable. The pull-out mechanisms of fibres are illustrated in Figure 2.4, Figure 2.5 and Figure 2.6. [24]

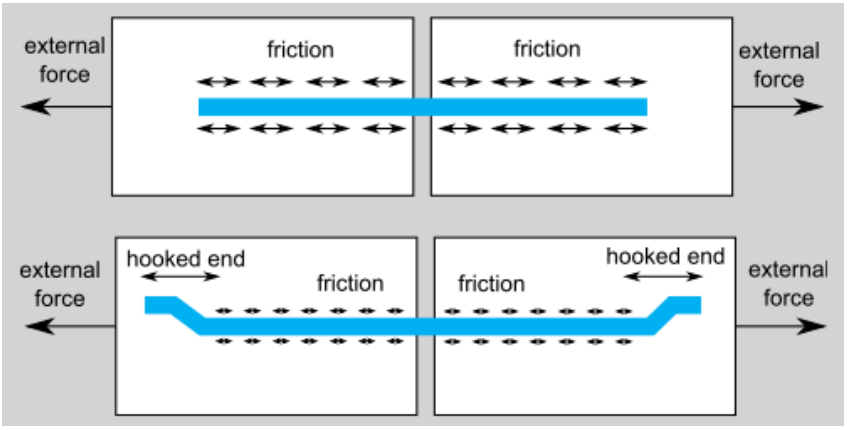

Figure 2.4. Illustration of the various internal and external forces acting on straight and hooked end steel fibres. [24]

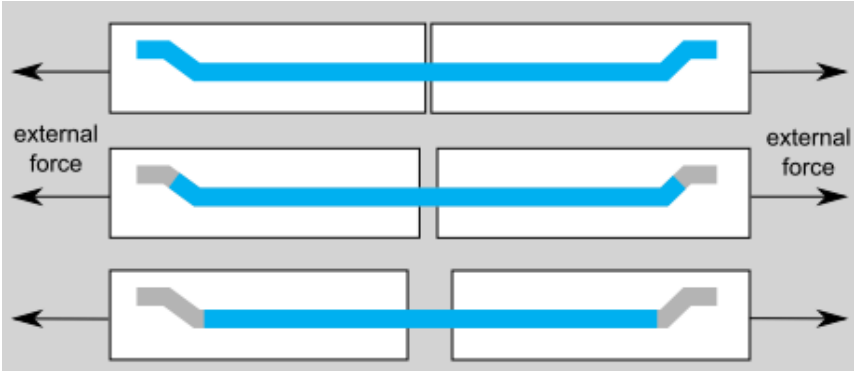

Figure 2.5. Illustration of pull-out steps of one steel fibre – without fibre rupture. [24]

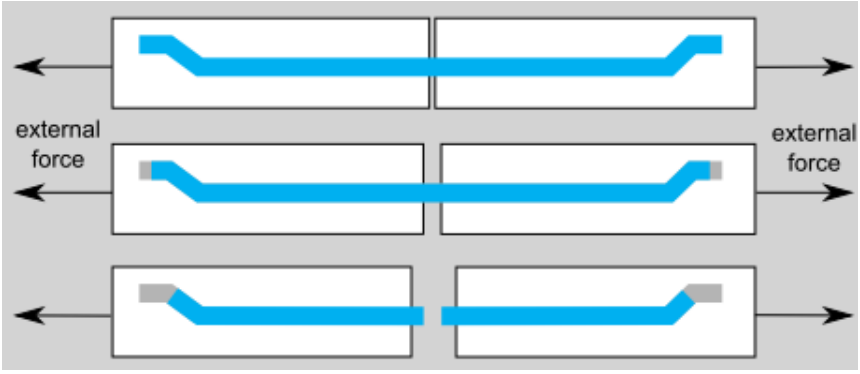

Figure 2.6. Illustration of pull-out steps of one steel fibre - with fibre rupture. [24]

2.3.2 Residual flexural tensile strength of steel fibre reinforced concrete

The strength of the hardened fibre reinforced concrete is characterized by the term "residual (or post-cracking) flexural tensile strength", which can be determined in different experimental ways. The residual flexural tensile strength is determined experimentally since it is not possible to calculate it with enough precision due to the complex interaction between concrete and fibres. [4]

To determine the residual flexural tensile strength, there are mainly two different standard tests to choose from; three or four point bending test. In the three point bending test, the maximum flexural tensile stress is in the middle of the specimen and in the four point test, the maximum stress is somewhere between the two loading points. Since the area where the specimen is expected to crack is larger in a four point test, it is more likely that somewhere in this area there will be a weak link that precipitates cracking, and consequently, the four point test is more likely to give a lower flexural tensile strength than a three point test. [1]

The Finnish guideline BY 56 [4] suggests that the residual flexural tensile strength of SFRC shall be determined in a three point bending test described in the ASTM C1018-9 (American Standards for Testing and Materials) [25]. In this standardised test, a notched beam with the dimensions 750 mm × 150 mm × 150 mm is loaded until a crack opening occurs. [4, 25]

The Swedish guideline SS 812310 [5] and the most recent guideline from the United Kingdom (TR 34) [8] use the European standard EN 14651 [26] to determine the residual tensile strength. According to SS 812310, the residual flexural tensile strength is determined by a three point bending test (illustrated in Figure 2.7) where the notched test specimen shall be prisms conforming to EN 12390-1: 2012 [27] with a nominal size (width and depth) of 150 mm and length between 550…700 mm. The distance between the circular supports shall be 500 mm (± 2.0 mm) and the length of these rollers shall be 10 mm longer than the width of the specimen. [26]

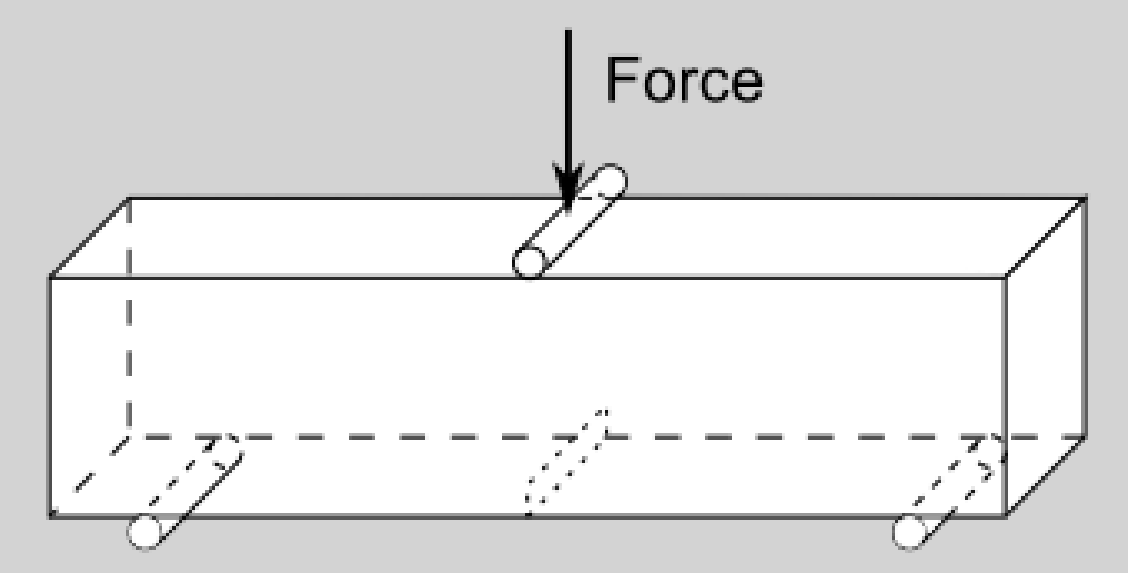

Figure 2.7. Layout of the three point bending test. [24]

The residual flexural strength is determined either by checking the load-deflection (δ) or the load-CMOD (Crack Mouth Opening Displacement) relationship. In a three point load-CMOD test, the testing machine is set to increase the CMOD at a constant rate of 0.05 mm/min until CMOD = 0.1 mm is reached. Thereafter, the rate is increased to 0.2 mm/min. At four different CMOD-values (0.5 mm, 1.5 mm, 2.5 mm and 3.5 mm) the corresponding load is obtained ($F_1 \ldots F_4$ in Figure 2.8). The residual flexural tensile strength ($f_{R,j}$) is then given by: [26, 1]

$$f_{R,j} = \frac{3F_j l}{2bh_{sp}^2} \tag{1}$$

where F_j is the load corresponding with $CMOD_j$ or δ_j, l is the span length, b is the width of the specimen and h_{sp} is the distance between the tip of the notch and the top of the specimen.

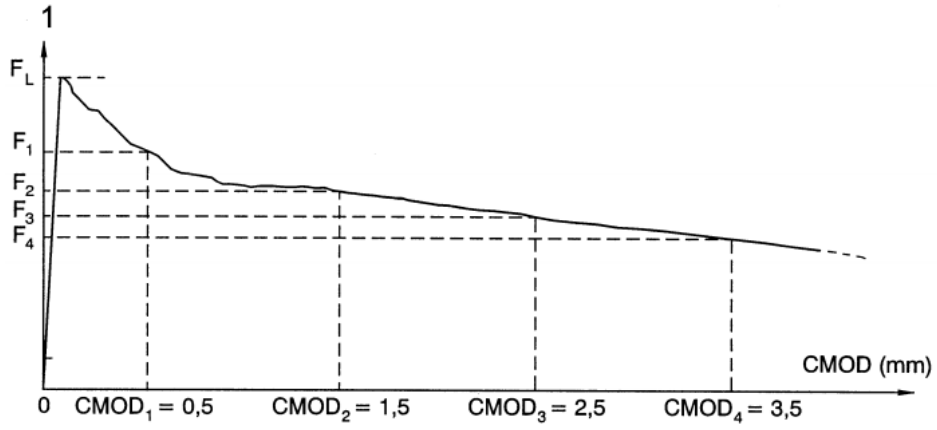

Figure 2.8. Load-CMOD diagram. [26]

2.3.3 Fibre orientation and distribution

The fibre orientation and distribution have a major influence on the properties of the hardened concrete. In fact, how well the SFRC performs in the post crack state correlates with the amount of fibres bridging the cracks, which, in turn, is influenced by the fibre dosage and fibre orientation. An assumption when examining SFRC is that the fibres are uniformly distributed and randomly oriented in the concrete. However, these assumptions are not entirely correct. There are several factors that affect the fibre orientation and the most important ones are the so-called wall effect, shear induced orientation and extensional stresses induced orientation. Other factors influencing the fibre orientation are the reinforcement layout, casting process, concrete rheology and fibre type and volume fraction. The following paragraphs will explain the first three phenomena in more detail. [24, 28]

The wall effect is illustrated in Figure 2.9. When casting SFRC the surrounding formwork makes it impossible for the fibres to be evenly dispersed, since the fibres will not penetrate the formwork. Therefore, the concentration of fibres is denser near the surface and the fibres tend to align in the direction of the surrounding flow. Besides the wall effect, the geometry and surface of the formwork also influence the fibre orientation. It has been observed that the rougher formwork surface, the more random fibre orientation is found in the vicinity of the formwork. [24]

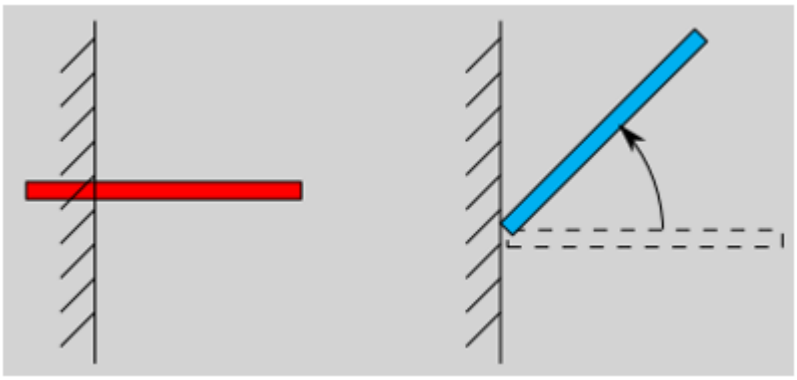

Figure 2.9. Wall effect: The red bar represent an impossible placement and the blue represent a possible placement of a fibre. [24]

When casting SFRC, shear induced orientation of steel fibres orientates the fibres in a direction that is almost parallel to the shear flow direction. As illustrated in Figure 2.10, the fibre will stay in that position when settled. Shear induced orientation takes approximately 0.5…5 seconds depending on the material properties. However, since 0.5…5 second is a short time compared to the casting process itself, the shear induced orientation is assumed to be instantaneous. [24]

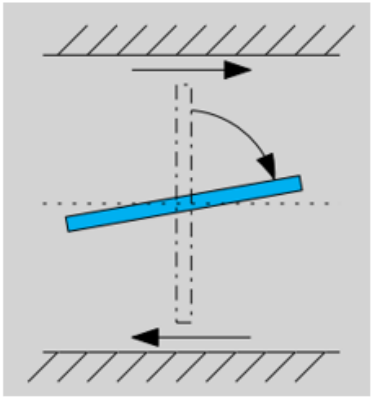

Figure 2.10. Shear induced orientation: Horizontal arrows represents the shear direction and the blue bar represents the final fibre position. [24]

An example of extensional stresses induced orientation is shown in Figure 2.11.When a slab is cast from a circular inlet positioned in the corner (brown circle), the mass will spread out in a circular shape. The further from the inlet, the slower is the "spread out speed" of the concrete. Close to the inlet, where the mass is moving fast, the fibres will orient in a direction parallel to the flow (red line). But, as the mass move further away from the inlet, the fibres tend to orient in a direction normal to the flow (blue line). [24]

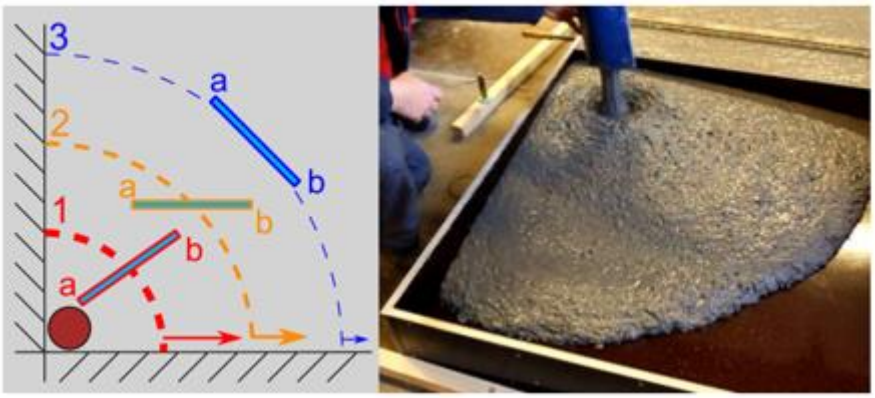

Figure 2.11. Extensional stresses induced orientation: Top view of plate casting. [24]

There are some ways to influence the orientation of the fibre after it has been casted as long as the concrete is still fresh. One way is to use a table vibrator. When vibrating, the fibres tend to align in a horizontal direction. [16] Another way is to drag a magnet trough the concrete, which will also align the fibres in a horizontal direction. [29]

2.4 Producing, mixing and casting steel fibre reinforced concrete

Producing SFRC is exactly like producing ordinary concrete except the extra step of adding steel fibres and superplasticizers to the mix. When adding fibres, the challenge is to add them to the mixture so they will not form clumps, which occur easily especially for fibres with deformed ends. To prevent fibres from clumping they can be collated into bundles of 10 – 30. These fibres are glued together with a water-soluble glue that dissolves when the fibres are added to the wet concrete mix (Figure 2.3, right). After the fibres are added, it will take the mixer approximately 30…40 revolutions to disperse the fibres throughout the matrix. For practical reasons, ERMCO [1] recommends that instead of numbers of revolutions, the minimum mixing time should be five minutes (or one minute per m^3). If loose fibres are used it is important that they are added free of clumps, since these will not dissolve in the mixer. Hence, the clumping problem is usually only in dosing and may be caused because:

- the fibres are added too quickly to the mix and therefore land on each other;
- the fibres are added to the mix before the other ingredients; or
- the amount of fibres are too high.

In conclusion, if the fibres are added free of clumps, they tend to stay that way and if they are added in clumps, they tend to remain in clumps. [16]

Fibres are added either at the concrete plant or on site. For health and safety reasons, manual handling of steel fibres should be restricted to a minimum. It is therefore recommended that fibres are dispersed on a conveyer belt by automatic means and fed into the fresh concrete from there. If the fibres are added on site, the manufacturer shall provide instructions on how to add fibres to the fresh concrete so that the fibres are evenly distributed without clumps. However, fibre producers are often unwilling to allow fibres to be added on site. This is not only because of health and security risks, but also for quality control reasons. [1]

The best way to ensure good SFRC quality is to add the fibres at the plant after the other components are thoroughly mixed. Today, producers have different kind of automatic dosing systems, which are often able to regulate the fibre content with high accuracy. [1] BY 56 [4] recommends that the fibre content is expressed in steps of 5 kg/m^3.

Once there is a ready SFRC mixture, the casting process is in many aspects same as for plain concrete. Pumping SFRC does not require special equipment, though it may be useful to have a vibrator on the grid of the pump. The workability of the matrix may be affected by the amount of fibres and their aspect ratio. As the fibre content and/or aspect ratio increase so does the impact on the workability. Adding superplasticizers to the matrix often solves the workability issue. [22]

2.5 Quality control of steel fibre reinforced concrete

For all building materials, there must be regularly quality control conducted. For SFRC in Finland the standards and guidelines regarding quality control that must be followed are:

- SFS-EN 206 Concrete - Specification, performance, production and conformity [30];
- SFS-EN 14889-1 Fibres for concrete - Part 1: Steel fibres - Definitions, specifications and conformity [23]; and
- BY 56 Teräskuitubetonirakenteet 2011 [4].

According to BY 56 [4], the fibre content should be checked regularly. The amount of fibres is tested by taking at least six random samples from the fibre concrete matrix at a minimum of five litres. Though, the recommended volume is about ten litres. Because of the random dispersion of fibres, the bigger the sample volume and number of samples, the more reliable results. After the samples are gathered, the fibres are collect, washed and thereafter weighted. The amount (kg) of fibres from one single sample must not be less than 20 % from the target content, and the average fibre content from all samples must not be less than 10 % from the target content [4]

There are two levels of attestation of conformity defined in EN 14889-1 [23]: System 1 and System 3. System 1 is applicable when the fibres have a structural function (e.g., in load bearing structures) and system 3 is applicable in other non-structural applications, e.g., when the fibres are used for reducing the risk of plastic shrinkage. System 1 fibres require regular surveillance of the manufacturing process by an independent Certifying Body, which provides the certificate of conformity (CE-mark). For System 3, the producer alone may declare that the quality is in accordance with the requirements of the standard, i.e. no surveillance of a third party is compulsory. [23, 1]

In Europe, only CE-labelled (European Conformity) steel fibres that conform to EN 14889-1 [23] may be used in concrete structures. Once one fibre type fulfils all requirements, it is provided the CE-mark. The CE-marking shall be done according to the CE-marking directive 93/68/EC [31] and an example of CE-labelling is represented (with explanations to the right) in Figure 2.12.Apart from the CE-label, the package should also include the quantity of fibres in every bag and a declaration of performance document for the given fibre type. [1, 4, 23]

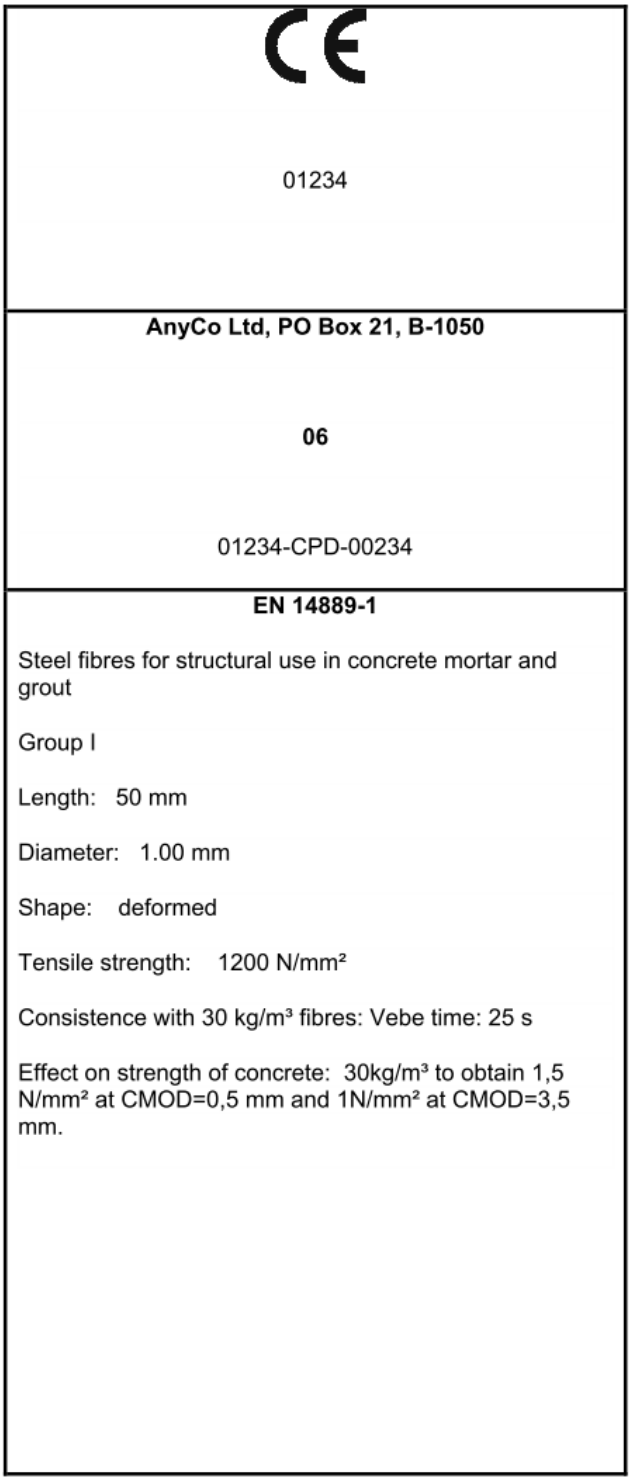

Figure 2.12. Example of CE-marking information. [23]

2.6 Applications of fibre reinforced concrete

The use of FRC has increased steadily since its introduction in the late 1960s, but its market share is still relatively small. Today, the main applications for FRC are in industrial floors and in shotcrete applications, e.g., for rock strengthening. Other common FRC applications are in pavements, claddings and architectural applications. [16]

In Finland, first larger floors with SFRC were realized at the end of 1980 (e.g. Kaukas, Lappeenranta) but the recession in 1990 stopped the development. SFRC gained new interest with the new millennium and today SFRC is the main solution in larger industrial floors. Furthermore, using FRC in elevated floors and precast concrete applications, for example wall panels, are slowly gaining interest in Finland. [22]

As a result of the raised interest to FRC and increased expertise, especially SFRC is increasingly utilized in more demanding structural applications. [2] In fact, in 2003 the world's first prestressed elevated floor made SFRC was completed in Ingolstadt, Germany. That floor is 250 mm thick with a span width of 5 m × 5 m. Yes, a reinforcement mesh was put into the floor to have somewhere to fix the heating pipes. But since the mesh is located in the centre of the neutral zone of the slab it is regarded ineffective to the load-bearing capacity of the slab. [32] After the Ingolstadt floor, SFRC has been used in several load-bearing structural application in Europe. For instance, all slabs in the sixteen story high Rocca-Al-Mare office building in Tallinn, Estonia, are made of SFRC (Figure 2.13, right). However, to prevent a progressive collapse, so called APC (anti-progressive collapse) reinforcement was added in the pillar lines (Figure 2.13, left) [2].

Figure 2.13. Rocca-Al-Mare in Tallinn. Left: under construction. [20]

3 Shear and punching resistance of concrete slabs

3.1 The shear and punching phenomenon

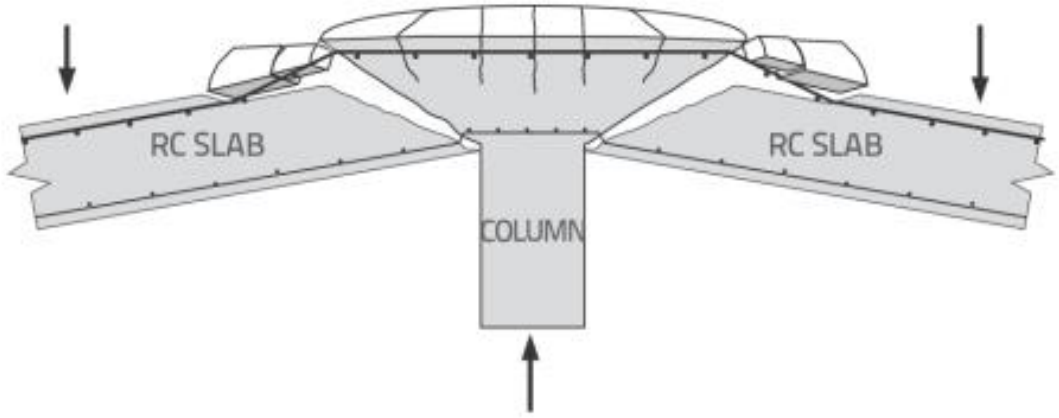

Figure 3.1. Schematic view of punching failure. [33]

In the early 1960s, Kinnunen and Nylander (Sweden) developed a theoretical model to determine the punching resistance for concrete slabs. On the basis of their test results, they concluded that the punching capacity of a slab is reached at a certain critical rotation. Their model predicts that the critical rotation could be determined by assuming a bilinear moment-curvature relationship and by simplifying the kinematics of the concrete slab. When published, this model described the phenomenon of punching better than any other model and also provided the most accurate results. However, due to the complex character of Kinnunen and Nylander's model, it was never included in any codes of practice, though it did serve as a basis for building codes, such as the Swedish and Swiss codes in the 1960s. [34]

Because of the complexity of the model a, number of studies have attempted to improve and simplify it [10, 11]. The model that is considered to describe best today the shear and punching behaviour for concrete slabs is the critical shear crack theory (CSCT). The CSCT model has been widely accepted and forms the basis for the shear and punching part in the Model Code 2010 [35, 9]

CSCT is based on the assumption that the punching resistance of a concrete slab decreases with increasing rotation of the slab. When a slab is exposed for a specific load, it will start to rotate around its point/line of support, resulting in a critical crack, as illustrated in Figure 3.2. The amount of load that can be bridged across this crack depends on the roughness of the crack, which consequently correlates with the maximum aggregate size. Hence, the main parameters when calculating the punching resistance according to the CSCT are the slab rotation, the effective depth and the maximum aggregate size. Since the effective depth and the aggregate size remain constant, the punching capacity can be defined as a function of the slab rotation [34] given by:

$$\frac{V_R}{b_0 d\sqrt{f_{ck}}} = \frac{3/4}{1+\frac{15\psi d}{d_{g0}+d_g}} \qquad (2)$$

where b_0 is the critical control perimeter set at a distance of $0.5d$ from the vicinity of the column (Figure 3.10) where d is the effective depth of the slab. f_{ck} is the concrete compression strength, ψ is the slab rotation, $d_{g0} = 16\ mm$ is a reference aggregate size and d_g is the maximum aggregate size.

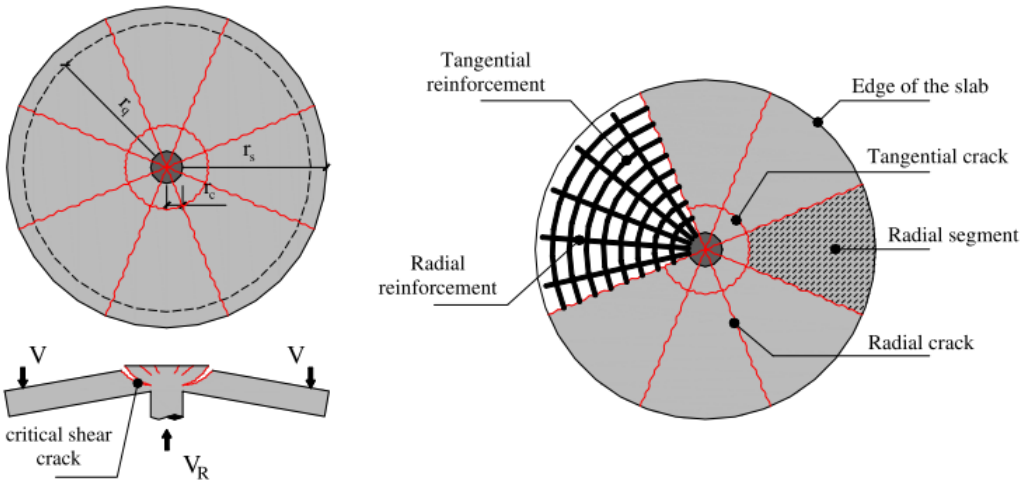

Figure 3.2. RC slab with axisymmetric structural conditions, crack pattern at ultimate limit state and reinforcement arrangement. [13]

Although the CSCT model was found to provide good estimations for the punching capacity, it assumes that the punching failure mechanism occurs with only rigid body rotations of the slab outside the punching cone. This assumption contradicts experimental evidence showing that rotation and sliding occurs in the failure region, and the CSCT model may therefore lead to inaccurate results. Moreover, CSCT is more complicated to use for routine designs than traditional methods. [36]

3.2 Failure mechanisms

There are three different failure modes for pile-supported slabs. The first failure mode is when the structure fails because of crushing of concrete or by internal diagonal cracking (Figure 3.3, left). The second mode is when the structure fails as a result of reinforcement yielding (Figure 3.3, middle). The third and last mode is a combination of previous two failure modes (Figure 3.3, right). Failures can be avoided through the use of various measures, including increasing the slab thickness, increasing the amount of flexural reinforcement or adding shear reinforcement. [37]

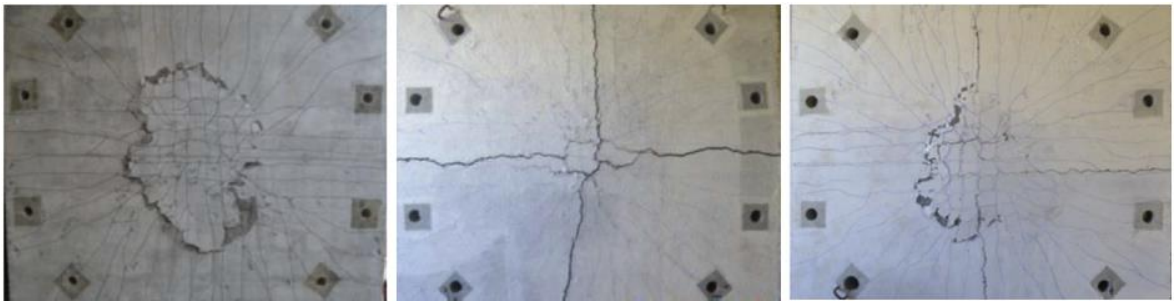

Figure 3.3. Different failure modes. Left: punching failure, middle: bending failure, right: combination of punching and bending. [12]

For slabs provided with shear reinforcement, there are several different possible failure modes which are illustrated in Figure 3.4. Furthermore, Figure 3.5 presents different types of shear reinforcement.

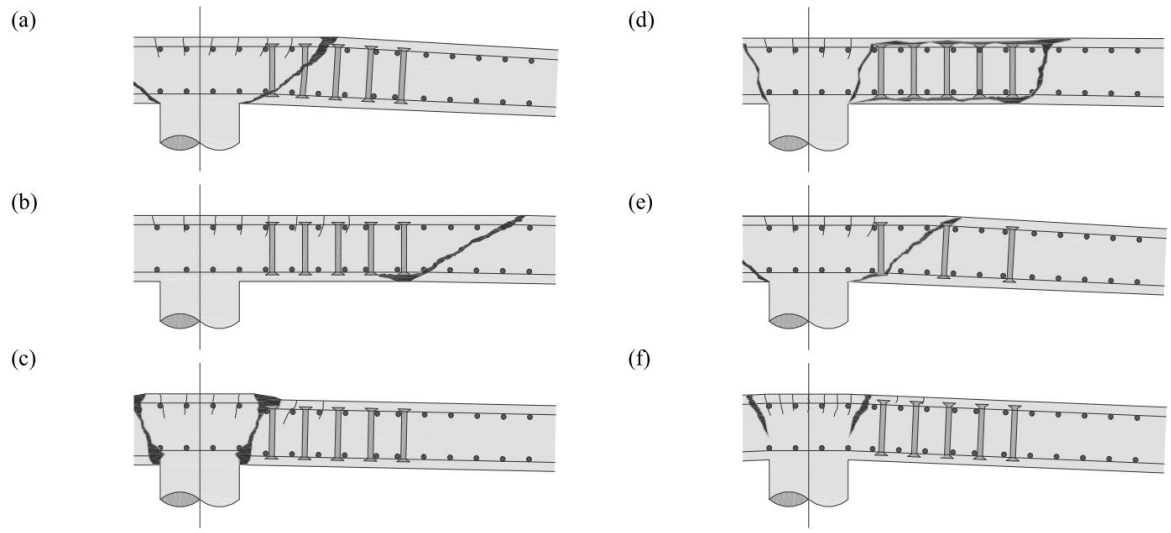

Figure 3.4. Possible failure modes of slabs with shear reinforcement: (a) failure within shear-reinforced area, (b) failure outside shear-reinforced area, (c) failure close to the column due to crushing of concrete, (d) delamination of the concrete core, (e) failure between the transverse reinforcement, and (f) flexural failure. [38]

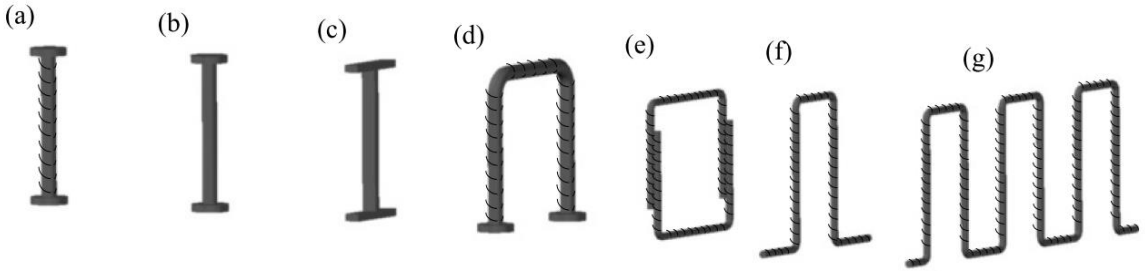

Figure 3.5. Examples of shear reinforcement systems: (a) corrugated double headed shear studs, (b) smooth double headed shear studs, (c) steel offcuts, (d) headed stirrups, (e) stirrups with lap at the vertical branch, (f) stirrups or shear links, (g) continuous stirrups or cages of shear links. [38]

When a slab begins to fail, cracks start to form inside the slab, and hence, it is generally difficult to observe the failure propagation. [37] For SFRC slabs, the failure process can be divided into three general stages. In the first stage, diffuse micro-cracks occur within the structure. Secondly, micro-cracks propagate to macro-cracks. And lastly, macro-cracks grow until the fibres are not able to transfer loads between the cracks and the structure fails. [19] Figure 3.6 illustrates the shear and punching failure for slabs, where (a) illustrates a case where the slab fails as a wide beam, and (b) demonstrates a punching failure. [37]

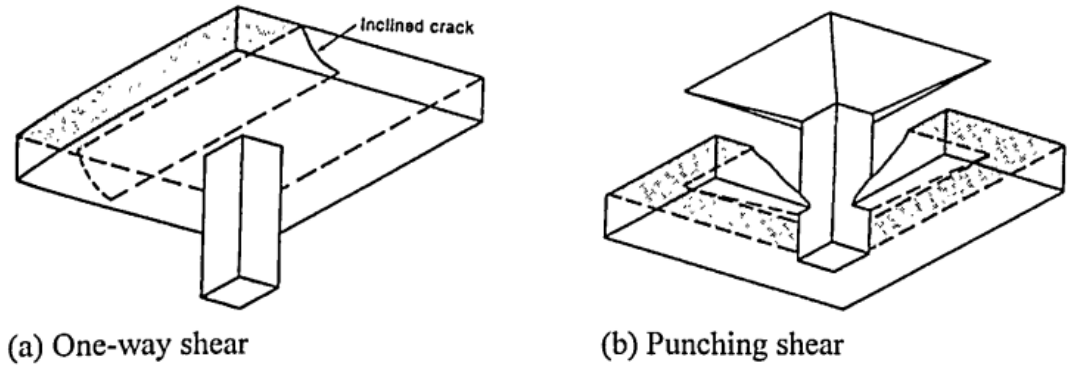

Figure 3.6. Shear and punching failure in a slab. [37]

Concrete structures may show either a strain-softening or a strain-hardening behaviour after the macro-cracks have started to develop (also known as the post crack-stage), which is illustrated in Figure 3.7. If the load bearing capacity in the post-crack stage is higher than in the un-cracked stage then the structure is described to behave in a strain-hardening manner. This is the case in most conventionally reinforced concrete structures. On the contrary, if the structure is still able to carry loads after cracking but not as much as in the un-cracked stage then the structure behaves in a strain-softening manner. This is typically the situation for SFRC with fibre dosages up to approximately 40 kg/m^3 (depending on the fibre type). [19]

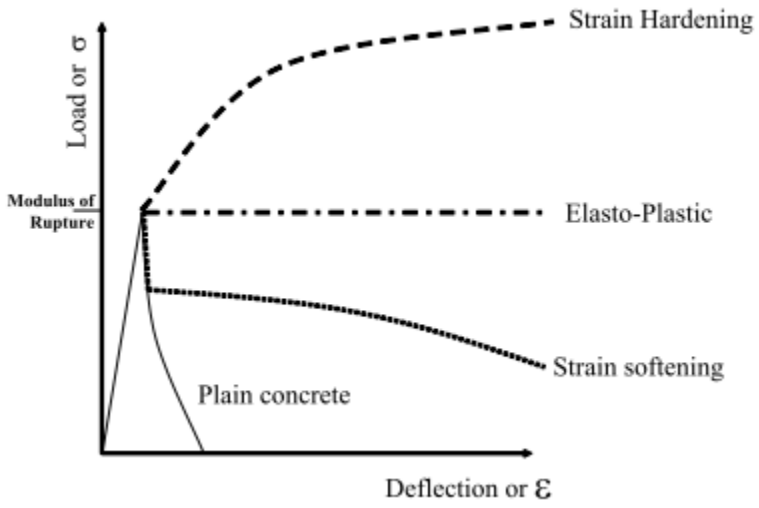

Figure 3.7. Typical load/deflection (stress/strain) plots of FRC. [19]

3.3 European standards and guidelines

The typical approach when determining the shear resistance for a SFRC slab is to first calculate the concrete contribution, then the fibre contribution and lastly, if needed, the contribution from shear reinforcement. However, in this thesis slabs provided with shear reinforcement are not investigated. The concrete contribution, is in most guidelines calculated according to equation (6.2.a) in Eurocode EN 1992-1-1 (EC2) [39], which is given by:

$$V_{Rd,c} = [C_{Rd,c}k(100\rho f_{ck})^{1/3} + k_1\sigma_{cp}]b_w d \quad (3)$$

with a minimum of

$$V_{Rd,c} = (v_{min} + k_1\sigma_{cp})b_w d \quad (4)$$

where v_{min}, is given by:

$$v_{min} = 0.035k^{3/2}f_{ck}^{1/2} \quad (5)$$

$C_{Rd,c}$ may be taken as:

$$C_{Rd,c} = 0.18/\gamma_c \quad (6)$$

where $\gamma_c = 1.5$ is the partial factor for concrete. k is defined as:

$$k = 1 + \sqrt{200/d} \leq 2 \quad (7)$$

ρ is the ratio between the tensile reinforcement and concrete given by:

$$\rho = A_{sl}/b_w d \quad (8)$$

where A_{sl} is the tensile reinforcement area and b_w is the width of the cross section. k_1 may be taken as 0.15 in shear applications and 0.10 in punching applications and σ_{cp} is defined as:

$$\sigma_{cp} = N_{Ed}/A_c < 0.12f_{cd} \quad (9)$$

where N_{Ed} is the cross section normal force (taken as = 0 if the there are no normal forces acting on the section) and A_c is the concrete area of the examined cross section.

The approach for punching is basically the same. The contribution from concrete, fibres and shear reinforcement is summarized and lastly, the punching resistance is checked at a critical control parameter, μ_1. The expression for punching in EC2 is given by:

$$V_{Rd,c} = C_{Rd,c}k(100\rho f_{ck})^{1/3} + k_1\sigma_{cp} \geq (v_{min} + k_1\sigma_{cp}) \quad (10)$$

EC2 defines the critical control parameter at a distance of $2d$ from the vicinity of the column (Figure 3.9). MC2010, on the other hand, defines the critical control parameter at a distance of $0.5d$ (Figure 3.10).

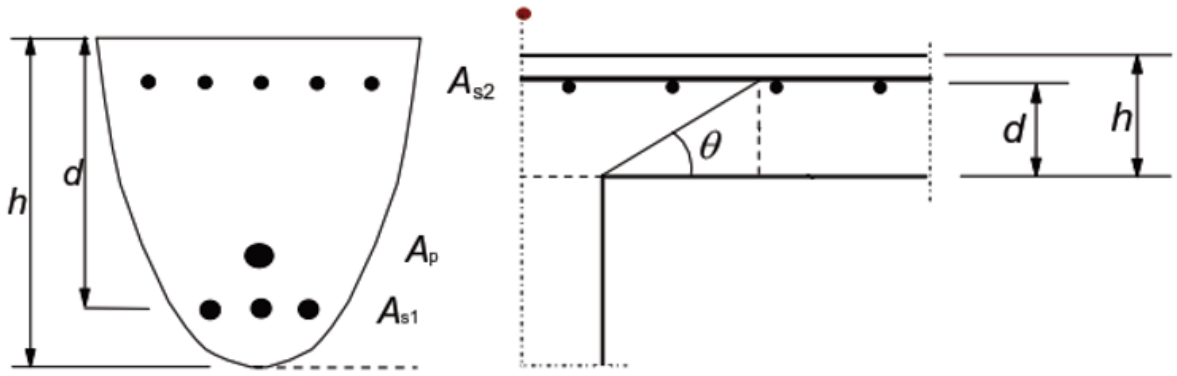

Figure 3.8. Definition of effective depth, h, according to Eurocode 2. Left: shear situation. Right: Punching situation. Modified from Reference [39].

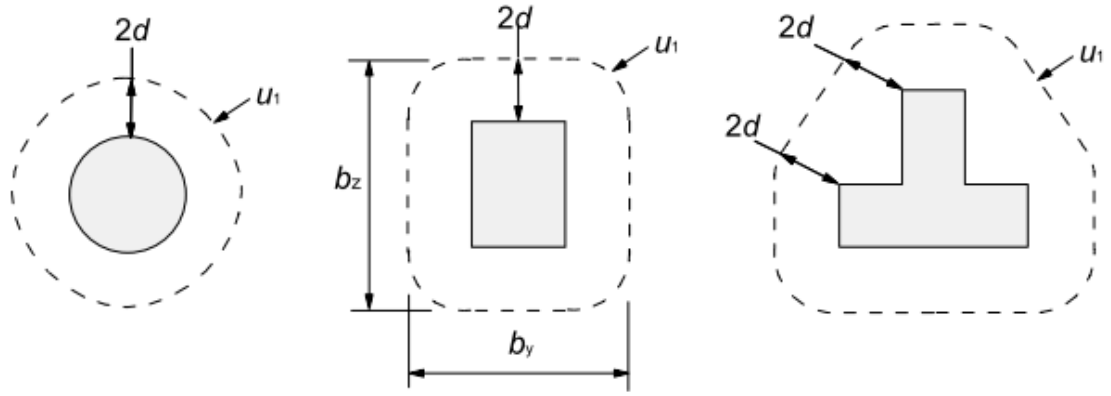

Figure 3.9. Typical basic control parameters around loaded areas according to Eurocode 2. [39]

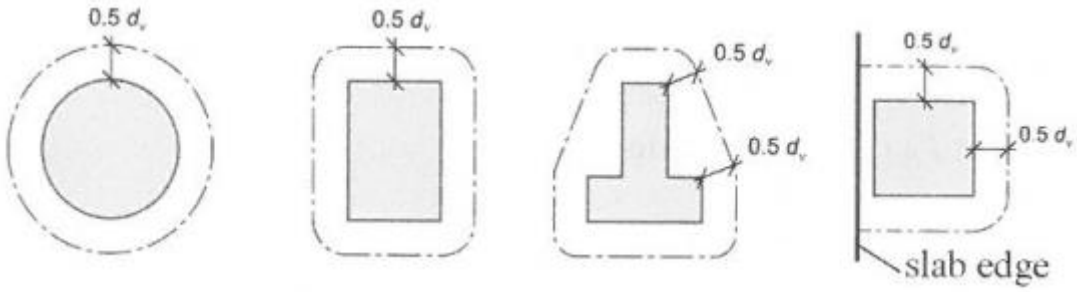

Figure 3.10. Typical basic control parameters around loaded areas according to MC2010. [9]

3.3.1 Finland – BY 56

BY 56 is an aid for making preliminary calculations for the capacity for SFRC ground or pile-supported slabs in industry buildings, storehouses or parking halls. The Finnish Concrete Association (Suomen Betoniyhdistys r.y (BY)) published this guideline in 2011. The authors claim that by using BY 56 designers are able to estimate the required fibre content with an accuracy of 10…20 percent (on the safe side). [4]

BY 56 has in its formula for shear and punching resistance adopted the concrete contribution from EC2 (Eq. (3)) and the fibre contribution from the third edition of TR 34. The formula for shear resistance in BY 56 is given by:

$$V_{Rd,c} = [C_{Rd,c}k(100\rho f_{ck})^{1/3} + k_1\sigma_{cp} + v_{fd}\,]b_w d \qquad (11)$$

where v_{fd} is the fibre contribution defined as:

$$v_{fd} = 0.7 k_f k \tau_{fd} \quad (12)$$

where k_f is a reduction factor taking into account T-shaped cross-sections (for rectangular cross-sections it may be taken as = 1) and is defined as:

$$k_f = 1 + n(h_f/b_w)(h_f/d) \leq 1.5 \quad (13)$$

where h_f is the height of the flange. n is given by:

$$n = (b_f - h_f)/h_f \leq 3 \quad (14)$$

where b_f is the widht of the flange. τ_{fd} is the steel fibre contribution defined as:

$$\tau_{fd} = 0.12 R_{20,50} f_{cbk} \quad (15)$$

where $R_{20,50}$ is the residual flexural strength for the SFRC and f_{cbk} is the unreinforced concrete flexural strength given by:

$$f_{cbk} = [1 + (200/h)^{0.5}] f_{ctk(0.05)} \leq 2 f_{ctk(0.05)} \quad (16)$$

where h is the slab total thickness and $f_{ctk(0.05)}$ is the characteristic axial tensile strength of concrete.

For fast preliminary calculations, BY 56 defines a term “virtual fibre”, which is an assumption of how much a certain fibre content increases the capacity of the slab. These values are listed in Table 3.1. That is to say, for a quick preliminar calculation the designer can pick a value from Table 3.1 and put it into the Eq. (15). [4]

Table 3.1. The residual tensile strength for the virtual fibre for different fibre contents [4]

Amount of fibres, ρ_k [kg/m^3]	**Residual tensile strength for ground slabs, $R_{10,20}$**	**Residual tensile strength for pole slabs, $R_{20,50}$**
25	0.57	0.52
30	0.64	0.58
35	0.70	0.65
40	0.77	0.71
45	0.83	0.77
50	0.90	0.84

The formula for calculating the punching capacity is very similar to the shear formula and is defined as [4]:

$$V_{Rd,c} = C_{Rd,c} k (100 \rho f_{ck})^{1/3} + k_1 \sigma_{cp} + \tau_{fd} \quad (17)$$

The punching capacity should then be checked at the critical control parameter (distance $2d$ from the column) defined in EC2 (Figure 3.9).

BY 56 is, as mentioned, only for preliminary calculations. However, there is an on-going work on a new standard in Finland and it is expected to be based on the Swedish standard (SS 812310), which is presented next. [22]

3.3.2 Sweden – SS 812310

The Swedish standard SS 812310:2014 Fibre Concrete – Design of Fibre Concrete structures, was published in 2014 and replaced the earlier guideline for SFRC in Sweden "Betongrapport nr 4" (published in 1997). SS 812310, which is written in English, is not a Eurocode but it is a complement to EC2. That is to say, when using SS 812310, EC2 has to be read in parallel, since SS 812310 often refers to EC2 to avoid repetitions. The heading and numbering is also made to match the numbering in EC2. The committee used the term fibre concrete instead of steel fibre concrete on purpose, with the idea that this standard should be material-independent. SS 812310 is applicable for both steel and polymer fibres that conforms to the standards EN 14889-1 [23] and EN 14889-2 [40]. Hence, SS 812310 does not cover class, carbon, basalt or any other fibre type. [5, 41]

SS 812310 states that the residual flexural tensile strength, $f_{ft,R3}$ (= characteristic value of the flexural tensile strength after cracking) shall be determined from a three point bending test according to EN 14651 [26]. This is different from their earlier standard where the residual flexural tensile strength should be determined from a four point bending test. [5]

The residual flexural tensile strength is provided in Table 3.2, where class R_1 is required for designs in service limit state (SLS) and class R_1 and R_3 are required for designs in ultimate limit state (ULS). By following the classifications provided in Table 3.2, SS 812310 suggests that fibre concrete may be expressed as, e.g., C30/37-$R_1$3/$R_3$2. Here, the fibre concrete corresponds to a concrete with a compressive strength of 30 MPa (cylinder) or 37 MPa (cube) and a residual flexural strength of 3 MPa in class R_1 and 2 MPa in class R_3. [5, 41]

Table 3.2 Residual flexural strength classes (R-classes) for fibre concrete [5]

Class R_1	$f_{R,1}$ (MPa)	Class R_3	$f_{R,3}$ (MPa)	Class R_4	$f_{R,4}$ (MPa)
$R_1$1	1,0	$R_3$1	1,0	$R_4$1	1,0
$R_1$2	2,0	$R_3$2	2,0	$R_4$2	2,0
$R_1$3	3,0	$R_3$3	3,0	$R_4$3	3,0
$R_1$4	4,0	$R_3$4	4,0	$R_4$4	4,0
$R_1$5	5,0	$R_3$5	5,0	$R_4$5	5,0
$R_1$6	6,0	$R_3$6	6,0	$R_4$6	6,0

Note 1 Residual flexural tensile strength is the characteristic value obtained from beam testing in accordance to SS-EN 14651 at a CMOD (crack mouth opening displacement) of 0,5; 2,5 and 3,5 mm respectively for $f_{R,1}$, $f_{R,3}$ and $f_{R,4}$, see Figure 3.1.

Note 2 Higher residual flexural tensile strength than given in the table may be utilised if the specified value is verified by test results according to SS-EN 14651.

Note 3 The following conditions must be satisfied: $C_1 = 100 \cdot f_{R,1}/f_{ctk,0.05} \geq 50$ % and $100 \cdot f_{R,3}/f_{R,1} \geq 50$ %. The intention is to ensure a certain minimum ductility of the fibre concrete.

Note 4 In most cases $f_{R,1}$ is higher than or equal to $f_{R,3}$ and $f_{R,1}$ is lower than $f_{ct,L}^{f}$, so called bending softening behaviour, see Figure 3.1.

The formula for shear in cases without shear reinforcement in SS 812310 originates from the Italian fibre standard CNR-DT 204/2006 "Guide for the Design and Construction of Fiber-Reinforced Concrete Structures". SS 812310 differs from other guidelines in that content that it does not determine the concrete contribution and fibre distribution separately

Instead, the total capacity is determined using one equation. This equation is very similar to Eq. (3) where the only difference is the addition of a factor that takes into account the fibre contribution. It is notable that the formula requires that there is some existing flexural reinforcement. Otherwise, the value will be zero. The formula for shear resistance is given by [5, 42]:

$$V_{Rd,cf} = \{\frac{0.18}{\gamma_c} k[100\rho(1 + 7.5\frac{f_{ft,R3}}{f_{ctk}} f_{ck}]^{1/3} + 0.15\sigma_{cp}\} b_w d \quad (18)$$

where f_{ctk} is the characteristic axial tensile strength of concrete and $f_{ft,R3}$ is the characteristic residual tensile strength of FRC given by:

$$f_{ft.R3} = 0.37 f_{R,3} \quad (19)$$

where $f_{R,3}$ is the residual flexural tensile strength of FRC.

For column bases without shear reinforcement, SS 812310 has separate formulas for calculating the punching capacity depending on whether the slab is provided with conventional bar reinforcement or not. For column bases with conventional bar reinforcement, the formula is basically the same as Eq. (18) and is given by:

$$V_{Rd,cf} = \frac{0.18}{\gamma_c} k[100\rho(1 + 7.5\frac{f_{ft,R3}}{f_{ctk}} f_{ck}]^{1/3} + 0.15\sigma_{cp} \quad (20)$$

The capacity should then be checked at a control parameter at a distance of $2d$ (Figure 3.9). For column bases without conventional bar reinforcement a formula suggested by Johan Silfwerbrand in 2000 is implemented and is given by:

$$V_{Rd,cf} = V_{Rd,f} = (k/2) C f_{R,3} / \gamma_f \quad (21)$$

where C is a constant (=0.45), $f_{R,3}$ is the residual flexural tensile strength in class R_3 and $\gamma_f = 1.5$ is the partial factor for fibre concrete. [5] When SS 812310 was published, the punching capacity in Eq. (21) was to be checked at the same critical control parameter as in Eq. (20), i.e., at a distance $2d$ from the vicinity of the column (Figure 3.9). However, according to Silfwerbrand [42], there is an error in SS 812310 and instead the punching capacity is to be checked at a distance $0.5d$ from the vicinity of the column when calculating the punching capacity for slabs without conventional bar reinforcement using Eq. (21), i.e., as in MC2010 (Figure 3.10). Again, if Eq. (20) is used then the critical control parameter is $2d$ and if Eq. (21) is used then the critical control parameter is $0.5d$.

3.3.3 Germany – DAfStb-Richtlinie Stahlfaserbeton

Germany is a major actor in the SFRC field in Europe, but it was relatively late until they had their first national guideline. Since the 1990s, the principal applications for SFRC in Germany have been industrial floors and tunnels. Guides to Best Practice published by the German Society for Concrete and Construction Technology (Deutscher Beton- und Bautechnik-Verein E.V. (DBV)) in the 1990s, was back then the best aid they had for such members. Later, in 2001, the DBV published "Guide to Best Practice for Steel Fibre Reinforced Concrete". Although this publication did not have the status of a standard, it was a valuable guide for designers of SFRC applications. [6]

In March 2010, the German Committee for Reinforced Concrete (DAfStb) published Richtlinie Stahlfaserbeton, which is today the governing German standard for SFRC. DAfStb [6] is applicable for steel fibres that conform to EN 14889-1 and aims to cover, together with EC2, the design and construction of load bearing SFRC and RC structures with compressive strength classes up to C50/60. [6]

DAfStb has been revised since it was published. In 2015, the German Committee for Reinforced Concrete published "Commentary on the DAfStb Guideline "Steel Fibre Reinforced Concrete"" where the content of the DAfStb (2012 edition) is clarified. The Commentary publication on DAfStb is divided into Part A and Part B, where the provisions of the guideline are explained in Part A and Part B contains background information on the safety concept, the derivation of the design residual tensile strengths and aids to application of the Guideline in the form of design charts. [6]

DAfStb divides SFRC into two different performance classes based on their residual flexural strength (determined from a four point bending test) [6, 1]:

- L1 (SLS) – performance class for minor deformations
- L2 (ULS) – performance class for larger deformations

The design engineer shall specify the correct performance class of the SFRC. Thereafter, the SFRC manufacturer shall determine the composition of the concrete including fibre type and dosage. According to DAfStb the minimum amount of shear reinforcement may be reduced to zero by taking into account the fibre effect. [6]

DAfStb expresses the design shear resistance for members not requiring design shear reinforcement in Section Re 6.2.2 as:

$$V_{Rd.c}^{f} = V_{Rd,c} + V_{Rd,cf} \tag{22}$$

where $V_{Rd,cf}$ is the SFRC contribution given by:

$$V_{Rd,cf} = \alpha_c^f f_{ctR,u}^f b_w h/\gamma_{ct}^f \tag{23}$$

where $\alpha_c^f = 0.85$ is a reduction factor which is aligned with the concept of DAfStb to allow for long-term effects on the residual tensile strength of SFRC, $\gamma_{ct}^f = 1.25$ is partial safety factor for residual tensile strength of SFRC and $f_{ctR,u}^f$ is the calculated residual tensile strength of SFRC in ULS and is given by:

$$f_{ctR,u}^f = \kappa_F^f \kappa_G^f f_{ct0,u}^f \tag{24}$$

where $f_{ct0,u}^f$ is the basic value of residual tensile strength given in Table 3.3, column 5, and κ_F^f and κ_G^f are reduction factors taking into account the fibre orientation and member size respectively (illustrated in Figure 3.11):

$\kappa_F^f = 0.5$ for level, horizontally manufactured slab type members ($b > 5h$) or in cases in which the fibre orientation is unfavourable with respect to the structural stresses acting on a member, such as, vertically casted walls that are subjected to bending around the horizontal axis.

$\kappa_F^f = 1.0$ for bending and tensile loads in beams.

$\kappa_G^f = 1.0 + A_{ct}^f 0.5 \leq 1.70$, where A_{ct}^f is the tension zone in cracked concrete cross-sections or plastic hinges for a given equilibrium system (in [m^2]). When calculating $f_{ctR,u}^f$, $A_{ct}^f = b_w d \leq 1.5$ must be used since experimental investigations have been conducted up to around 1.5 m.

Table 3.3. Performance classes L1 and L2 for SFRC with corresponding basic value of residual tensile strength [6]

Column	1	2	3	4	5	6
	Basic values of residual tensile strength f^f_{ct0} in N/mm²					
	Deformation 1		Deformation 2			
Row	L1	$f^f_{ct0,L1}$	L2	$f^f_{ct0,L2}$	$f^f_{ct0,u}$	$f^f_{ct0,s}$ [c]
1	0	< 0.16	0	-	-	-
2	0.4 [a]	0.16	0.4 [a]	0.10	0.15	0.15
3	0.6	0.24	0.6	0.15	0.22	0.22
4	0.9	0.36	0.9	0.23	0.33	0.33
5	1.2	0.48	1.2	0.30	0.44	0.44
6	1.5	0.60	1.5	0.38	0.56	0.56
7	1.8	0.72	1.8	0.45	0.67	0.67
8	2.1	0.84	2.1	0.53	0.78	0.78
9	2.4	0.96	2.4	0.60	0.89	0.89
10	2.7 [b]	1.08	2.7 [b]	0.68	1.00	1.00
11	3.0 [b]	1.20	3.0 [b]	0.75	1.11	1.11

[a] for slab type structures only ($b > 5h$).

[b] steel fibre reinforced concrete of these performance classes will require general building inspectorate approval or permission in each individual case.

[c] applies to L2/L1 ≤ 1.0; for L2/L1 > 1.0 see paragraph (4)P.

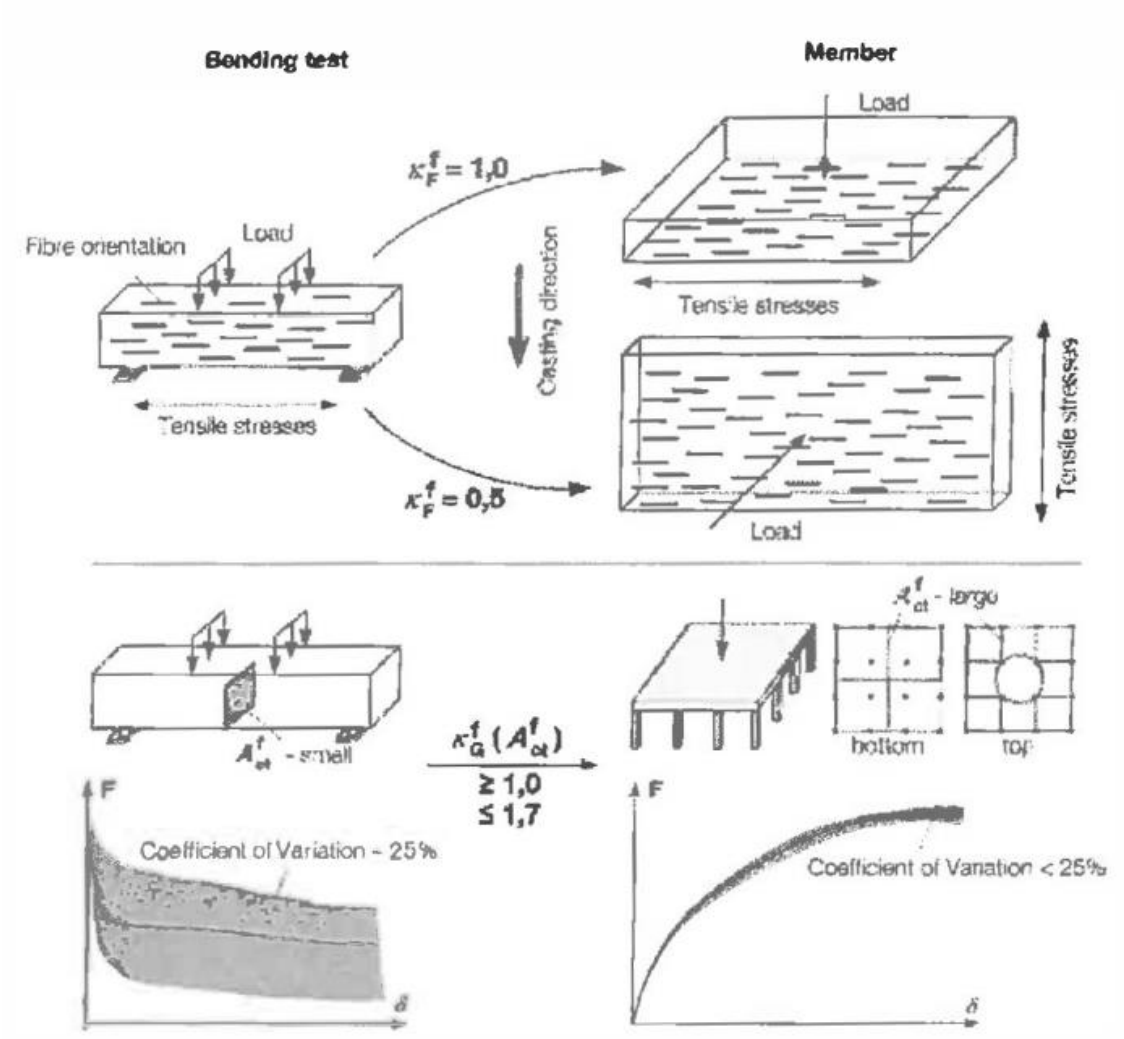

Figure 3.11. Explanation of factors κ_F^f and κ_G^f. [6]

For SFRC slabs or column bases without punching shear reinforcement, the punching shear is given by [6]:

$$V_{Rd,c}^f = 2d/aV_{Rd.c} + V_{Rd,cf} \leq V_{Rd,max} \tag{25}$$

where $a = 2d$ for slabs and $V_{Rd,cf}$ is given by:

$$V_{Rd,cf} = 0.85\alpha_c^f f_{ctR,u}^f/\gamma_{ct}^f \tag{26}$$

The punching is to be checked at a control parameter of $2d$ (Figure 3.9). [6]

3.3.4 UK – Technical Report 34

TR 34 fourth edition [8] by The Concrete Society was first published in August 2013 and has since then been reprinted two times, June 2014 and March 2016. TR 34 is a complement to EC2 for designing concrete industrial ground floors and the third reprint has been expanded to include comprehensive guidance on the design of pile-supported floors. [8]

The punching and shear resistance for SFRC slabs is calculated with the same formula in TR 34. TR 34 uses the symbol P_p for the "punching shear" resistance and is given by:

$$P_p = (V_{Rd,c} + V_{Rd,cf})\mu_1 d \tag{27}$$

where μ_1 is the length of the critical control parameter at a distance of $2d$ from the support (Figure 3.9). According to TR 34 d should be taken as $0.75h$ for FRC or unreinforced concrete. $V_{Rd,c}$ and $V_{Rd,cf}$ are the concrete and steel fibre contribution respectively. The concrete contribution, $V_{Rd,c}$ is the same as in EC2 (Eq. (3)) and the fibre contribution is defined as:

$$\begin{aligned} V_{Rd,cf} &= [0.12(f_{r1} + f_{r2} + f_{r3} + f_{r4})/4]/2 \\ &= 0.015(f_{r1} + f_{r2} + f_{r3} + f_{r4}) \end{aligned} \tag{28}$$

where f.r1…f.r4 are the residual flexural strength in $CMOD_1$…$CMOD_4$, of which values are provided from a three point beam test that conform to EN 14651 [26]. Eq. (28) is based on RILEM TC 162-TDF [43] which suggests that the increase in shear capacity due to steel fibres is 0.12 times the mean residual flexural strength. However, TR 34 chooses to reduce the fibre contribution by 50%, hence the denominator 2. [8, 43]

The method for calculating punching shear has been changed in the fourth edition of TR 34. The earlier third edition defined the punching shear capacity for SFRC as [7]:

$$P_p = (V_{Rd,c} + 0.12R_{e,3}f_{cbk})\mu_1 d \tag{29}$$

where $R_{e,3}$ is the equivalent flexural strength ratio. [39]

3.3.5 Fib Model Code 2010

The International Federation for Structural Concrete (fib) published Model Code for Concrete Structures 2010 (MC2010) [9] in 2013 with the main intention *"to contribute to the development of improved design methods and the application of improved structural materials"*. The predecessors of fib, CEB (Comité Euro-International du Béton) and FIP (Fédération Internationale de la Précontrainte), published the first code-like recommendation in 1964 and 1970. The motive was to gather practical experience and knowledge into practical documents, so that national code commissions could take advantage of it. Before MC2010, fib published The Model Code 1978 and The Model Code 1990, of which the later served as an important basis for the most recent version of EC2. [9]

MC2010 uses a design strategy where analyses are performed on a certain level of approximation (LoA) where each level provides different accuracy. There are four different LoA defined in the MC2010 and they are [9]:

I. Preliminary design
II. Typical design
III. Detailed design or assessment of existing structure
IV. Numerical design.

The higher the LoA, the more complex and time-consuming is the approximation method. Level I approximation method is used in preliminary designs where a simple, yet reliable, analysis is required. Once a preliminary approximation is performed, it can be refined to achieve more accurate results, either by analytical or numerical methods. In Levels II and III the physical parameters of the design equation are typically evaluated through simplified analytical formulas. These LoAs are usually sufficient in most design cases and should not be very time-consuming. Level II should already give good estimates for simple cases but in more complex cases with irregular geometry higher LoAs may be much more accurate. Level IV provides the most accurate estimation but is similarly very time-consuming and therefore only advised in complex structures. Figure 3.12 illustrates accuracy as a function of time for different LoAs. [35, 9]

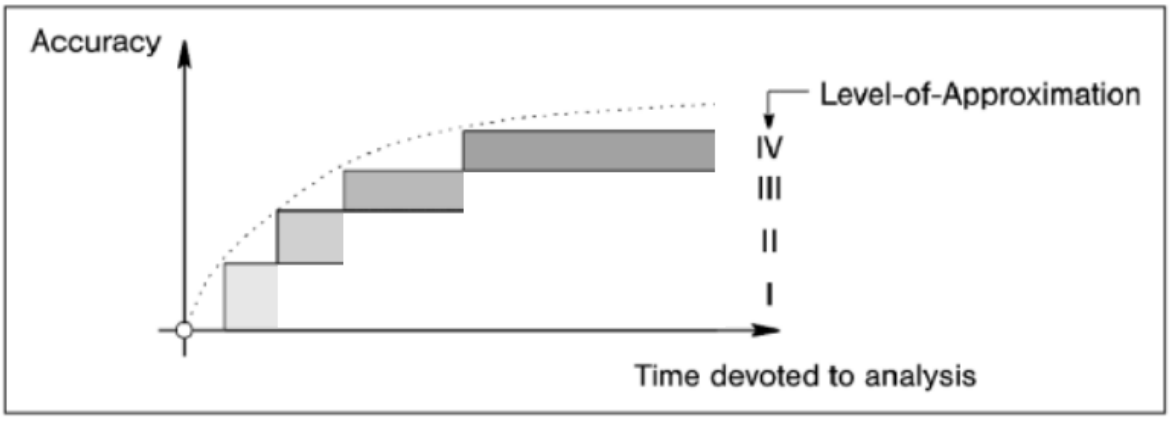

Figure 3.12. Accuracy on the estimate of the actual behaviour as a function of time devoted to the analysis for various levels of approximation. Modified from MC2010. [9]

In MC2010 [9] there is no formula for determining the shear resistance of FRC slabs. However, there is a formula for determining the shear resistance for FRC beams and that formula is the same as in the Sweidish standard SS 812310 [5] for determining the shear resistance in for FRC slabs (Eq. (18)). In other words, since no formula for determining the shear resistance for FRC slabs is presented in MC2010 Eq. (18) shall be used.

As stated earlier, the CSCT model is applied in MC2010 since the shear and punching capacity depends on the crack widths, which propagates with the rotation of the slab. Contrary to shear in beams, the load-rotation behavoir in slabs is significantly non-linear. A general approach for obtaining the load-rotation relationship has been investigated by Aurelio Muttoni and the resulting expression was derived on the basis of a quadrilinear moment-curvature diagram (Figure 3.13 b-h). For design applications the expression by Muttoni has been simplified in MC2010 and will be presented latter in this sub section. [35]

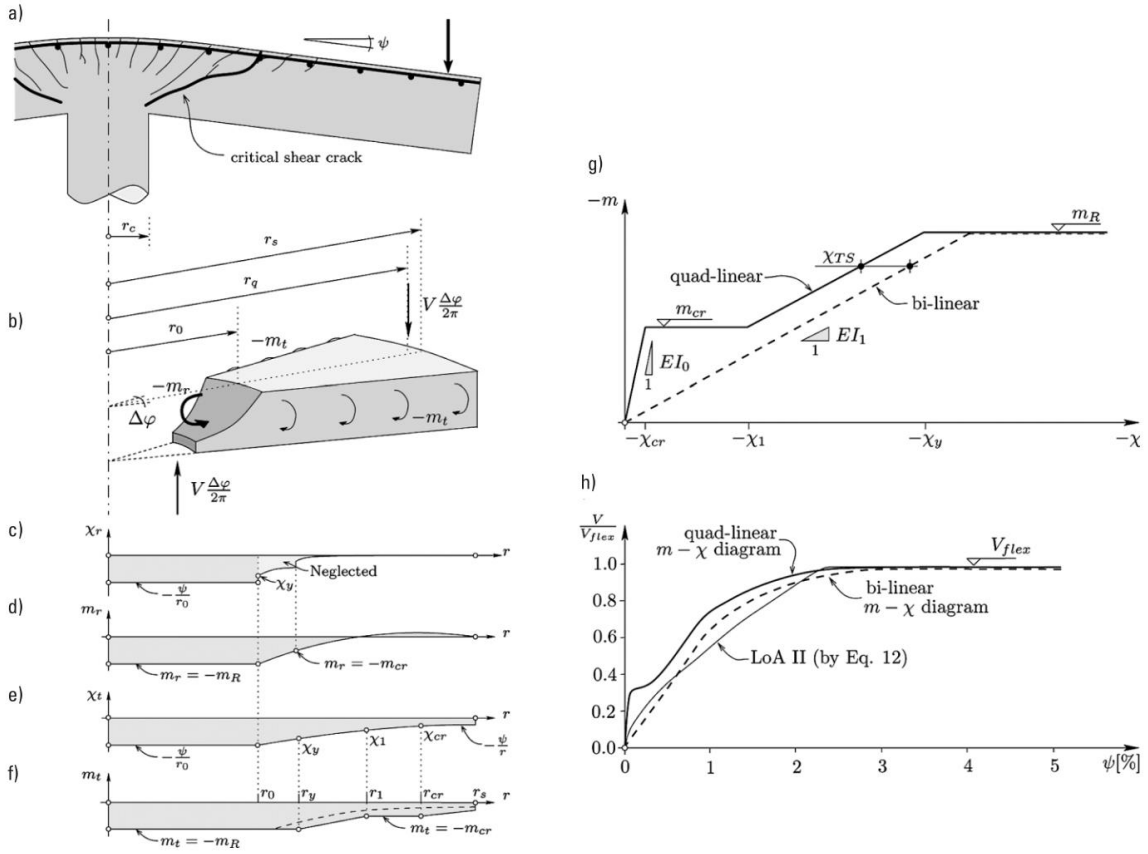

Figure 3.13. Physical model for obtaining suitable load-rotation relationships in flat slabs: a) region investigated and critical shear crack, b) moments, forces and dimensions, c) radial curvature, d) moments, e) tangential curvature, f) moments, g) quadrilinear moment-curvature diagram, and h) corresponding load-rotation relationships. [35]

The fundamentals of how to determine the punching resistance according to MC2010 is illustrated in Figure 3.14. All entities should be in SI units (International System of Units). Firstly, the rotation of the slab is to be checked for the corresponding shear force acting (V_E). Then, the capacity of the slab (V_R) is to be checked at the corresponding rotation and lastly check if the slab fullfils the condition $V_E \leq V_R$. [35]

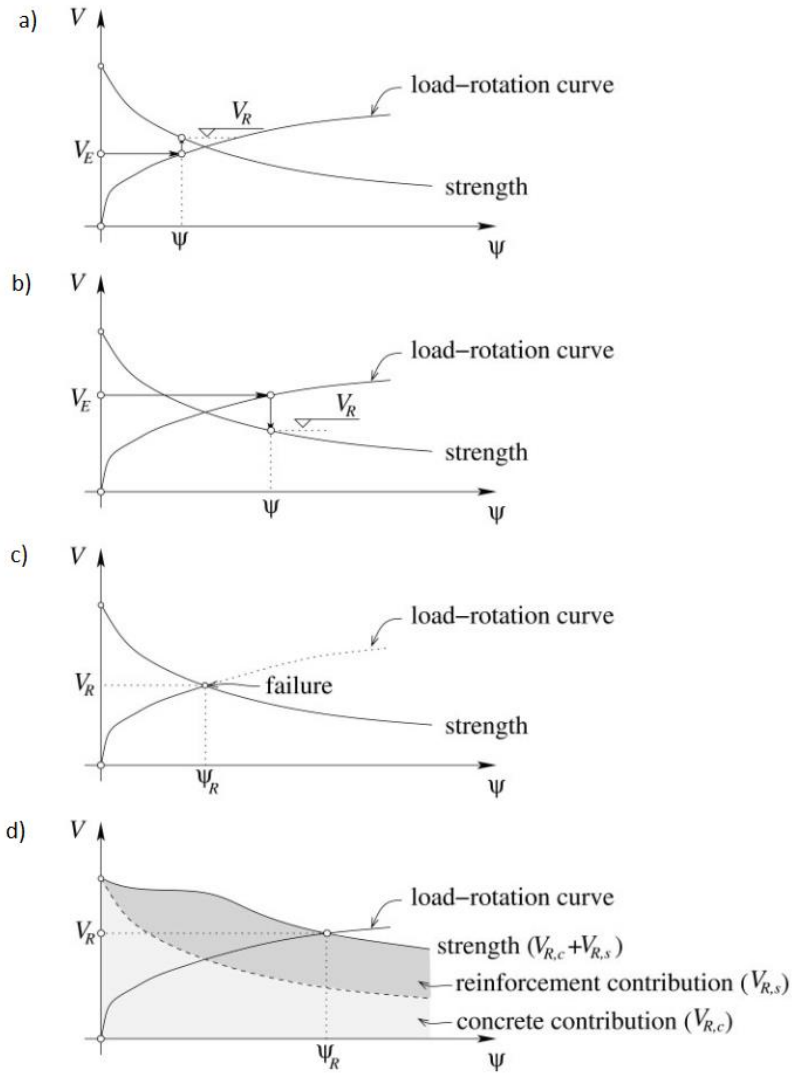

Figure 3.14. a) and b); calculating of punching shear strength V_R for rotation developed for a given applied load V_E, c) intersection between failure criterion and load-rotation curve for calculation of punching shear strength V_R and d) failure criterion accounting for concrete and shear reinforcement contributions. [35]

For FRC slabs, the formula for punching capacity is defined as:

$$V_{Rd} = V_{Rd,F} + V_{Rd,s} \tag{30}$$

where $V_{Rd,s}$ is the design shear resistance provided by the stirrups (given in [9] Eq. 7.3-67) and $V_{Rd,F}$ is the FRC contribution given by:

$$V_{Rd,F} = V_{Rd,c} + V_{Rd,f} \tag{31}$$

where $V_{Rd,c}$ is the concrete contribution and $V_{Rd,f}$ is the fibre contribution. By replacing $V_{Rd,c}$, $V_{Rd,f}$ and $V_{Rd,s}$ by their respective expression, the formula for V_{Rd} may be taken as:

$$V_{Rd} = k_\psi \frac{\sqrt{f_{ck}}}{\gamma_c} b_0 d + \frac{f_{Ftuk}}{\gamma_f} b_0 d + \sum A_{sw} k_e \sigma_{swd} \tag{32}$$

where k_ψ depends on the deformations (rotations) of the slab and is given by:

$$k_\psi = \frac{1}{1.5+0.9k_{dg}\psi d} \leq 0.6 \quad (33)$$

where the parameter ψ refers to the rotation of the slab depending on which LoA is used (more about this later). For concrete with maximum aggregate size not less than 16 mm, the parameter k_{dg} may be taken as $= 1$. For maximum aggregate size less than 16 mm, k_{dg} is given by:

$$k_{dg} = \frac{32}{16+d_g} \geq 0.75 \quad (34)$$

For high strength and lightweight concrete the value for d_g can be taken as = 0 due to the risk for aggregate particles to brake, resulting in a reduced aggregate interlock contribution.

$\gamma_f = 1.5$ is the partial safety factor for FRC and f_{Ftuk} is the characteristic value of the ultimate residual tensile strength for FRC given by:

$$f_{Ftuk} = f_{Fts} - \frac{w_u}{CMOD_3}(f_{Fts} - 0.5f_{R3} + 0.2f_{R1}) \geq 0 \quad (35)$$

where $w_u = 1.5\,mm$ is the maximum crack opening accepted in structural design and $CMOD_3 = 2.5\,mm$. f_{R1} and f_{R3} are the residual flexural tensile strength of FRC corresponding to respective CMOD ($= CMOD_j$) and f_{Fts} may be taken as:

$$f_{Fts} = 0.45f_{R1} \quad (36)$$

In the last part of Eq. (32), $\sum A_{sw}$ is the sum of the cross-sectional area of all shear reinforcemen. k_e is the coefficient of eccentricity which can be taken as 0.90 for inner columns, 0.70 for edge columns, 0.65 for corner columns and 0.75 for corner of walls and σ_{swd} refers to the stress that is activated in the shear reinforcement and can be calculated using [9] Eq. (7.3-67).

When shear reinforcement is needed for punching resistance, a minimum amount of fibres and applicable transverse reinforcement shall fullfil the requirement given in Eq. (7.7-21):

$$V_{Rd,s} + V_{Rd,f} \geq 0.5V_{Ed} \quad (37)$$

where V_{Ed} is the design shear force.

Level I approximation

As mentioned, the value for ψ (illustrated in Figure 3.13 a) depends on which LoA the analyse is based on. For a regular flat slab a preliminary safe estimation for ψ at approximation level I is given by:

$$\psi = 1.5\frac{r_s}{d}\frac{f_{yd}}{E_s} \quad (38)$$

where r_s denotes the position where the radial bending moment is zero with respect to the support axis, which in LoA I can be taken as 0.22 times the span length in systems where

the ratio of the spans (L_x/L_y) is between 0.5…2.0. f_{yd} is the design yield strength and E_s is the modulus of elasticity of the reinforcement.

Level II approximation

For a more accurate estimation of ψ, the equation at approximation level II is given by:

$$\psi = 1.5\frac{r_s}{d}\frac{f_{yd}}{E_s}\left(\frac{m_{Ed}}{m_{Rd}}\right)^{1.5} \quad (39)$$

where r_s may be taken as in LoA I and m_{Ed} is the avarage bending moment acting on the support strip (for the considered direction). For inner columns where the slab is provided with top reinforcement in each direction m_{Ed} is given by:

$$m_{Ed} = V_{Ed}\left(\frac{1}{8} + \frac{|e_{u,i}|}{2b_s}\right) \quad (40)$$

where V_{Ed} is the design shear force, b_s is the widht of the bending moment support strip and $e_{u,i}$ is the load eccentricity. For edge and corner columns m_{Ed} is defined in [9] Eq. 7.3-72…7.3-74. In Eq. (39) m_{Rd} is the design avarage flexural strength per unit length in the support strip (for the considered direction) and is calculated according to rigid-plasticity theory as:

$$m_{Rd} = \rho d^2 f_{yd}(1 - 0.5 f_{yd}/f_{cd}) \quad (41)$$

For prestressed slabs Eq. (39) may be replaced by:

$$\psi = 1.5\frac{r_s}{d}\frac{f_{yd}}{E_s}\left(\frac{m_{Ed}-m_{Pd}}{m_{Rd}-m_{Pd}}\right)^{1.5} \quad (42)$$

where m_{Pd} denotes the avarage decompression moment due to prestressing.

Level III approximation

The coefficient 1.5 in Eq. (39) and Eq. (42) can be replaced by 1.2 if r_s is calculated using a linear elastic (uncracked) model and m_{Ed} is calculated from a linear elastic (uncracked) model as the avarage value of the moment for design of the flexural reinforcement over the width of the support strip. [9]

Level IV approximation

MC2010 suggests that *"The rotation can be calculated on the basis of a nonlinear analysis of the structure and accounting for cracking, tension stiffening effects, yielding of the reinforcement and any other nonlinear effects relevant for providing an accurate assessment of the structure"*. [9]

3.4 Comparison of methods

A Mathcad file was created for fast comparisons between guidelines regarding the punching capacity for different fibre content and amount of bending reinforcement. Except for fibre content and amount of bending reinforcement the user can also set compression (pre-stressing) force, column width and concrete cover. Here, in all calculations, the later input variables will remain constant. After selecting desired input variables, the program will calculate the punching capacity for the slab as a function of the slab thickness. A draft from the Mathcad file is shown in Figure 3.15. Figure 3.16 illustrates the resulting LD curves. To illustrate the improvement in punching resistance with increased fibre content, the punching capacity curve according to EC2 for a corresponding concrete slab with no fibres is plotted as a dotted red line in Figure 3.16. For a complete draft of the Mathcad file and all LD curves, see Appendix 4 respectively Appendix 5.

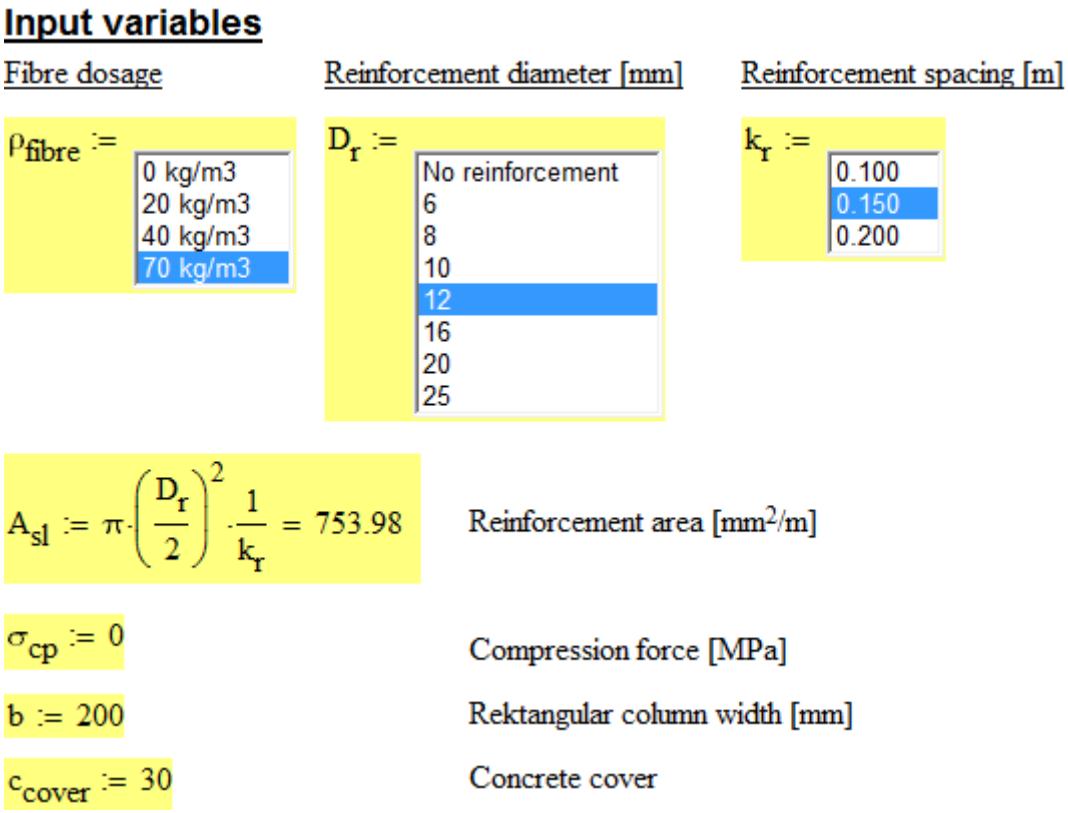

Figure 3.15. Screen view of input variables in Mathcad.

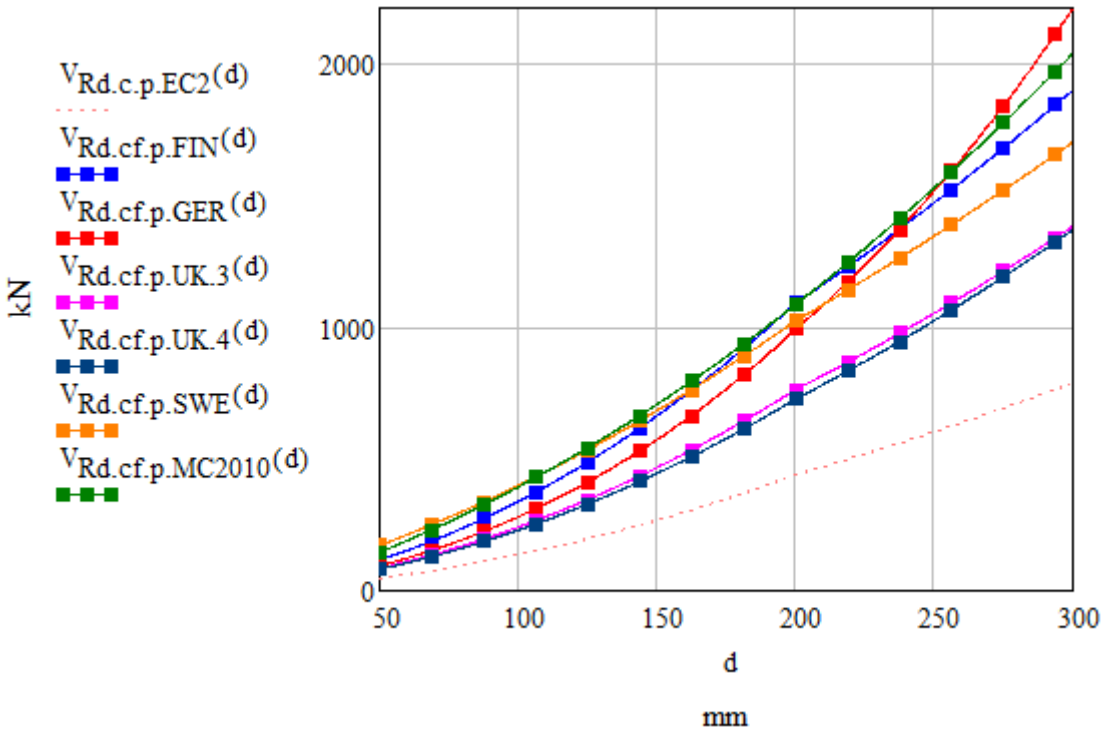

Figure 3.16. Punching capacity for SFRC70 ⌀12 c/c 150.

Abbreviations used are:

- EC2 – Eurocode EN 1992-1-1
- FIN – Finland, BY 56
- GER – Germany, DAfStb
- UK3 – United Kingdom, TR 34 third edition
- UK4 – United Kingdom, TR 34 fourth edition
- SWE – Sweden, SS 812310:2014
- MC2010 – fib Model Code for concrete structures 2010

Laboratory test results from a four point bending test that was performed in January 2015 for three different fibre dosages are used as reference in this thesis. The test setup from the bending test is illustrated in Figure 3.17. The target dimension of the beam was 150 ×150 × 700 and it is simply supported where the distance between the supports was 600 mm. The fibre type is Hendix Prime 75/52 and the three dosages that were tested were 20, 40 and 70 kg/m^3. Hereafter, these dosages will be referred to as SFRC20, SFRC40 and SFRC70 respectively.

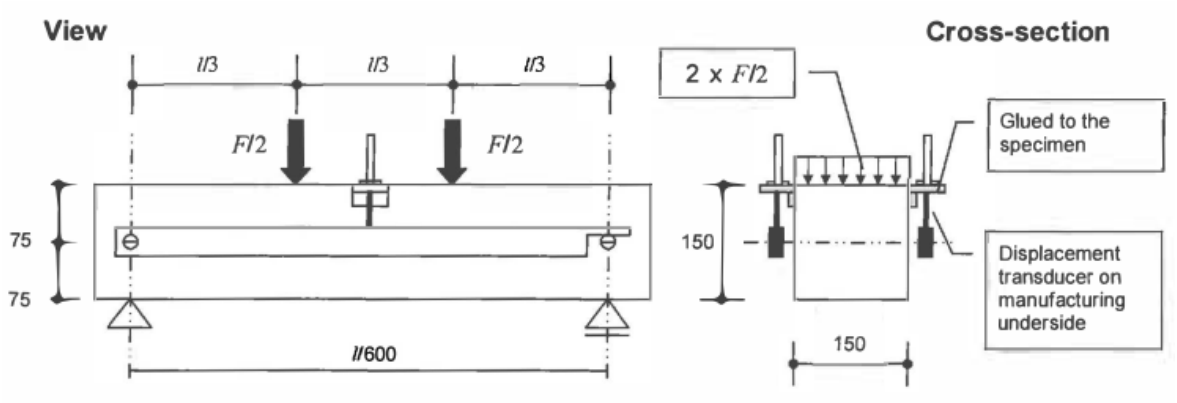

Figure 3.17. Four point bending test setup. [6]

About half of the previous guidelines use three point bending test and the other half four point bending test for determining the residual tensile strength values for FRC. Since the reference test results used in this thesis are from a four point bending test the reference test results had to be transformed so that calculations according to guidelines using three point bending test could be performed as well. To do that, the deflection values from the reference test results was transformed into corresponding CMOD values using Table 3.4 and with the principle illustrated in Figure 2.8.

Table 3.4. Relationship between CMOD and δ [26]

CMOD (mm)	***δ*** (mm)
0,05	0,08
0,1	0,13
0,2	0,21
0,5	0,47
1,5	1,32
2,5	2,17
3,5	3,02
4,0	3,44

To clarify, to obtain the value of, e.g., F_3, a line is drawn upwards at position 2.17 mm on the x-axis ($CMOD_3$ = 2.5 mm → δ = 2.17 mm). Then, at the intersection of the LD curve, a line is drawn parallel to the x-axis until it crosses the y-axis. After this, its corresponding residual flexural tensile strength value ($f_{R,j}$) could be determined using Eq. (1). This is not a standardised or accepted method and it is only done here to be able to make preliminary approximations according to standards in favour of three point bending test. Table 3.5 summaries the F_j-values from the reference laboratory test and Figure 3.18 illustrates how the F_j-values are obtained.

The guidelines of which the R-values are provided from the test results are the German (DAfStb) and British (TR 34 3rd edition) guidelines. Since the Finnish guideline (BY 56) uses the concept of virtual fibres it is possible to use that standard as well. Calculations according to the other guidelines (TR 34 fourth edition (UK4), SS 812310 (Sweden) and Model Code 2010) are considered unreliable since the R-values were determined using the method as described above.

Table 3.5. Summary of F_j-values (in Newton)

	$CMOD_1$	**$CMOD_2$**	**$CMOD_3$**	**$CMOD_4$**
SFRC 20	17500	17700	16700	14900
SFRC 40	28500	27500	24900	21000
SFRC 70	45800	50000	44800	37300

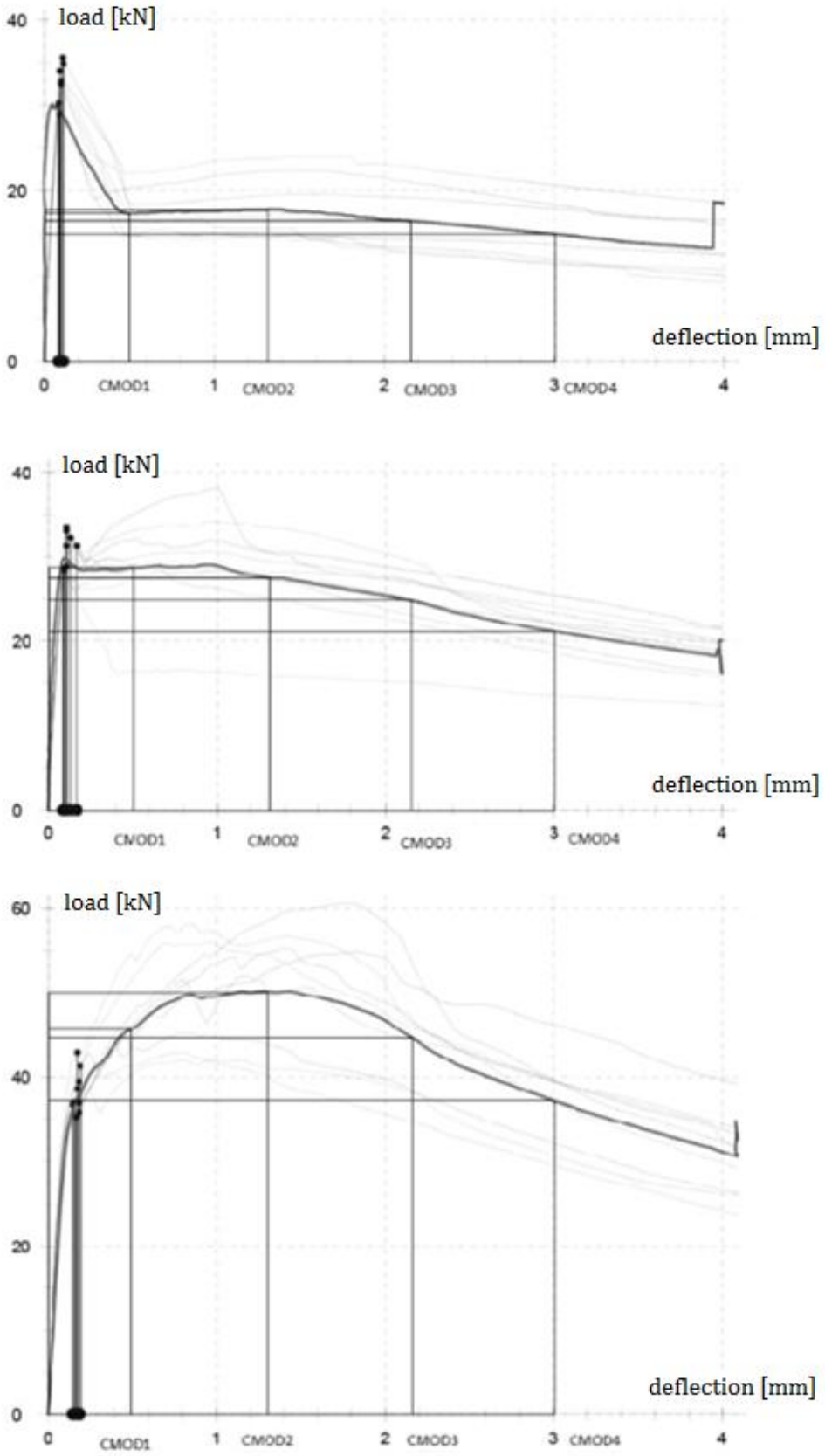

Figure 3.18. Load-deflection curves from the reference test results and their corresponding F_j-values. Top: 20 kg/m3, middle: 40 kg/m3 and bottom: 70 kg/m3 fibre content. Grey curves: test results. Black curves: mean values.

4 Non-linear finite element simulation

4.1 Introduction to non-linear analysis

Numerical simulation is a powerful tool for solving complex non-linear structural problems. It is sometimes an alternative to physical laboratory testing, since the simulation is not limited by the size of the structure, amount of loads or load cases and testing facilities. Numerical simulations do not give exact same results as physical tests and the results must therefore always be reviewed critically. However, by using numerical methods, it is possible to predict the structural behaviour under different type of loading and environmental conditions.

When using non-linear analysis, the typical situation is that the software introduces some advanced material model, which divides the non-linear analysis into incremental segments. The solution is an iterative predictor-corrector process, which is stopped when the difference between the predictor and the corrector is in acceptable tolerance. The process, which is illustrated in Figure 4.1, starts with the predictor (point 1), in which the solution is estimated by linear analysis based on tangent or initial material stiffness D. The corrector (point 2) then improves the the solution based on non-linear constitutive law F. [9]

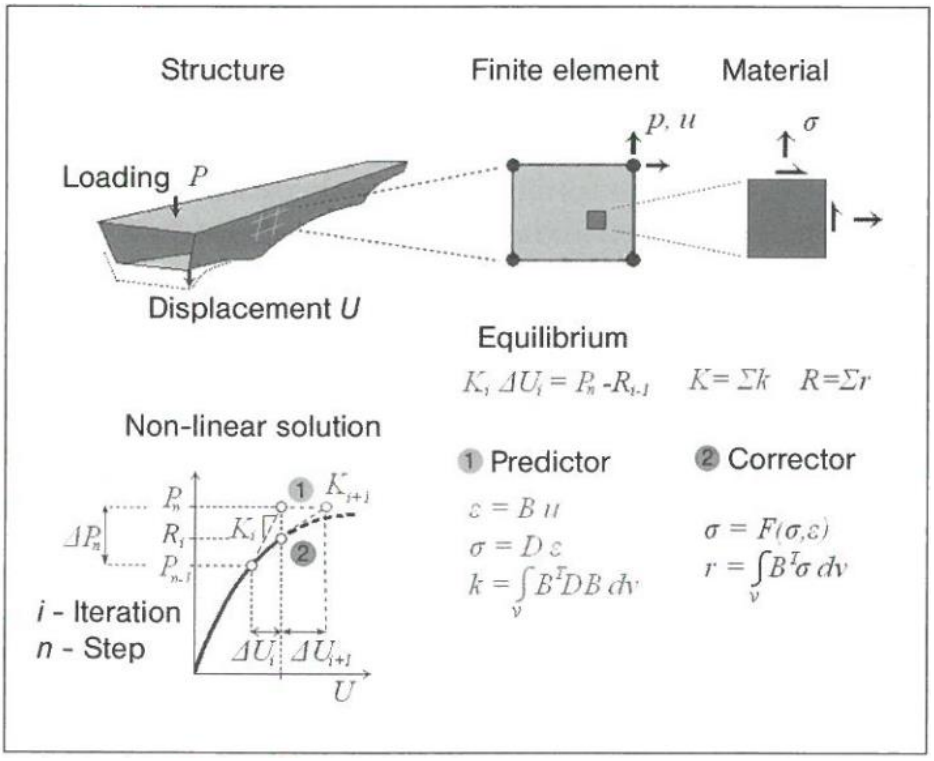

Figure 4.1. Typical algorithm for non-linear element analysis. [9]

There are several FEM software products available today. Here a software named ATENA 3D (version 5.3.4.13272) will be used. ATENA, which is developed by Červenka Consulting is a software for non-linear FEM analysis that is specially designed for concrete and it is, according to the developer, able to simulate the real structural behaviour both RC and SFRC, including concrete cracking, crushing and reinforcement yielding. Furthermore, the software supports dynamic, static, thermal and moisture analysis.

4.2 Determination of the material parameters for steel fibre reinforced concrete

Before simulating a punching test for FRC the material parameters for the given fibre type must be defined. Since there is no predefined list of different fibre types in ATENA the user will need to define the material parameters himself so that they are similar enough to the desired fibre type. There are two possible methods to do this. The first method is manual inverse analysis (which is used here) and the other is by using a program called Consoft. The chapter that describes how to determine the material parameters with Consoft is at the time of writing still under construction in [44] and will therefore not be investigated.

To perform an inverse analysis the user needs test results from an either three or four (recommended) point bending test. The test setup shall be replicated in ATENA (in pre-processor mode) and the user will have to adjust the material parameters until the load-deflection (LD) curve from the simulated bending test resembles the LD curve from laboratory test. Once the material parameters are defined the punching test can be modelled and the material parameters from the simulation are inserted.

When replicating the laboratory test, for symmetrical reasons, only half of the beam was modelled where the right surface is fixed in x-direction (Figure 4.2). Furthermore, the loading points are made wider than in the actual tests not to risk that the stress concentration at the loading points will be too high and cause simulation errors.

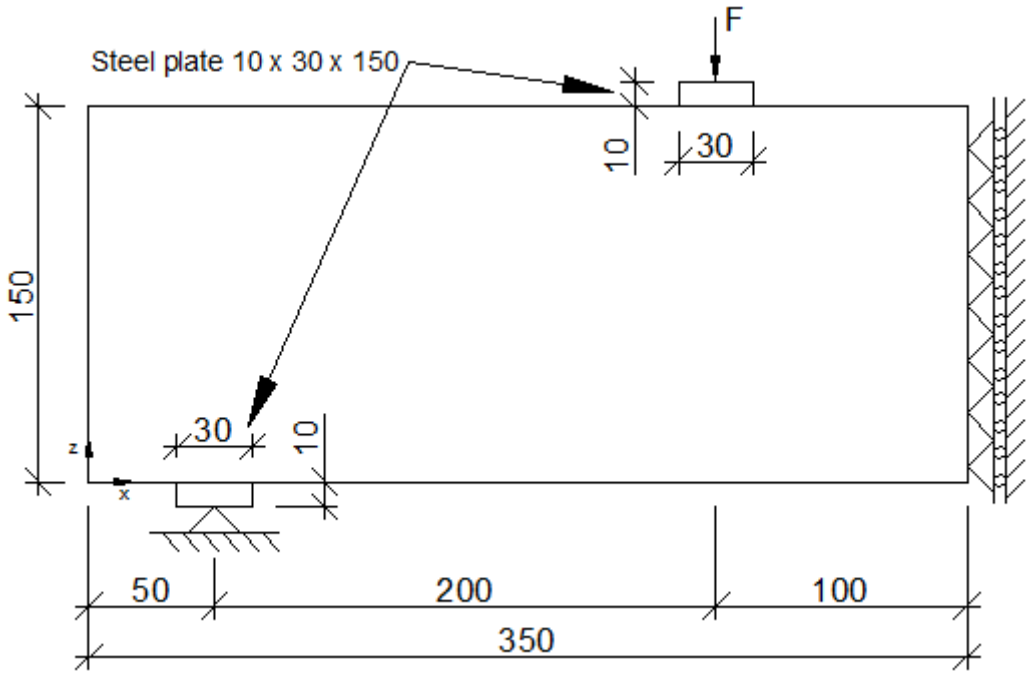

Figure 4.2. Four point bending test simulation setup. Dimensions in mm.

In ATENA, it is possible to create different mesh types for each macro-element. There are four different mesh options to choose from: brick, tetra, extrude or a combination of brick and tetra. Here, brick mesh with size 25 mm × 30 mm × 25 mm (x, y, z) was used for the beam. Because of the small size of the supports (10 mm × 30 mm × 150 mm), tetra type was

chosen for them. A monitoring point was added on the top loading point to measure the applied load and at the middle right to measure the deflection. For each load step the load was set to increase at a rate of 0.1 mm in the vertical direction. In Figure 4.3 the FEM mesh is illustrated to the left and support conditions and monitoring points to the right

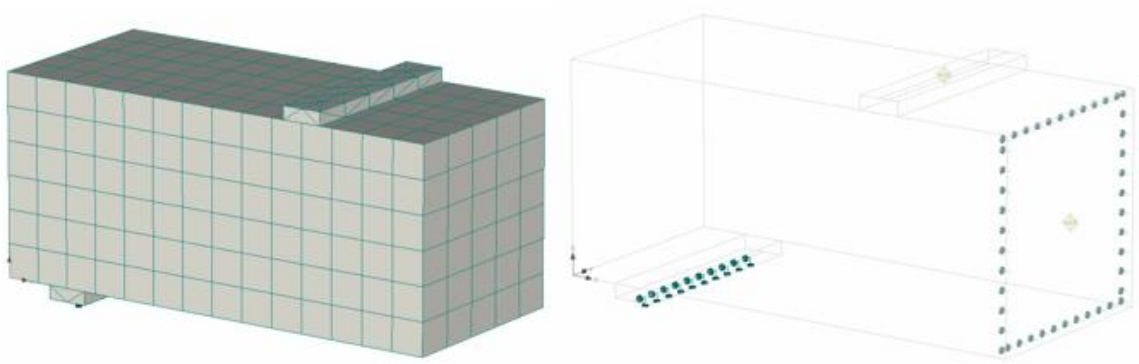

Figure 4.3. FEM mesh to the left. Supports and monitoring points to the right.

There are two different iteration solution procedures to choose from in ATENA: the Newton-Raphson (N-R) method and arc length (AL) method. In short, the N-R method keeps the load increment unchanged and iterates displacements until equilibrium is satasfied within the given tolerance. The AL method on the other hand keeps the solution path constant and iterates both increasement of displacement and forces. If the force is increased up to failure (or further) then the AL method is recommended. In all other situations (e.g., displacement control), N-R is recommended and was therefore chosen here [45]. Figure 4.4 shows the solution parameters used in all simulations. For more information about the solution methods the author refers to ATENA program documentation [46].

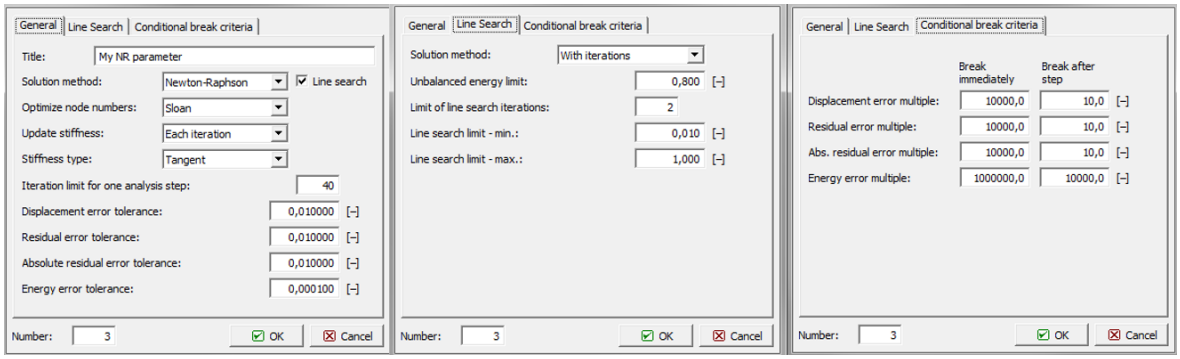

Figure 4.4. Screen view of solution parameters.

After the bending test setup was modelled the process of determining the material parameters started. Different material types in ATENA are listed in Figure 4.5. The material type that shall be used for SFRC is the "3D Nonlinear Cementitious 2 User", which is a type that allows a user definition of some material laws.

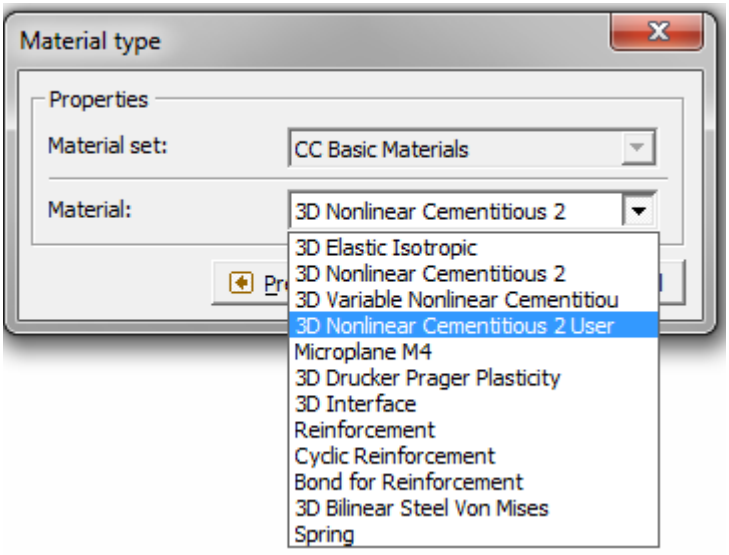

Figure 4.5. Screen view of ATENA material type options.

The key material parameters for SFRC are the tensile strength, tension function, compressive function and the compressive strength reduction due to cracking function. The tensile strength is given by:

$$F_t = \frac{F_{max}\, l}{bh^2} \tag{43}$$

where F_{max} is the load corresponding to the tensile strength (first peak in the LD diagram), l is the span length (600 mm), b is the beam widht (150 mm) and h the beam height (150 mm).

Setting the compressive function and the compressive strength reduction due to cracking function is done based on the experience of the developers of the software. The compressive function is modified so that the first point is moved 100 times due to the fact that FRC has higher ductility in compression than ordinary concrete (Figure 4.6). The compressive strength reduction due to cracking function is modified so that it has a constant value of 1 (Figure 4.7).

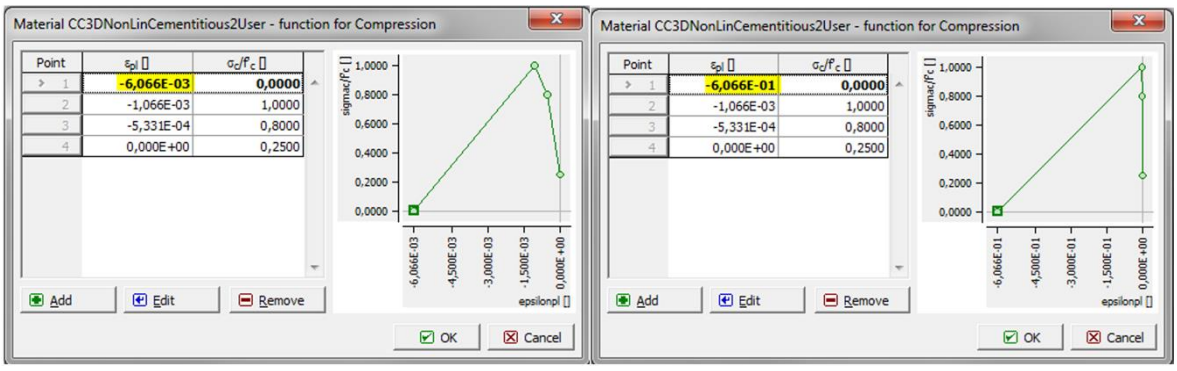

Figure 4.6.Screen view of the compressive function. Right: adjusted function.

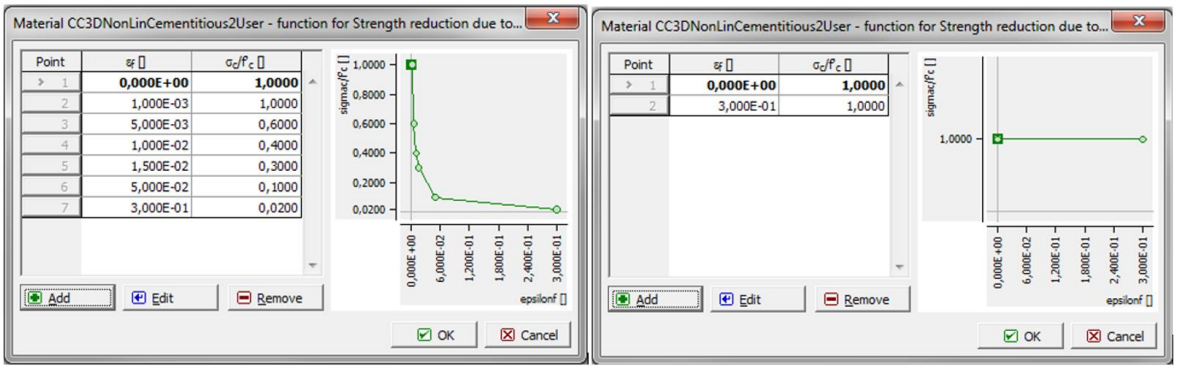

Figure 4.7. Screen view of the compressive strength reduction due to cracking function. Right: adjusted function.

Once these three parameters/functions are set, the user may run the simulation. In ATENA the results from the simulation are checked in the post-processor. Here the user may study different properties for the specimen for each load step. One example can be seen in Figure 4.8, which illustrates the cracking (cracks not smaller than 1.0 mm) in the SFRC20 specimen after load step 40.

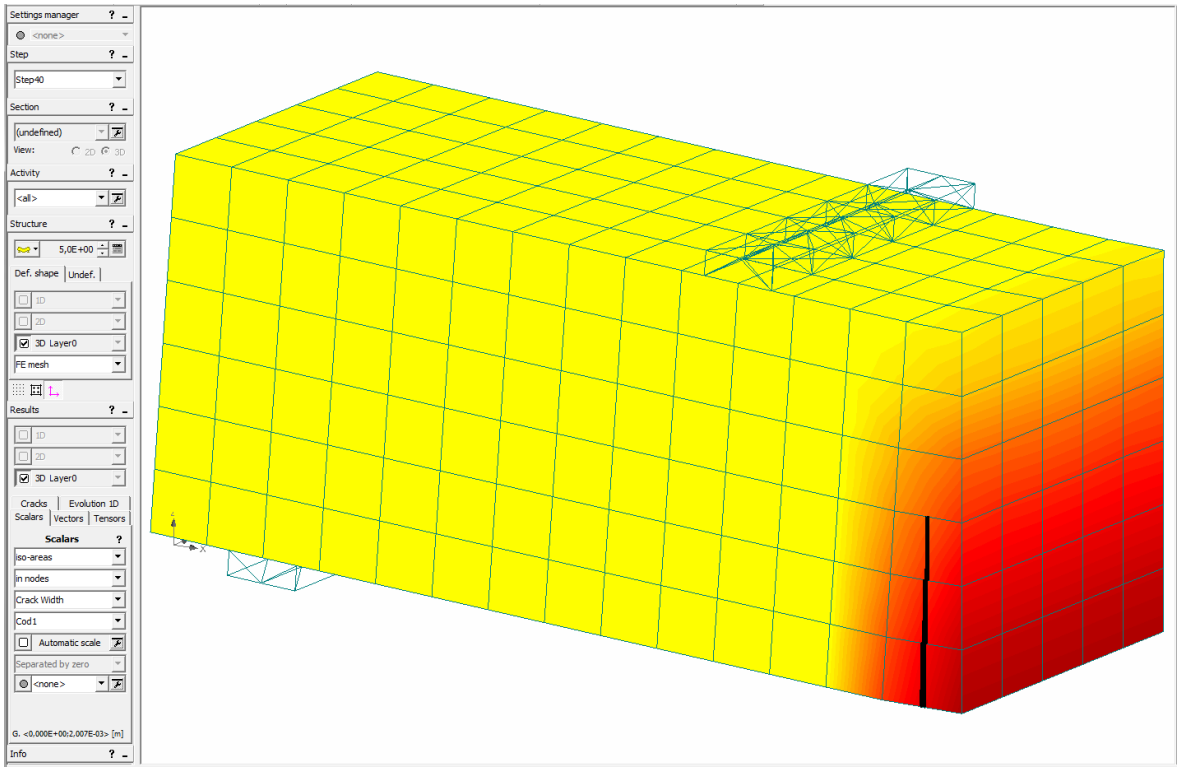

Figure 4.8. Crack pattern from a four point bending test simulation.

From the post-processor the user may transfer the LD data into a spreadsheet and there the LD graph is plotted and compared with the LD curve from the laboratory test. Hereafter, the last key parameter, the tension function (default tension function is shown in Figure 4.9), will be adjusted until the LD curves are similar enough. The other key parameters will not be adjusted anymore. How to adjust the tension function is described in Reference [44] and the process is illustrated in Figure 4.10, which demonstrates how the simulation result, after adjusting the tension function, got closer to the laboratory test result.

Note that there is a big scatter in the reference test results [47] and here the aim was to replicate the mean curve (red curve).

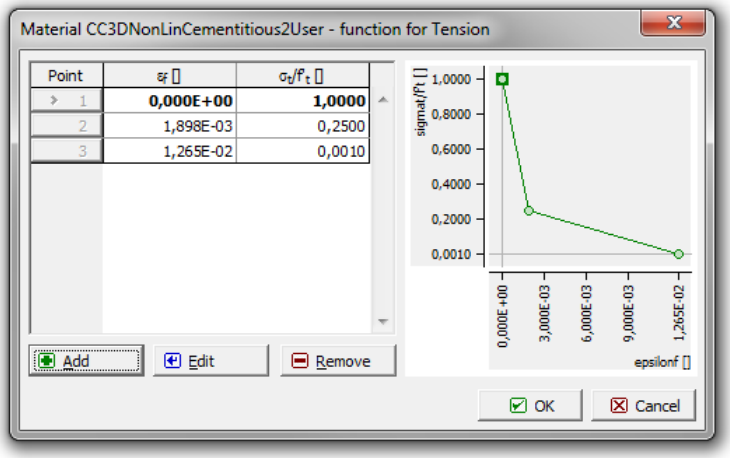

Figure 4.9. Screen view of default tension function for 3D Nonlinear Cementitious 2 User (f_{cu} = 45 MPa).

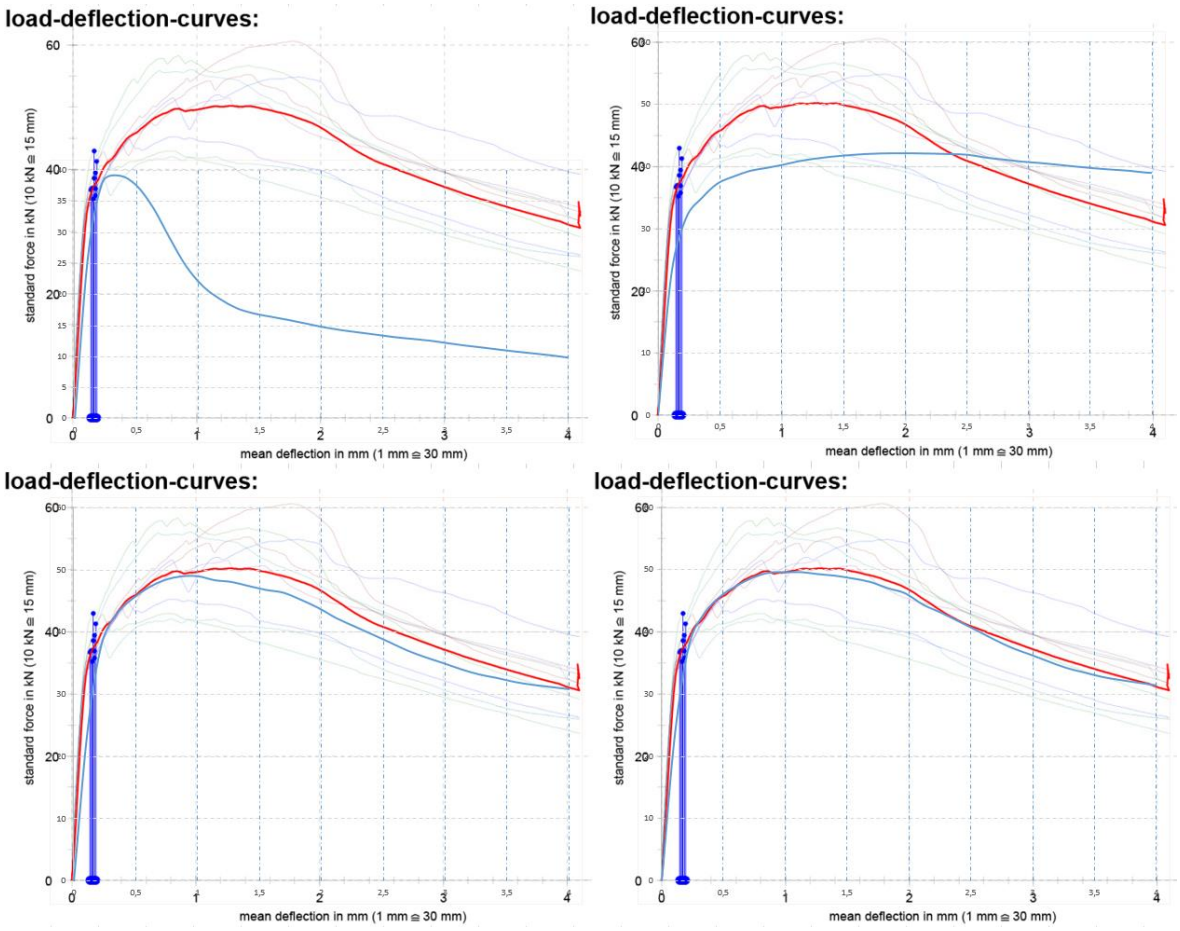

Figure 4.10. Modification of tension function for SFRC70. Red curve: reference test result [47]. Blue curve: simulations.

Figure 4.11 illustrates the final tension function and resulting LD curve for each fibre content. It is notable that the initial slope for each curve, which is determined by the modulus of elasticity, is not as steep as the reference curves. Instead of guessing a value for the modulus of elasticity, and risk overestimating its value, the author chose to use a mean value from the reference data.

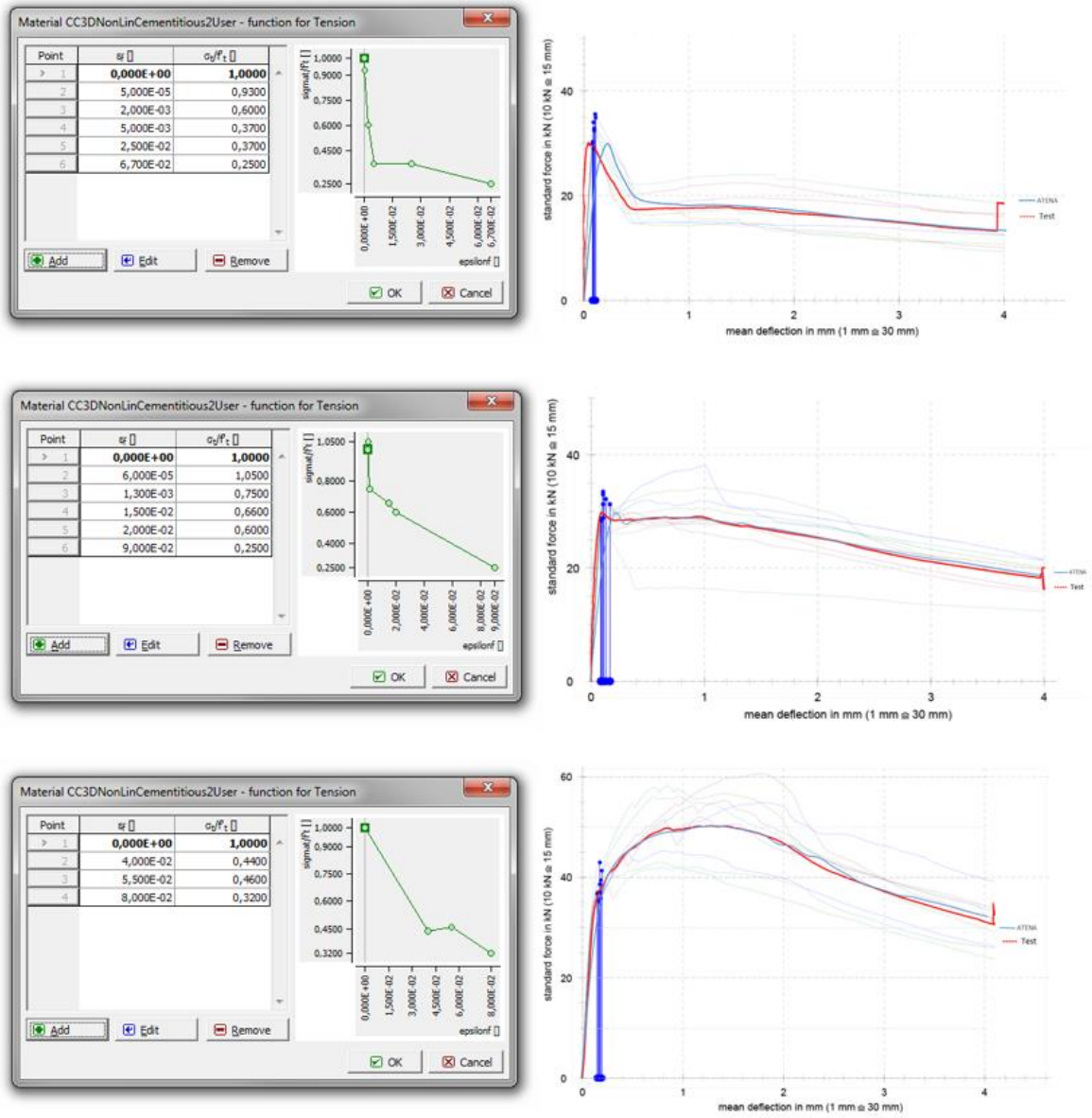

Figure 4.11. Tension functions and corresponding load-deflection curves for C30/37 containing different amount of Hendix prime 72/52 steel fibres. Fibre contents: Top: 20 kg/m^3, middle: 40 kg/m^3, bottom: 70 kg/m^3.

Another parameter that should be mentioned that was not modified is the shear function. The shear function influences the punching behaviour of the slab but to be able to modify the shear function one would need data from a shear test for the corresponding fibre, which does not exist in this case. However, a test simulation was performed to examine how the shear function influences the punching behaviour. The shear function was modified according to

the intuition of the author (see Figure 4.12). From Figure 4.13 it can be concluded that such modification has big impact on the post-peak behaviour of the slab and also seem to slightly increase its maximum capacity. Though, since there is no information about the shear behaviour the author uses the default shear function for 3D Nonlinear Cementitious 2 User in his simulations. For a complete list of input parameters see Appendix 2.

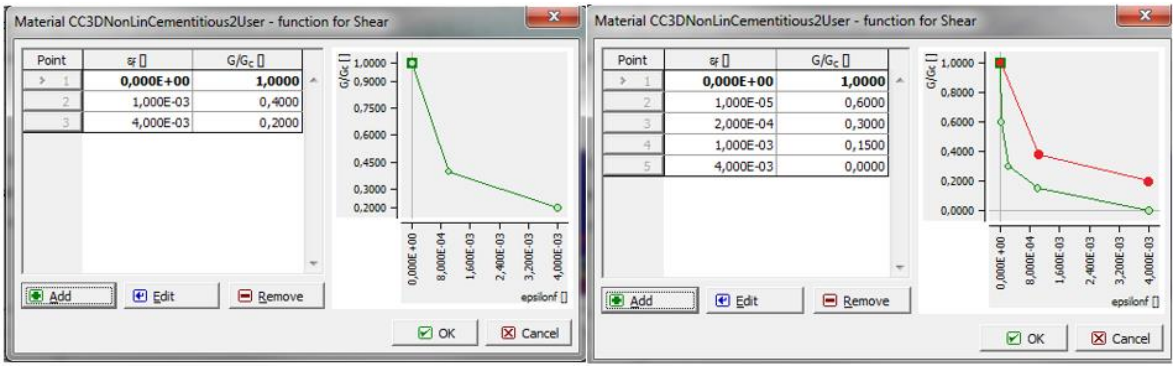

Figure 4.12. Screen view of modified shear functions. Left: modified shear function, right: modified shear function (red curve) and default shear function (green curve).

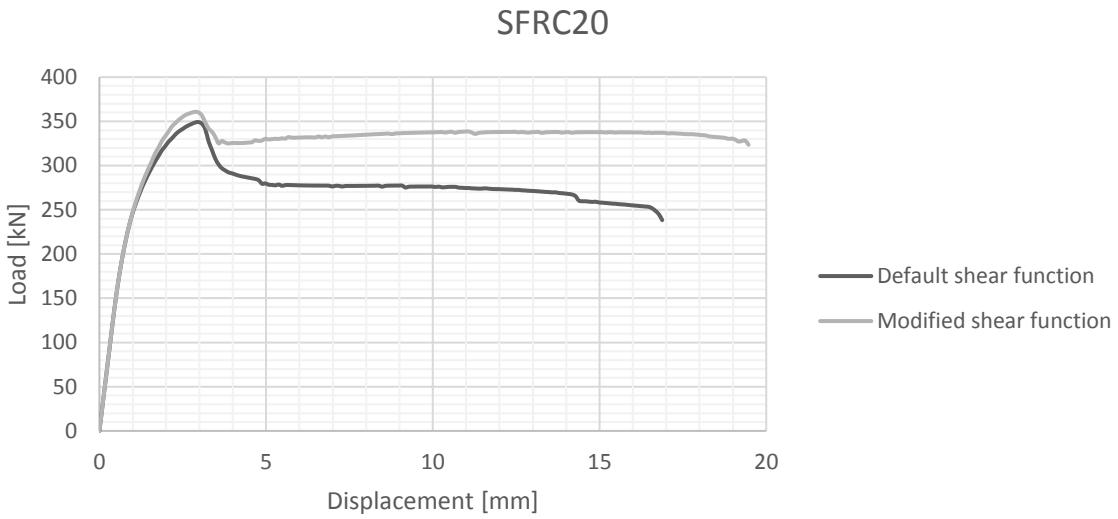

Figure 4.13. Comparison of default and modified shear function for SFRC20.

In 2006, Öman and Blomkvist [48] investigated how other parameters affect the simulation results. They simulated the punching behaviour for reinforced concrete slabs with various amount of reinforcement in ATENA and compared the simulation results to laboratory test results that were performed by Carl Erik Broms in the end of 1980s. In their thesis (Section 6.3) they perform a parameter study where they investigate how different parameters affect the simulation results. A summary of their conclusions is listed in Table 4.1.

Table 4.1 Influence of parameters on the simulation result according to [48]

Parameter	Impact on the result
Mesh size	Big
Tensile strength	Moderate
Compression strength	Moderate
Fracture energy* (tension function)	Big
Modulus of elasticity	Moderate
Critical compressive displacement, W_d*	None
Plastic strain at compression strength, ε_{cp}*	None
Multiplier for the plastic flow dir., β	None
Bond for reinforcement	Very small

**** For "3D Nonlinear Cementitious 2 User" material these parameters are adjustable as functions. I.e., not constants.***

From the parameter study one can conclude that the two main parameters are the mesh size and fracture energy. In this thesis the tension function is determined as a function of the fracture energy and it is already concluded that it has a big impact on the results (Figure 4.10). In the beginning of this section it is stated that the tensile and compression strength are significant parameters, which is partly confirmed by Öman and Blomqvist [48]. It was also stated earlier that the modulus of elasticity impacts the slope of the LD curve and that is as well confirmed by Öman and Blomqvist [48]. (see Figure 4.14). Other parameters (Critical compressive displacement (W_d), Plastic strain at compression strength (ε_{cp}), Multiplier for the plastic flow dir. (β) and Bond for reinforcement)) have no or very small impact on the results according to Öman and Blomqvist [48].

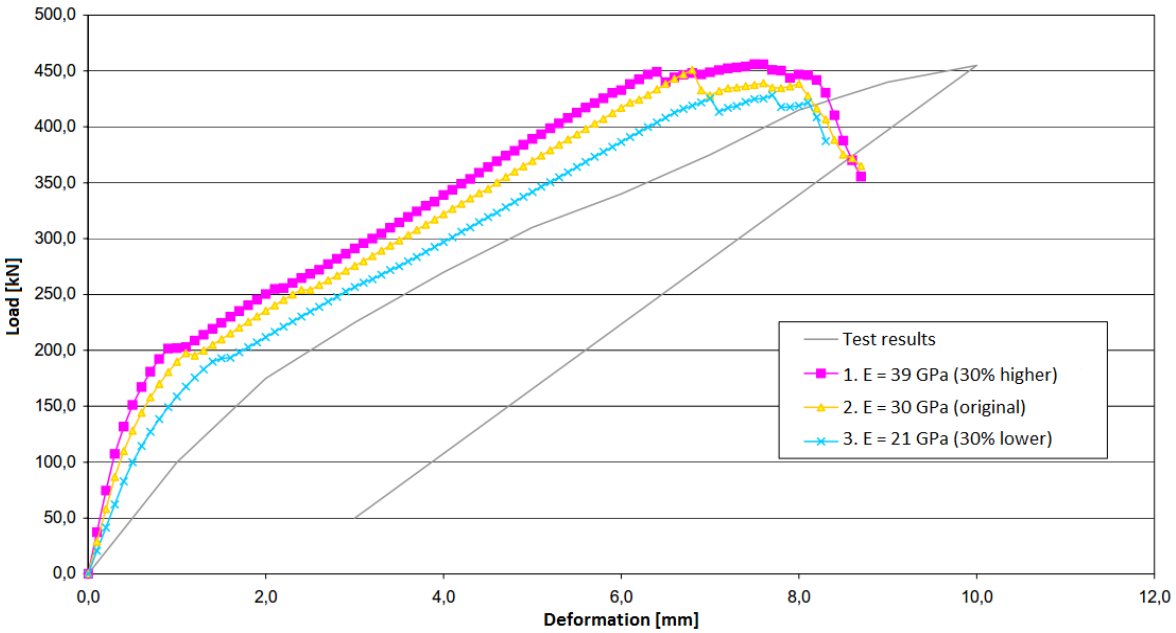

Figure 4.14. Influence of the modulus of elasticity on the LD curve. Yellow curve: E = 30 GPa, purple: E = 39 GPa (+30%), blue: E = 21 GPa (-30%).Modified from [48].

4.3 Punching simulation model setup

All in all 18 different slabs were simulated with various combinations of thickness, fibre content and reinforcement bars. Their properties are listed in Table 4.2.

Table 4.2. Properties of simulated slabs

	Specimen	Reinforcement diameter [mm] / spacing[mm]	Thickness, h [mm]
1	SFRC20		150
2	SFRC40		150
3	SFRC70		150
4	SFRC20 ⌀8 c/c 150	8 / 150	150
5	SFRC40 ⌀8 c/c 150	8 / 150	150
6	SFRC70 ⌀8 c/c 150	8 / 150	150
7	SFRC20 ⌀12 c/c 150	12 / 150	150
8	SFRC40 ⌀12 c/c 150	12 / 150	150
9	SFRC70 ⌀12 c/c 150	12 / 150	150
10	SFRC20		200
11	SFRC40		200
12	SFRC70		200
13	SFRC20 ⌀8 c/c 150	8 / 150	200
14	SFRC40 ⌀8 c/c 150	8 / 150	200
15	SFRC70 ⌀8 c/c 150	8 / 150	200
16	SFRC20 ⌀12 c/c 150	12 / 150	200
17	SFRC40 ⌀12 c/c 150	12 / 150	200
18	SFRC70 ⌀12 c/c 150	12 / 150	200

The punching simulation setup is inspired by the test setup by Barros et al. [12]. The slab measures 2600 × 2600 × d mm^3 and is supported in vertical direction by 12 steel plates (80 × 80 × 10 mm^3) at a radius of 1000 mm from the centre of the slab. The load is applied on a 200 × 200 × 50 mm^3 steel plate that is located in the bottom centre of the slab. In those slabs provided with bending reinforcement, the top reinforcement bars are located at a 30 mm distance from the top surface. The principal test setup is illustrated in Figure 4.15.

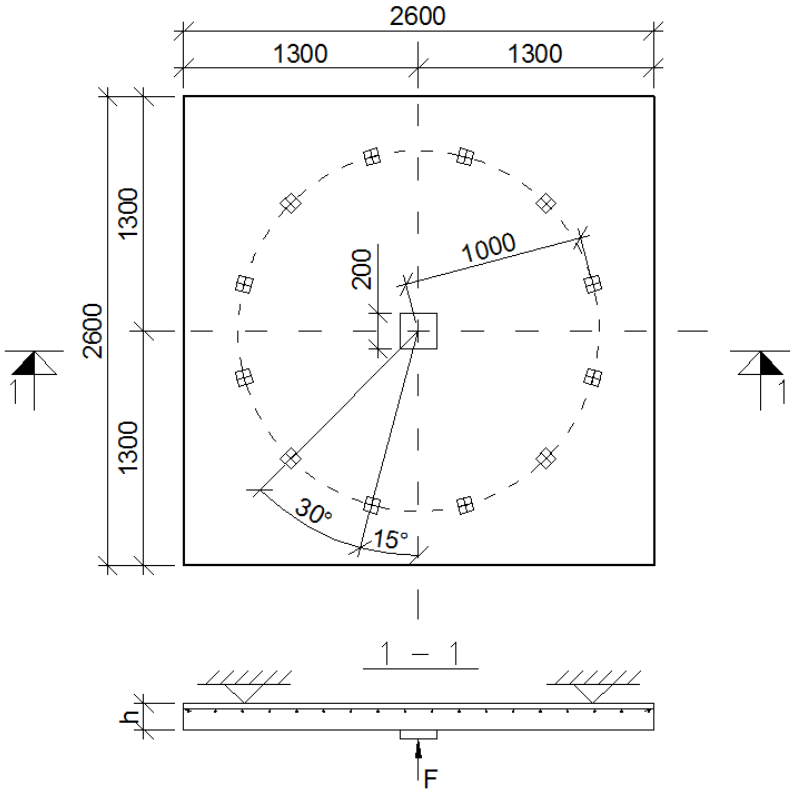

Figure 4.15. Punching test setup. Dimensions in mm.

For symmetrical reasons only one quarter of the slab is modelled and the size of the FEM mesh elements for the slab measures 50 mm × 50 mm × 25 mm (x, y, z) resulting in six elements in z-direction for the 150 mm slabs and eight elements for the 200 mm slabs (a minimum of 4-6 elements per thickness is recommended in the ATENA program documentation [49]). In total, the 150 mm slab consists of 4056 elements and the 200 mm slab of 5408 elements. The load is set to increase at 0.1 mm each load step and it is applied in the middle of the bottom steel plate and the deflection is measured in the bottom centre of the slab. Figure 4.16 illustrates the FEM mesh, supports and reinforcements for a 150 mm slab with bending reinforcement.

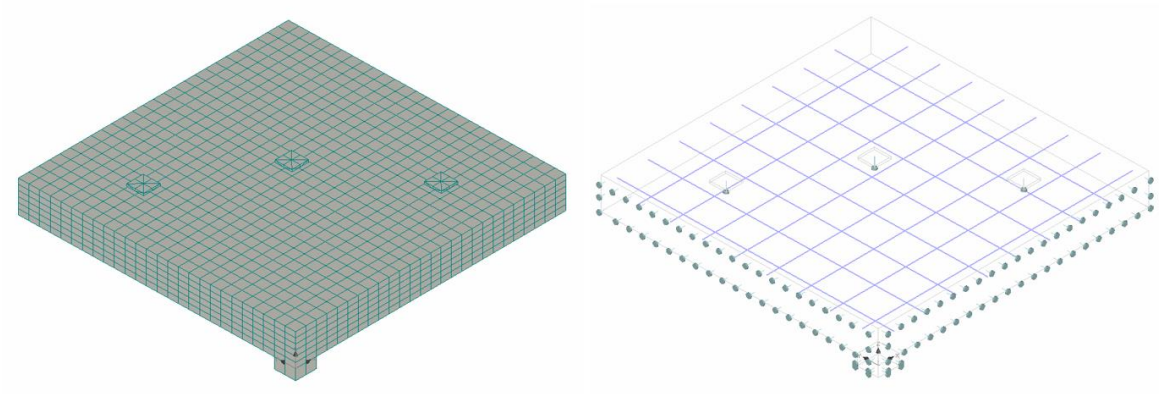

Figure 4.16. Left: FEM mesh. Right: Supports and reinforcement.

4.4 Punching simulation results

The results from the FEM simulation show some clear relationships in both the 150 mm and 200 mm thick slabs (see Figure 4.17 and Figure 4.18). It is evident that an increase in fibre content raises the punching capacity. Likewise, the amount of bending reinforcement also has a big impact on the punching capacity. Looking at Figure 4.17 and Figure 4.18, the graphs on the left side show how the capacity increases as the amount of bending reinforcement is kept constant. Likewise, the graphs to the right shows how the capacity increases when the fibre content is kept constant. The simulations were stopped at the point where the software could no longer fullfill the convergence criterias (convergence criterias are illustrated in Figure 4.4). The maximum punching capacity for each slab is summarised in Table 4.3.

Table 4.3. Summary of FEM results

Specimen	h = 150 mm	h = 200 mm
SFRC20	349.2 kN	600.4 kN
SFRC40	392.4 kN	682.0 kN
SFRC70	616.0 kN	1061.6 kN
SFRC20 ø8 c/c 150	406.8 kN	690.4 kN
SFRC40 ø8 c/c 150	496.8 kN	861.6 kN
SFRC70 ø8 c/c 150	709.6 kN	1216.4 kN
SFRC20 ø12 c/c 150	518.0 kN	928.0 kN
SFRC40 ø12 c/c 150	649.2 kN	1099.2 kN
SFRC70 ø12 c/c 150	924.8 kN	1422.8 kN

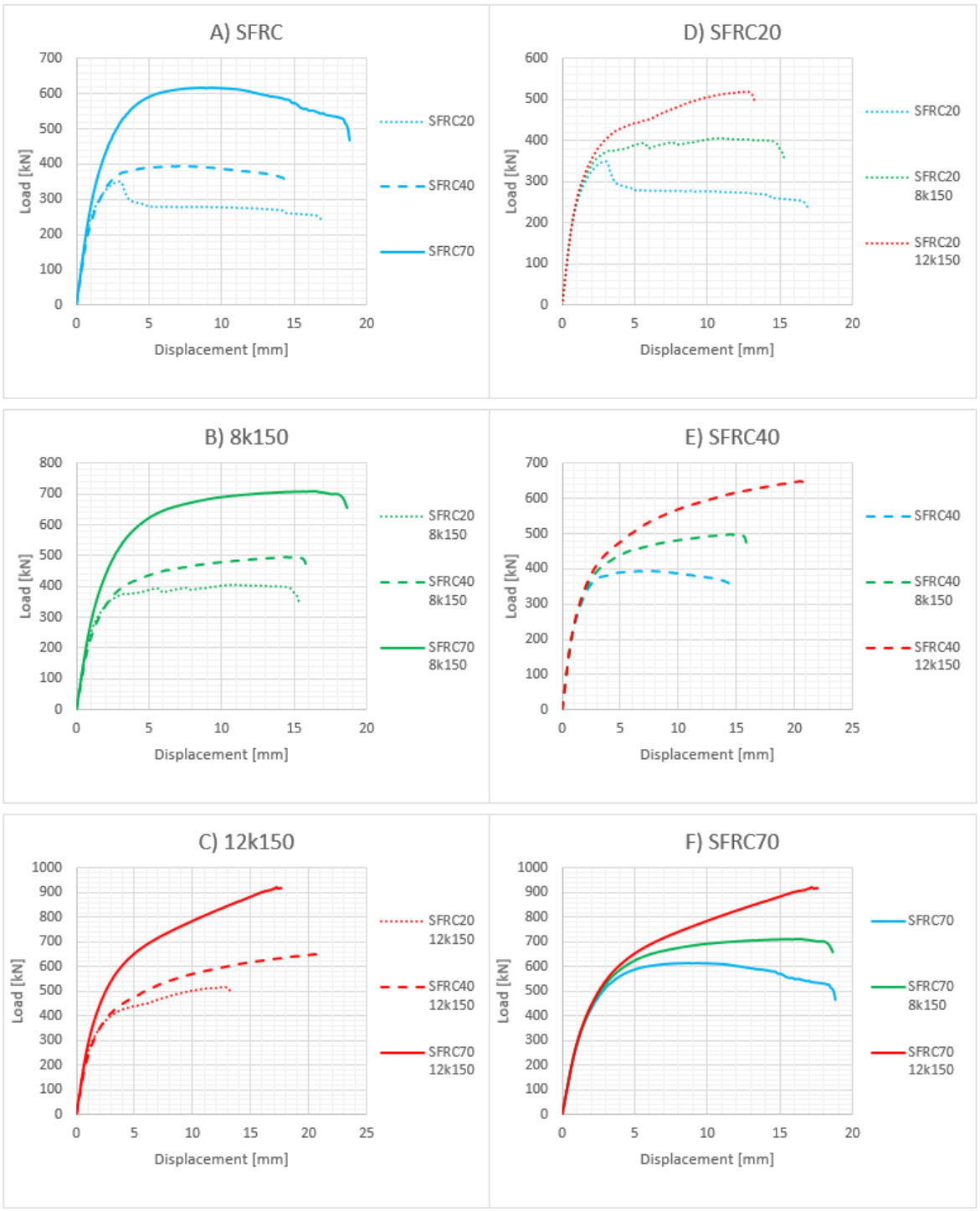

Figure 4.17. Load-deflection curves for 150 mm thick slabs. A: no bending reinforcement, fibre content varies. B: ⌀8 c/c 150 reinforcement, fibre content varies. C: ⌀12 c/c 150 reinforcement, fibre content varies. D: 20 kg/m3 fibre content, reinforcement varies. E: 40 kg/m^3 fibre content, reinforcement varies. F: 70 kg/m^3 fibre content, reinforcement varies.

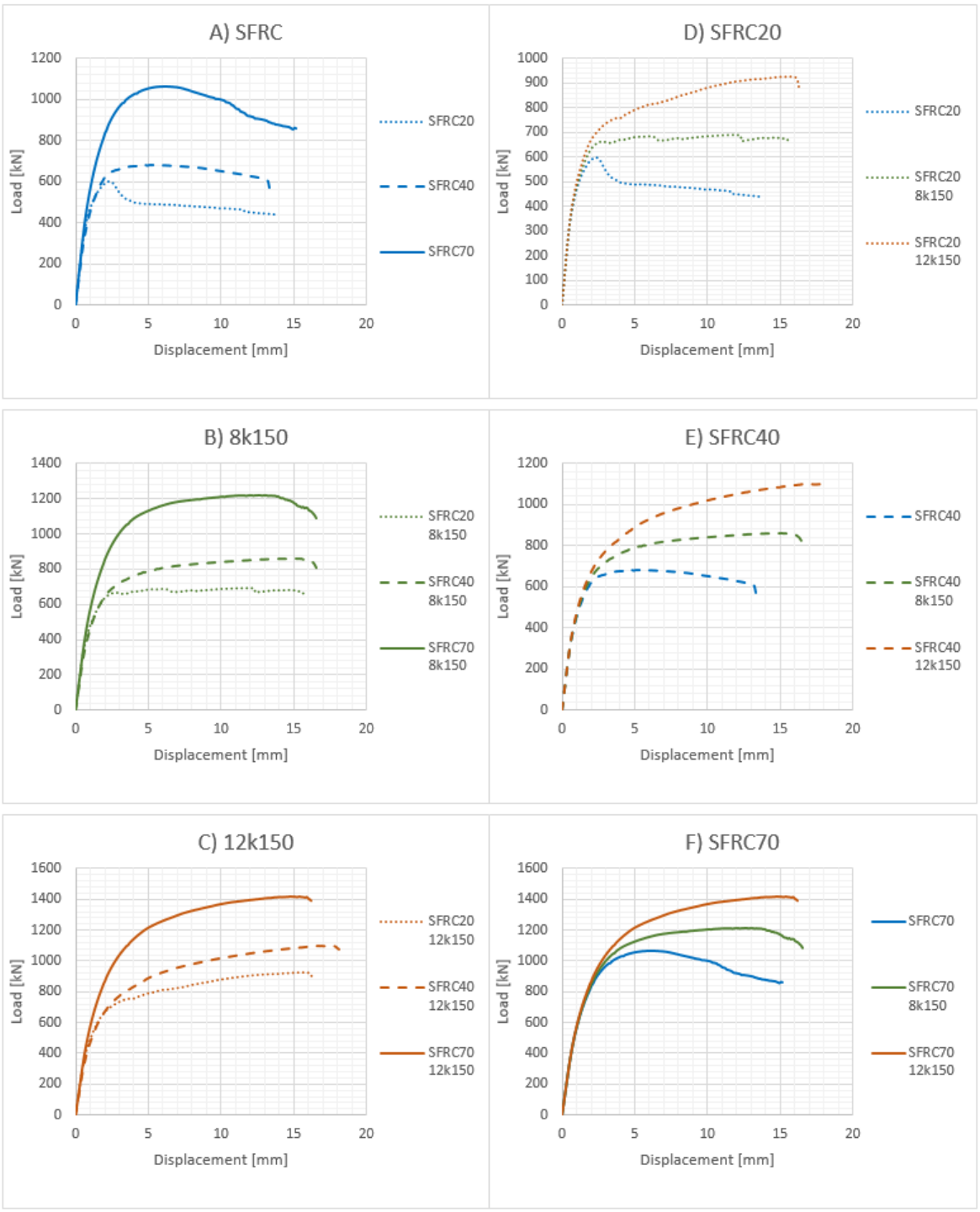

Figure 4.18. Load-deflection curves for 200 mm thick slabs. A: no bending reinforcement, fibre content varies. B: ⌀8 c/c 150 reinforcement, fibre content varies. C: ⌀12 c/c 150 reinforcement, fibre content varies. D: 20 kg/m3 fibre content, reinforcement varies. E: 40 kg/m^3 fibre content, reinforcement varies. F: 70 kg/m^3 fibre content, reinforcement varies.

5 Synthesis of results

5.1 Comparison between finite element simulation and guidelines

Table 5.1…Table 5.4 show the calculated punching values according to the standards in Section 3.3 and how much they differ from the FEM simulation results. Abbreviations used are the same as defined in Section 0, where the residual flexural strength value (R-value) for GER and UK3 are adopted directly from the reference test results and FIN assumes the R-value using the concept of virtual fibres from Table 3.1. The rest (UK4, SWE and MC2010) received their R-values by the approximation method described in Section 3.4. In other words, the guidelines in Table 5.3 and Table 5.4 use approximated R-values and therefore it is not possible to say how good the approximations according to these guidelines are.

Table 5.1. h = 150

Specimen	FEM [kN]	Punching capacity*					
		FIN		GER		UK3	
		[kN]	Error	[kN]	Error	[kN]	Error
SFRC20	349.2	429.2	22.9 %	391.2	12.0 %	256.6	-26.5 %
SFRC40	392.4	552.7	40.8 %	451.7	15.1 %	311.3	-20.7 %
SFRC70	616.0	662.9	7.6 %	572.7	-7.0 %	365.0	-40.8 %
SFRC20 ø8 c/c 150	406.8	429.2	5.5 %	391.2	-3.8 %	358.7	-11.8 %
SFRC40 ø8 c/c 150	496.8	552.7	11.3 %	451.7	-9.1 %	413.4	-16.8 %
SFRC70 ø8 c/c 150	709.6	662.9	-6.6 %	572.7	-19.3 %	467.1	-34.2 %
SFRC20 ø12 c/c 150	518.0	429.2	-17.1 %	391.2	-24.5 %	358.7	-30.8 %
SFRC40 ø12 c/c 150	649.2	522.7	-19.5 %	451.7	-30.4 %	413.4	-36.3 %
SFRC70 ø12 c/c 150	924.8	662.9	-28.3 %	572.7	-38.1 %	467.1	-49.5 %
Average			1.8 %		-11.7 %		-29.7 %
Standard deviation			20.8 %		17.1 %		11.3 %

Table 5.2. h = 200 mm

Specimen	FEM [kN]	Punching capacity*					
		FIN		GER		UK3	
		[kN]	Error	[kN]	Error	[kN]	Error
SFRC20	600.4	706.3	17.6 %	663.8	10.6 %	415.0	-30.9 %
SFRC40	682.0	860.1	26.1 %	773.2	13.4 %	503.4	-26.2 %
SFRC70	1061.6	1090.8	2.7 %	992.0	-6.6 %	590.2	-44.4 %
SFRC20 ø8 c/c 150	690.4	706.3	2.3 %	663.8	-3.9 %	587.6	-14.9 %
SFRC40 ø8 c/c 150	861.6	860.1	-0.2 %	773.2	-10.3 %	676.0	-21.5 %
SFRC70 ø8 c/c 150	1216.4	1090.8	-10.3 %	992.0	-18.4 %	762.8	-37.3 %
SFRC20 ø12 c/c 150	928.0	706.3	-23.9 %	663.8	-28.5 %	587.6	-36.7 %
SFRC40 ø12 c/c 150	1099.2	860.1	-21.8 %	773.2	-29.7 %	676.0	-38.5 %
SFRC70 ø12 c/c 150	1422.8	1090.8	-23.3 %	992.0	-30.3 %	762.8	-46.4 %
Average			-3.4 %		-11.5 %		-33.0 %
Standard deviation			17.0 %		15.7 %		9.9 %

Table 5.3. h = 150

Specimen	FEM [kN]	Punching capacity**					
		UK4***		SWE		MC2010****	
		[kN]	Error	[kN]	Error	[kN]	Error
SFRC20	349.2	231.9	-33.6 %	267.5	-23.4 %	205.4	-41.2 %
SFRC40	392.4	266.9	-32.0 %	379.9	-3.2 %	311.2	-20.7 %
SFRC70	616.0	342.6	-44.4 %	683.4	10.9 %	548.8	-10.9 %
SFRC20 ø8 c/c 150	406.8	334.0	-17.9 %	267.5	-34.3 %	374.2	-8.0 %
SFRC40 ø8 c/c 150	496.8	369.0	-25.7 %	379.9	-23.5 %	476.9	-4.0 %
SFRC70 ø8 c/c 150	709.6	444.7	-37.3 %	683.4	-3.7 %	714.5	0.7 %
SFRC20 ø12 c/c 150	518.0	334.0	-35.5 %	314.3	-39.3 %	363.5	-29.8 %
SFRC40 ø12 c/c 150	649.2	369.0	-43.2 %	379.9	-41.5 %	469.3	-27.7 %
SFRC70 ø12 c/c 150	924.8	444.7	-51.9 %	683.4	-26.1 %	706.8	-23.6 %
Average			-35.7 %		-20.5 %		-18.4 %
Standard deviation			9.6 %		17.0 %		12.9 %

Table 5.4. h = 200 mm

Specimen	FEM [kN]	Punching capacity**					
		UK4		SWE		MC2010****	
		[kN]	Error	[kN]	Error	[kN]	Error
SFRC20	600.4	375.1	-37.5 %	440.1	-26.7 %	307.8	-48.7 %
SFRC40	682.0	431.6	-36.7 %	569.0	-16.6 %	466.2	-31.6 %
SFRC70	1061.6	554.1	-47.8 %	1023.8	-3.6 %	822.1	-22.6 %
SFRC20 ø8 c/c 150	690.4	547.7	-20.7 %	440.1	-36.3 %	580.1	-16.0 %
SFRC40 ø8 c/c 150	861.6	604.2	-29.9 %	569.0	-34.0 %	739.6	-14.2 %
SFRC70 ø8 c/c 150	1216.4	726.7	-40.3 %	1023.8	-15.8 %	1094.5	-10.0 %
SFRC20 ø12 c/c 150	928.0	547.7	-41.0 %	523.0	-43.6 %	570.9	-38.5 %
SFRC40 ø12 c/c 150	1099.2	604.2	-45.0 %	585.6	-46.7 %	729.3	-33.7 %
SFRC70 ø12 c/c 150	1422.8	726.7	-48.9 %	1023.8	-28.0 %	1085.2	-23.7 %
Average			-38.6 %		-27.9 %		-26.6 %
Standard deviation			8.5 %		13.2 %		11.9 %

* *Residual tensile strength values from the test results*
** *Approximated residual tensile strength values*
*** *Slab thickness below recommended minimum slab thickness*
**** *Level of approximation 1*

First notable thing with the results is that the values in Table 5.1 and Table 5.2 are looping. This means that the contribution from the bending reinforcement is not taken into account. For UK3 the values for the fibre only slabs are lower than for the slabs with bending reinforcement but then for the slabs with bending reinforcement the values are looping. The explanation is that the guidelines in Table 5.1 and Table 5.2 suggest that the concrete contribution to punching resistance should be determined as in EC2 (Eq. (10)). Looking at Eq. (10), it suggest that the punching capacity is given by $V_{Rd,c} = C_{Rd,c}k(100\rho f_{ck})^{1/3}$ but it must have a minimum resistance of $v_{min} = 0.035k^{3/2}f_{ck}^{1/2}$ of which the later formula only takes into account the concrete compression strength and slab thickness. Since neither FIN nor GER clarifies how the concrete contribution shall be determined for slabs without bending reinforcement it is assumed that for slabs with no bending reinforcement the effective depth is equal to the total depth of the slab. I.e., the minimum punching capacity for concrete slabs is given by:

$$V_{Rd,c,min} = [v_{min} + k_1\sigma_{cp}]u_1 h \quad (44)$$

UK3 (and UK4) suggests that for slabs with no bending reinforcement the effective depth shall be taken as $d = 0.75h$. However, when bending reinforcement is added the effective depth is then calculated in the same way as in FIN and GER. Because of this assumption ($d = h$) $V_{Rd,c,min}$ is governing and bending reinforcement is not, according to the calculations, contributing to the punching resistance.

Table 5.5 shows how the calculated punching capacity for different cases of concrete slabs differs depending on which equation is used. It presents cases for both unreinforced (6.2.b) and reinforced (6.2a) slabs with different thicknesses and different ways of assuming the effective depth.

Table 5.5. Overview of calculated punching resistance for a concrete slabs according to Eurocode 2. Values in kN

Row	Formula (EC2)	Specimen, effective depth	Slab thickness		
			150 mm	200 mm	800 mm
1	**6.2.b**	**No reinforcement,** $d = h$	267.45	440.05	3745.03
2	**6.2.b**	**No reinforcement,** $d = d_{eff}$*	169.01	311.58	3482.58
			-36.81 %	-29.19 %	-7.01 %
3	**6.2.b**	**No reinforcement,** $d = 0.75h$	165.38	267.45	2327.42
			-38.16 %	-39.22 %	-37.85 %
4	**6.2.a**	**With reinforcement ⌀8 c/c 150,** $d = d_{eff}$**	147.79	239.91	1814.82
			-44.74 %	-45.48 %	-51.54 %
5	**6.2.a**	**With reinforcement ⌀12 c/c 150,** $d = d_{eff}$**	189.3	309.12	2369.27
			-29.22 %	-29.75 %	-36.74 %
6	**6.2.a**	**With reinforcement ⌀20 c/c 100,** $d = d_{eff}$**	258.19	480.71	3784.19
			-3.46 %	9.24 %	1.05 %

*$d_{eff} = h - 30 - 6$, ** concrete cover = 30 mm

In Table 5.5 the dark shaded areas show how much smaller/bigger the value is compared to the value in row 1. Row 6 is added to show approximately how much steel should be added for Formula 6.2.a to become governing. ⌀20 c/c 100 reinforcement equals 3141.59 mm^2/m steel. For a 150 mm thick slab, the maximum value for ρ $(= 0.02)$ is reached with 3000 mm^2/m steel, meaning that after adding 3000 mm^2/m of reinforcement the capacity will not increase anymore (according to EC2). The corresponding value for a 200 mm thick slab is 4000 mm^2/m. In other words, for 150 mm thick slabs Formula 6.2.b will always be governing regardless how much steel is put into the slab and therefore the results in Table 5.1 and Table 5.2 are looping, which in turn leads to relatively high standard deviations.

UK3 and UK4 show relatively similar results although they use different approaches for determining the R-value. Their average errors are relatively high but their standard deviation values are clearly the lowest. Notable is that in UK4, the recommended minimum design thickness for a pile-supported slab is 200 mm. For MC2010 (Table 5.3 and Table 5.4), only calculations according to LoA I was performed since the R-value is unreliable.

A looping behaviour is also present in SWE. Again, SWE has separate formulas for slabs with (Eq. 20) and without (Eq. 21) bending reinforcement, but when the fibre content is over approximately 40 kg/m^3 Eq. 21 becomes governing. The behaviours of Eq. 20 and Eq. 21 are illustrated in Figure 5.1.

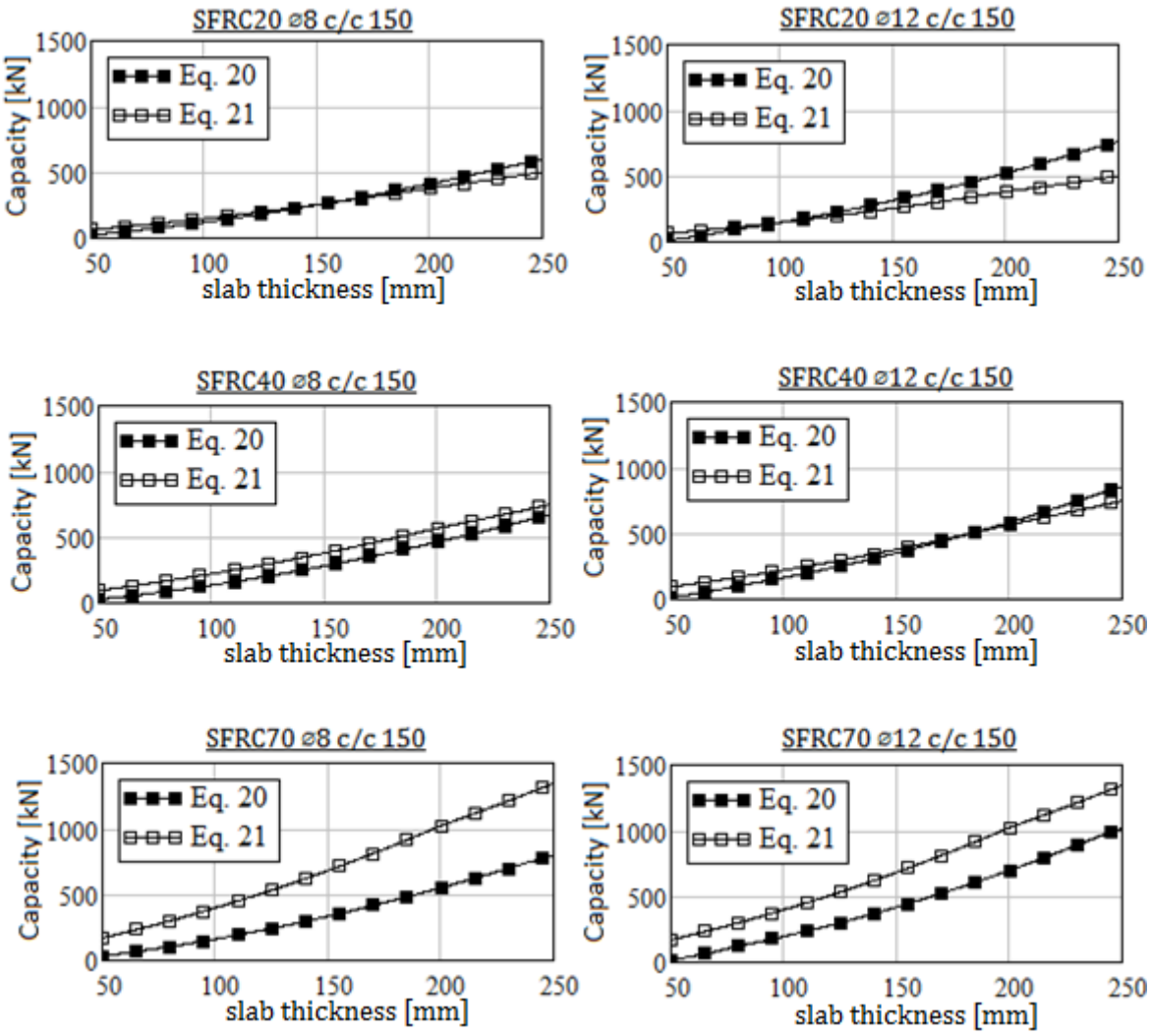

Figure 5.1. Behaviour of Eq. 20 and Eq. 21 for various fibre content and amount of bending reinforcement.

For fibre only slabs with 40 kg/m^3 of fibres (SFRC40) the calculated values are in general higher than for other fibre content. It is possible that the material parameters for SFRC40 are not determined as accurately as for SFRC20 and SFRC70. Though, the opposite is also possible, i.e., the material parameters for SFRC40 are more accurate than SFRC20 and SFRC70.

5.2 Alternative method based on finite element results

Since there are big differences between the reviewed guidelines an attempt was made to investigate if it is possible to establish an improved theoretical model that is based on the FEM results. To do this, some of the guidelines presented in Section 3.3 are combined with modifications with all partial factors neglected.

Two formulas were established and compared. The first formula (Karv1) is a combination of EC2, UK4 and GER. Karv1 adopts the concrete contribution for unreinforced concrete from UK4 which suggests that the effective depth for an unreinforced concrete slab should be taken as $0.75h$. I.e., the concrete contribution for a slab without bending reinforcement is given by Eq. (4) where $d = 0.75h$. If the slab is provided with bending reinforcement the concrete contribution is calculated as in Eq. (3). The fibre contribution is inspired by DAfStb (Eq. (26)) but it is modified so that the factor 0.85 is taken as 1 and the partial factor is removed. Also, the partial factor for concrete in Eq. (3) is neglected. Hence, the formula for punching capacity (without compression forces) according to Karv1 is given by:

$$V_{Rk.cf.p.Karv1} = [C_{Rd,c}k(100\rho f_{ck})^{1/3} + \alpha_c^f f_{ctR,u}^f]u_1 d \quad (45)$$

with a minimum of

$$V_{Rk.cf.p.Karv1} = v_{min}u_1 0.75h \quad (46)$$

where the value of $C_{Rd,c}$ is taken as 0.2 ($C_{Rd,c} = 0.18$ in EC2), k is a thickness dependent factor defined in Eq. (7), ρ is the reinforcement ratio (Eq. (8)) and f_{ck} is the concrete compression strength. $\alpha_c^f = 0.85$ is a factor taking into account long-term effects on the residual tensile strength of SFRC and $f_{ctR,u}^f$ is the calculated residual tensile strength of SFRC in ULS defined in Eq. (24). μ_1 is the length of the critical control parameter at a distance of $2d$ from the support (Figure 3.9) where d is the effective depth of the slab. h is the total thickness of the slab.

The second formula (Karv2) is similar to Karv. The difference is that here the fibre contribution is taken directly from UK3 instead of DAfStb. Hence, the punching capacity according to Karv2 is defined as:

$$V_{Rk.cf.p.Karv2} = [C_{Rd,c}k(100\rho f_{ck})^{1/3} + 0.12R_{e,3}f_{cbk}]u_1 d \quad (47)$$

with a minimum capacity defined in Eq. (46). $R_{e,3}$ is the equivalent flexural strength ratio for SFRC and f_{cbk} is the unreinforced concrete flexural strength defined in Eq. (16). Calculated values according to Karv1 and Karv2 and how they differ from the simulation results can be seen in Table 5.6 and Table 5.7.

Table 5.6. h = 150

Specimen	FEM [kN]	Punching capacity			
		Karv1		Karv2	
		[kN]	Error	[kN]	Error
SFRC20	349.2	347.4	-0.5 %	312.9	-10.4 %
SFRC40	392.4	436.3	11.2 %	401.3	2.3 %
SFRC70	616.0	614.2	-0.3 %	488.2	-20.8 %
SFRC20 ø8 c/c 150	406.8	417.2	2.6 %	382.8	-5.9 %
SFRC40 ø8 c/c 150	496.8	506.2	1.9 %	471.2	-5.1 %
SFRC70 ø8 c/c 150	709.6	684.1	-3.6 %	558.0	-21.4 %
SFRC20 ø12 c/c 150	518.0	476.0	-8.1 %	441.6	-14.7 %
SFRC40 ø12 c/c 150	649.2	564.9	-13.0 %	530.0	-18.4 %
SFRC70 ø12 c/c 150	924.8	742.9	-19.7 %	616.8	-33.3 %
Average			-3.3 %		-14.2 %
Standard deviation			8.6 %		10.1 %

Table 5.7. h = 200

Specimen	FEM [kN]	Punching capacity			
		Karv1		Karv2	
		[kN]	Error	[kN]	Error
SFRC20	600.4	596.5	-0.6 %	510.2	-15.0 %
SFRC40	682.0	757.4	11.1 %	655.7	-3.9 %
SFRC70	1061.6	1079.1	1.6 %	798.5	-24.8 %
SFRC20 ø8 c/c 150	690.4	715.6	3.6 %	629.3	-8.8 %
SFRC40 ø8 c/c 150	861.6	876.5	1.7 %	774.8	-10.1 %
SFRC70 ø8 c/c 150	1216.4	1198.2	-1.5 %	917.6	-24.6 %
SFRC20 ø12 c/c 150	928.0	818.4	-11.8 %	731.1	-21.2 %
SFRC40 ø12 c/c 150	1099.2	979.2	-10.9 %	877.5	-20.2 %
SFRC70 ø12 c/c 150	1422.8	1301.0	-8.6 %	1020.4	-28.3 %
Average			-1.7 %		-17.4 %
Standard deviation			7.1 %		7.9 %

Karv1 turned out to have an average error value significantly lower than Karv2 and also a little lower standard deviation. In the unreinforced slabs and the slabs with ⌀8 c/c 150 reinforcement, the calculated values according to Karv1 are very close to the FEM results (except for the SFRC40 sample). In slabs with ⌀12 c/c 150 reinforcement, Karv1 tends to underestimate the capacity. In conclusion, Karv1 provides results, which for both 150 mm and 200 mm slabs, are both closer and with lower standard deviation than all other methods examined.

6 Conclusions

Six different national standards/guidelines have been in evaluated in this thesis in terms of their methods to determine shear and punching capacity for SFRC slabs. Also, punching failures were simulated using a FEM software product where the results from the simulations were compared to the national standards/guidelines. Lastly, based on the simulation results, an alternative theoretical model was developed.

Since no punching test results have been evaluated in this thesis it is neither possible to say that that one method is more accurate than the other nor to consider the FEM simulation results as anything but a rough approximation of the punching resistance of the slab. However, the FEM simulation results seem realistic. The punching capacity increased both when the fibre content increased and when bending reinforcement was added. When comparing the FEM results to the guidelines (Table 5.1…Table 5.4) in general the guidelines underestimates the capacity, which they also should so that the approximation is safe. However, the approximated punching resistance for a SFRC slab varies significantly depending on which guideline the approximation is based on. For instance, as shown in Table 5.4, the punching capacity for a 200 mm thick slab with 70 kg/m^3 of Hendix Prime 75/52 (SFRC70) is according to TR 34 fourth edition (UK4) 554.1 kN and according to the Swedish SS 812310:2014 (SWE) 1023.8 kN. Furthermore, in many cases the contribution from bending reinforcement is not taken into account, i.e., same resistance in punching is reached regardless whether the slab is provided with bending reinforcement or not. Given these points, there is a need for a common European standard for FRC. As no such standard exists, a designer today can simply pick one method and, as shown, the approximated punching capacity may differ significantly depending on the method chosen.

One of the alternative methods suggested in Section 5.2 (Karv1) turned out to differ less to the FEM results than any other guideline/standard investigated in this thesis. The average error and standard deviation were both lower using the Karv1 method. The fact that the average error is lower is logical since all partial factors are removed. After all, the aim was to develop a formula that would have an as low as possible average error. The fact the standard deviation is lower in Karv1 compared to other guidelines/standards indicates that the Karv1 method is more consistent and reliable compared to other methods presented in this thesis. However, since Karv1 is only a theoretical model developed to achieve results close to the FEM simulation, the author does not recommend it to be used before further investigations have been conducted.

It is easy to learn the basics of the FEM software (ATENA) used in this thesis. The user interface is pleasant and the essentials are clearly demonstrated in the tutorials, which can be found from the website of Červenka Consulting. There is also a theory manual and a user manual from where the user will find in-depth information about the software. If the user is unable to find answers from there, the staff at Červenka Consulting are quick to reply to questions sent by e-mail. However, a couple of issues are notable. While building a model is easy there are some restrictions to the geometry. The software only supports geometries consisting of straight lines and making modifications to the model after it is complete it is more time consuming than it should be. For instance changing the thickness of the reinforcement could not be done automatically. Instead, all bars had to be modified individually. Therefore, the user should know exactly what to model before starting. It took the software about five to ten minutes to perform the four point bending test simulation but

for the punching failure simulation it could take up to 5 hours (processor: Intel (R) Xeon(R) CPU ES-1620 0 @ 3.60 GHz). For the 200 mm thick slabs the model consisted of 5408 FEM elements and the file size of such a model is between 1.5…2.5 GB.

The author recommends that more large-scale tests should be performed for FRC. Obviously, with more test data it would be easier to develop an international standard that would be more reliable than current guidelines. Again, SFRC has shown good potential in structural applications but with more test data and an international standard it would become easier to make safe designs using this material.

References

[1] ERMCO. (2012) Guidance to fibre concrete - Properties, Specification and Practice in Europe.

[2] J. Mandl. (2008) Flat slabs made of steel fibre-reinforced concrete. CPI – Concrete Plant International. no. 1. pp. 210-215.

[3] J. Mandl and M. Matsinen. (2015) Halkeilun hallinta maanvaraisissa betonilattioissa ja pintabetoneissa teräskuitubetonia käyttäen. Betoni. vol. 85. no. 2. pp. 66-73.

[4] BY 56. (2011) Teräskuitubetonirakenteet 2011. Suomen Betoniyhdistys ry. Helsinki: BY-Koulutus Oy. ISBN 978-952-67169-4-7.

[5] SS 812310. (2014) Fiber Concrete - Design of Fibre Concrete Structures. Stockholm: Swedish Standard Institute.

[6] Commentary on the DAfStb Guideline. (2015) Steel Fibre Reinforced Concrete, Berlin: German Committee for Structural Concrete.

[7] Technical Report 34 (2003) Concrete Industrial Ground Floors - Third Edition. The Concrete Society. ISBN 1 904482 01 5

[8] Techincal Report 34 (2016) Concrete Industrial Ground Floors - Fourth Edition. The Concrete Society. ISBN 978-1-904482-77-2

[9] fib Model Code For Concrete Structures. (2010) Lausanne, Switzerland: International Federation for Structural Concrete (fib). ISBN 978-3-433-03061-5

[10] K.-K. Choi, M. M. Reda Taha, H.-G. Park and A. K. Maji. (2007) Punching shear strength of interior concrete slab–column connections reinforced with steel fibers. Cement and Concrete Composites. vol. 29. no. 5. pp. 409-420.

[11] M. Harajli, D. Maalouf and H. Khatib. (1995) Effect of Fibers on the Punching Shear Strength of Slab-Column Connections. Cement and Concrete Composites. vol. 17. no. 2. pp. 161-170.

[12] J. A. O. Barros, B. N. M. Neto, G. S. S. A. Melo and C. M. Frazão. (2015) Assessment of the effectiveness of steel fibre reinforcement for the punching resistance of flat slabs by experimental research and design approach. Composites Part B. vol. 78. pp. 8-25.

[13] B. N. M. Neto, J. A. O. Barros and G. S. S. A. Melo. (2013) Model to Simulate the Contribution of Fiber Reinforcement for the Punching Resistance of RC Slabs. Journal of Materials in Civil Engineering. vol. 26. no. 7.

[14] A. B. Poole and I. Sims. (2015) Concrete Petrography: A Handbook of Investigative Techniques. Second Edition. ISBN 9781856176903

[15] The Roman Pantheon [Online]. Available: http://www.crystalinks.com/romepantheon.html. [Accessed 18 November 2016].

[16] A. Bentur and S. Mindess. (2007) Fibre Reinforced Cementitious Composites. Second edition. Abingdon: Taylor & Francis. ISBN 10: 0-415-25048-X

[17] ACI Committee 544. (2002) State-of-the-Art-Report on Fiber Reinforced Concrete. American Concrete Institute.

[18] The Concrete Society. [Online]. Available: http://www.concrete.org.uk/fingertips-nuggets.asp?cmd=display&id=376. [Accessed 18 November 2016].

[19] CCANZ. (2009) INFORMATION BULLETIN: IB 39. Cement & Concrete Assosiation of New Zealand, Wellington.

[20] J. Mandl and M. Matsinen. 2014. Teräskuitubetonin käyttäminen kantavissa rakenteissa. Betoni. vol. 84. no. 1. pp. 60-69.

[21] PiiMat Oy. [Online]. Available: http://www.piimat.fi/tuotteet/betonilattiat/kuitubetoni. [Accessed 11 April 2016].

[22] J. Mandl and M. Matsinen [Interview]. 12 July 2016.

[23] EN 14889-1 (2006) Fibres for concrete - Part 1: Steel fibres - Definitions, specifications and conformity, CEN - European Committee for Standardization.

[24] L. Nyholm Thrane, S. Oldrich, M. Strøm and T. Kasper. (2013) Guideline for execution of steel fibre reinforced SCC. Taastrup: Danish Technological Institute. Concrete Centre.

[25] ASTM C1018. Standard Test Method for Flexural Toughness and First-Crack Strength of Fiber-Reinforced Concrete (Using Beam With Third-Point Loading).

[26] EN 14651 + A1. (2005) Test Method for Metallic Fibre Concrete. Measuring The Flexural Tensile Strength (Limit of Proportionality (Lop), Residual). CEN - European Committee for Standardization.

[27] EN 12390-1. (2000) Testing hardened concrete - Part 1: Shape, dimensions and other requirements for specimens and moulds. CEN - European Committee for Standardization.

[28] Nordic Concrete Research. (2015) Characterisation of fibre content, distribution and orientation to predict Fibre Reinforced Concrete behavior. Norsk Betongforening. Oslo.

[29] R. West, S. Zhang and J. Mandl. (2015) Aligning Long Steel Fibres In Fresh Concrete. ICE Virtual Library. [Online]. Available: http://www.icevirtuallibrary.com/doi/10.1680/ccfdc.34013.0052. [Accessed 18 November 2016].

[30] EN 206. (2003) Concrete - Specification, performance, production and Conformity. Brussels: European Committee for Standardization.

[31] Council Directive 93/68/EC. (1993) The Council of the European Communities.

[32] J. Mandl. (2003) Free suspended elevated flat slab with post tension and without active traditional reinforcemnt is proved to be ready for practice. Readymix AG. Bayreuth. Innovation price avarded.

[33] M. Bartolac, D. Damjanović and I. Duvnjak. (2015) Punching strength of flat slabs with and without shear reinforcement. Građevinar. vol. 67. no. 8. pp. 771-786.

[34] A. Muttoni. (2008) Punching Shear Strength of Reinforced Concrete Slabs without Transverse Reinforcement. American Concrete Institute.

[35] A. Muttoni, M. F. Ruiz, E. Bentz and V. Sigrist. (2013) Background to the Model Code 2010 Shear Provisions - Part II Punching Shear. Structural Concrete.

[36] P. V. P. Sacramento, M. P. Ferreira, D. R. C. Oliveira and G. S. S. A. Melo. (2012) Punching strength of reinforced concrete flat slabs without shear reinforcement. Ibacron Structures And Materials Journal. vol. 5. no. 5. pp. 659-691.

[37] B. T. Lim. (1997) Punching shear capacity of flat slab-column junctions (a study by 3-D non-linear finite element analysis) Doctoral thesis. University of Glasgow, Department of Civil Engineering. pp. 265

[38] S. Lips. (2012) Punching of Flat Slabs with Large Amounts of Shear Reinforcement. Doctoral thesis. Ecole Polytechnique Fédérale de Lausanne, Structural Concrete Laboratory (IBETON). pp. 210

[39] EN 1992-1-1. (2004) Design of concrete structures - Part 1-1: General rules and rules for buildings. CEN - European Committee for Standardization.

[40] EN 14889-2. (2006) Fibres for concrete - Part 2: Polymer fibres - Definitions, specifications and conformity. CEN - European Committee for Standardization.

[41] J. Silfwerbrand. (2014) Structural Design of Load-Bearing Fibre Concrete Structures. Finnish Concrete Day, 23 October 2014, Helsinki.

[42] J. Silfwerbrand. (2015) Bärande möjlighet för fibrerna. Betong. vol. 1. pp. 51-54.

[43] RILEM TC 162-TDF. (2003) Test and design methods for steel fibre reinforced concrete. Materials and Structures. ISBN 2-912143-38-1

[44] T. Sajdlová. (2016) ATENA Program Documentation Part 4-7, ATENA Science – GiD FRC Tutorial, Step by step guide for nonlinear analysis of fiber reinforced concrete structures with ATENA and GiD. Prague: Červenka Consulting.

[45] P. Dobromil and J. Červenka. (2016) ATENA Program Documentation Part 11, Troubleshooting Manual. Prague: Červenka Consulting.

[46] V. Červenka, L. Jendele and J. Červenka. (2016) ATENA Program Documentation Part 1. Prague: Červenka Consulting.

[47] J. Mandl. (2015) Test report of SFRC performance with Hendix Prime 75/52. Rendered at University of Weimar in 2015 (Not published).

[48] D. Öman and O. Blomkvist. (2006) Icke linjär 3D finit elementanalys av genomstansade armerade betongplattor. Master's thesis. Kungliga Tekniska Högskolan, Institutionen för byggvetenskap. Stockholm. pp. 104

[49] V. Červenka and J. Červenka. (2014) ATENA Program Documentation Part 2-2, User's Manual for ATENA 3D, Version 5.1.1. Prague: Červenka Consulting.

Appendices

Appendix 1 Standards, guidelines for fibre concrete and other references

Appendix 2 ATENA material parameters data

Appendix 3 ATENA macro elements data

Appendix 4 Mathcad calculations

Appendix 5 Graphs showing punching capacity as a function of slab thickness

Appendix 1 Standards, guidelines for fibre concrete and other references

*From ERMCO [1]

** Not from ERMCO

i. prEN 206 Concrete - Specification, performance, production, and conformity (EN206-1 is in revision and the revision will be called EN206 as it combines Part 1 and Part 9). *

ii. EN 14650 Precast concrete products – General rules for factory production control of metallic fibred concrete. *

iii. Austria: ÖVBB Richtlinie Faserbeton (ÖVBB guideline fibre concrete), Österreichische Vereinigung für Beton- und Bautechnik, Vienna, 07/2008.

iv. Austria: ÖVBB Richtlinie Erhöht brandbeständiger Beton für unterirdische Verkehrsbauwerke (ÖVBB guideline higher fire resistance with concrete for underground buildings for traffic), Österreichische Vereinigung für Beton- und Bautechnik, Vienna, 07/2005. *

v. Belgium: NBN B 15-238, Proeven op vezelversterkt beton – Buigproef op prismatische proefstukken. *

vi. Denmark: Danish Technological Institute, Concrete Centre, Guidelines for Execution of Steel Fibre Reinforced SCC, 09/2013.**

vii. Denmark: Danish Technological Institute, SFRC Consortium, Design Guideline for Structural Applications of Steel Fibre Reinforced Concrete, 01/2014.**

viii. EN 14889-1: Fibres for concrete Part 1: Steel fibres - Definitions, specifications and conformity.**

ix. EN 14889-2: Fibres for concrete Part 2: Polymer fibres – Definitions, specifications and conformity.**

x. Germany: DAfStb-Guideline, Committee for Structural concrete DAfStb guideline Steel fibre reinforced concrete, Final version, 03/2010. *

xi. Italy: UNI 11039 Steel fibre reinforced concrete – Part I: Definitions, classification, specification and conformity – Part II: Test method for measuring first crack strength and ductility, 02/2003. *

xii. Netherlands: CUR: Recommendation 111 Steel fibre reinforced concrete Industrial floors on pile foundations Design and Construction, 10/2010. *

xiii. Norway: Publication Nr.7, Sprayed concrete for rock support, Norwegian concrete association *

xiv. Sweden: Swedish Standards Institute, SS 812310, Fibre Concrete – Design of Fibre Concrete Structures, 03/2014 (Old: Swedish Concrete Association Concrete Report No 4, Stålfiberbetong – rekommendationer för konstruktion, utförande och provning (Steel Fibre Reinforced Concrete – Recommendations for Design, Construction, and Testing), Stockholm, .2nd Ed 1997. (In Swedish).)**

xv. Switzerland: SIA 162/6, Empfehlung Stahlfaserbeton (recommendation steel fibre reinforced concrete), 02/1999. *

xvi. UK: Concrete Society Technical Report 34 – Concrete Industrial Ground Floors – A guide to design and construction, 4th Edition. Concrete Society. Blackwater, Camberley, Surrey, 2016.**

xvii. UK: Concrete Society Technical Report no 63 - Guidance for the Design of Steel-Fibre-Reinforced Concrete. Blackwater, Camberley, Surrey, 2007. *

xviii. UK: Concrete Society Technical Report No 65 - Guidance on the use of Macro synthetic- Fibre-reinforced Concrete, Concrete Society:. Blackwater, Camberley, Surrey, 2007. *

xix. Rilem TC 162 TDF Design of Steel fibre reinforced concrete – Method, recommendations, Material and Structures, 2002. *

xx. fib Model Code 2010 First complete draft, Volume 1, and 2, Bulletin 55, 3/2010. *

xxi. EFNARC European Specification for sprayed concrete, Guidelines for specifiers and contractors, 1996. *

Appendix 2 ATENA material parameters

MATERIAL 1	
Property	**Value**
Title	Steel
Type	CC3DElastIsotropic
Elastic modulus E [MPa]	2,100E+05
Poisson's ratio μ [–]	0,300
Specific material weight ρ [MN/m^3]	2,300E-02
Coefficient of thermal expansion α [1/K]	1,200E-05
MATERIAL 2	
Property	**Value**
Title	Reinforcement
Type	CCReinforcement
Elastic modulus E [MPa]	2,100E+05
Specific material weight ρ [MN/m^3]	7,850E-02
Coefficient of thermal expansion α [1/K]	1,200E-05
Reinf. type	Bilinear
σ_y [MPa]	550,000
In compression	active
MATERIAL 3	
Property	**Value**
Title	SFRC 20kg/m3
Type	CC3DNonLinCementitious2User
Elastic modulus E [MPa]	4,470E+04
Poisson's ratio μ [–]	0,200
Specific material weight ρ [MN/m^3]	2,300E-02
Coefficient of thermal expansion α [1/K]	1,200E-05
Tensile strength F_t [MPa]	5,700E+00
Compressive strength F_c [MPa]	-4,490E+01
Function for Tension (ε[]; σ_t/f'_t[])	(0,000E+00; 1,0000) (5,000E-05; 0,9300) (2,000E-03; 0,6000) (5,000E-03; 0,3700) (2,500E-02; 0,3700) (6,700E-02; 0,2500)
Tension ch.size [m]	0,02500
Tension loc.strain [–]	0,000E+00
Function for Compression (ε[]; σ_c/f'_c[])	(-6,075E-01; 0,0000) (-1,075E-03; 1,0000) (-5,377E-04; 0,8000) (0,000E+00; 0,2500)
Compression ch.size [m]	0,02500
Compression loc.strain [–]	-1,075E-03
Function for Strength reduction due to cracking (ε[]; σ_c/f'_c[])	(0,000E+00; 1,0000) (3,000E-01; 1,0000)

Function for Shear (ε[]; G/G_c[])	(0,000E+00; 1,0000) (1,000E-05; 0,6000) (2,000E-04; 0,3000) (1,000E-03; 0,1500) (4,000E-03; 0,0000)
Shear loc.strain [–]	0,000E+00
Function for Shear strength reduction due to cracking (ε_f[]; τ_c/f'_t[])	(0,000E+00; 1,1000) (1,000E-04; 0,8700) (5,000E-04; 0,5100) (1,000E-03; 0,3400) (2,000E-03; 0,2000) (3,000E-03; 0,1500) (5,000E-03; 0,0900) (1,000E-02; 0,0500)
Function for Tension - compression (σ_c/f'_c[]; σ_t/f'_t[])	(0,0000; 1,0000) (1,0000; 0,2000)
Exc.,def. the shape of fail.surface e [–]	0,520
Multiplier for the direction of the pl.flow β [–]	0,000
Fixed crack model coefficient [–]	1,000
MATERIAL 4	
Property	**Value**
Title	SFRC 40kg/m3
Type	CC3DNonLinCementitious2User
Elastic modulus E [MPa]	3,910E+04
Poisson's ratio μ [–]	0,200
Specific material weight ρ [MN/m3]	2,300E-02
Coefficient of thermal expansion α [1/K]	1,200E-05
Tensile strength F_t [MPa]	5,330E+00
Compressive strength F_c [MPa]	-4,440E+01
Function for Tension (ε[]; σ_t/f'_t[])	(0,000E+00; 1,0000) (6,000E-05; 1,0500) (1,300E-03; 0,7500) (1,500E-02; 0,6600) (2,000E-02; 0,6000) (9,000E-02; 0,2500)
Tension ch.size [m]	0,02500
Tension loc.strain [–]	0,000E+00
Function for Compression (ε[]; σ_c/f'_c[])	(-6,075E-01; 0,0000) (-1,075E-03; 1,0000) (-5,377E-04; 0,8000) (0,000E+00; 0,2500)
Compression ch.size [m]	0,02500
Compression loc.strain [–]	-1,075E-03
Function for Strength reduction due to cracking (ε[]; σ_c/f'_c[])	(0,000E+00; 1,0000) (3,000E-01; 1,0000)
Function for Shear (ε[]; G/G_c[])	(0,000E+00; 1,0000) (1,000E-05; 0,6000) (2,000E-04; 0,3000) (1,000E-03; 0,1500) (4,000E-03; 0,0000)
Shear loc.strain [–]	0,000E+00
Function for Shear strength reduction due to cracking (ε_f[]; τ_c/f'_t[])	(0,000E+00; 1,1000) (1,000E-04; 0,8700) (5,000E-04; 0,5100) (1,000E-03; 0,3400) (2,000E-03; 0,2000) (3,000E-03; 0,1500) (5,000E-03; 0,0900) (1,000E-02; 0,0500)
Function for Tension - compression (σ_c/f'_c[]; σ_t/f'_t[])	(0,0000; 1,0000) (1,0000; 0,2000)
Exc.,def. the shape of fail.surface e [–]	0,520
Multiplier for the direction of the pl.flow β [–]	0,000
Fixed crack model coefficient [–]	1,000
MATERIAL 5	

Property	Value
Title	SFRC 70kg/m3
Type	CC3DNonLinCementitious2User
Elastic modulus E [MPa]	4,460E+04
Poisson's ratio μ [–]	0,200
Specific material weight ρ [MN/m^3]	2,300E-02
Coefficient of thermal expansion α [1/K]	1,200E-05
Tensile strength F_t [MPa]	7,350E+00
Compressive strength F_c [MPa]	-4,500E+01
Function for Tension (ε[]; σ_t/f'_t[])	(0,000E+00; 1,0000) (4,000E-02; 0,4400) (5,500E-02; 0,4600) (8,000E-02; 0,3200)
Tension ch.size [m]	0,02500
Tension loc.strain [–]	0,000E+00
Function for Compression (ε[]; σ_c/f'_c[])	(-6,075E-01; 0,0000) (-1,075E-03; 1,0000) (-5,377E-04; 0,8000) (0,000E+00; 0,2500)
Compression ch.size [m]	0,02500
Compression loc.strain [–]	-1,075E-03
Function for Strength reduction due to cracking (□[]; □c/f'c[])	(0,000E+00; 1,0000) (3,000E-01; 1,0000)
Function for Shear (□[]; G/Gc[])	(0,000E+00; 1,0000) (1,000E-05; 0,6000) (2,000E-04; 0,3000) (1,000E-03; 0,1500) (4,000E-03; 0,0000)
Shear loc.strain [–]	0,000E+00
Function for Shear strength reduction due to cracking (□f[]; □c/f't[])	(0,000E+00; 1,1000) (1,000E-04; 0,8700) (5,000E-04; 0,5100) (1,000E-03; 0,3400) (2,000E-03; 0,2000) (3,000E-03; 0,1500) (5,000E-03; 0,0900) (1,000E-02; 0,0500)
Function for Tension - compression (□c/f'c[]; □t/f't[])	(0,0000; 1,0000) (1,0000; 0,2000)
Exc.,def. the shape of fail.surface e [–]	0,520
Multiplier for the direction of the pl.flow □ [–]	0,000
Fixed crack model coefficient [–]	1,000

MATERIAL 6	
Property	**Value**
Title	C30,37 characteristic values
Type	CC3DNonLinCementitious2
Elastic modulus E [MPa]	3,300E+04
Poisson's ratio μ [–]	0,200
Specific material weight ρ [MN/m^3]	2,300E-02
Coefficient of thermal expansion α [1/K]	1,200E-05
Tensile strength F_t [MPa]	2,000E+00
Compressive strength F_c [MPa]	-3,000E+01
Specific fracture energy G_f [MN/m]	6,662E-05
Critical compressive displacement W_d [m]	-5,000E-04
Exc.,def. the shape of fail.surface e [–]	0,520
Multiplier for the direction of the pl.flow β [–]	0,000

Fixed crack model coefficient [–]	1,000
Plastic strain at compressive strength ε_{cp} [–]	-1,291E-03
Onset of non-linear behavior in compression F_{c0} [MPa]	-4,200E+00
Reduction of compressive strength due to cracks $r_{c,lim}$ [–]	0,8
Crack Shear Stiff. Factor S_F [–]	20,0
Aggregate Size [m]	0,020
M A T E R I A L 7	
Property	**Value**
Title	C45,55 characteristic values
Type	CC3DNonLinCementitious2
Elastic modulus E [MPa]	3,600E+04
Poisson's ratio μ [–]	0,200
Specific material weight ρ [MN/m^3]	2,300E-02
Coefficient of thermal expansion α [1/K]	1,200E-05
Tensile strength F_t [MPa]	2,700E+00
Compressive strength F_c [MPa]	-4,500E+01
Specific fracture energy G_f [MN/m]	8,677E-05
Critical compressive displacement Wd [m]	-5,000E-04
Exc.,def. the shape of fail.surface e [–]	0,520
Multiplier for the direction of the pl.flow □ [–]	0,000
Fixed crack model coefficient [–]	1,000
Plastic strain at compressive strength □cp [–]	-1,150E-03
Onset of non-linear behavior in compression Fc0 [MPa]	-5,670E+00
Reduction of compressive strength due to cracks rc,lim [–]	0,8
Crack Shear Stiff. Factor SF [–]	20,0
Aggregate Size [m]	0,020

Appendix 3 ATENA macro-elements

Four point bending test

MACRO-ELEMENTS

MACROELEMENT 1

MACROELEMENT 1 - JOINTS

Number	X [m]	Y [m]	Z [m]
1	0,0000	0,0000	0,0000
2	0,3500	0,0000	0,0000
3	0,3500	0,1500	0,0000
4	0,0000	0,1500	0,0000
5	0,0000	0,0000	0,1500
6	0,3500	0,0000	0,1500
7	0,3500	0,1500	0,1500
8	0,0000	0,1500	0,1500

MAKROELEMENT 1 - LINES

Number	Joint at the beg.	Joint at the end		Number	Joint at the beg.	Joint at the end
1	1	2		7	7	6
2	2	6		8	3	4
3	6	5		9	4	8
4	5	1		10	8	7
5	2	3		11	4	1
6	3	7		12	5	8

MAKROELEMENT 1 - SURFACES

Number	List of boundary lines
1	1-4
2	2,5-7
3	6,8-10
4	4,9,11-12
5	1,5,8,11
6	3,7,10,12

MACROELEMENT 1 - PROPERTIES

Type of macroelement standard, azimuth = 0,00°, zenith = 0,00°

CS	Used	Material			
1	Yes	Ident	Material	Ratio [%]	
Basic	SFRC				

MACROELEMENT 2

MACROELEMENT 2 - JOINTS

Number	X [m]	Y [m]	Z [m]
1	0,0350	0,0000	0,0000
2	0,0350	0,0000	-0,0100

3	0,0500	0,0000	-0,0100
4	0,0650	0,0000	-0,0100
5	0,0650	0,0000	0,0000
6	0,0350	0,1500	-0,0100
7	0,0500	0,1500	-0,0100
8	0,0650	0,1500	-0,0100
9	0,0650	0,1500	0,0000
10	0,0350	0,1500	0,0000

MAKROELEMENT 2 - LINES

Number	Joint at the beg.	Joint at the end		Number	Joint at the beg.	Joint at the end
1	1	2		9	4	8
2	2	3		10	8	7
3	3	4		11	5	9
4	4	5		12	9	8
5	5	1		13	1	10
6	3	7		14	10	9
7	7	6		15	6	10
8	6	2				

MAKROELEMENT 2 - SURFACES

Number	List of boundary lines
1	1-5
2	2,6-8
3	3,6,9-10
4	4,9,11-12
5	5,11,13-14
6	1,8,13,15
7	7,10,12,14-15

MACROELEMENT 2 - PROPERTIES

Type of macroelement standard, azimuth = 0,00°, zenith = 0,00°

CS	Used	Material			
1	Yes	Ident	Material	Ratio [%]	
Basic	Steel				

MACROELEMENT 3

MACROELEMENT 3 - JOINTS

Number	X [m]	Y [m]	Z [m]
1	0,2350	0,0000	0,1500
2	0,2350	0,0000	0,1600
3	0,2500	0,0000	0,1600
4	0,2650	0,0000	0,1600
5	0,2650	0,0000	0,1500
6	0,2350	0,1500	0,1600
7	0,2500	0,1500	0,1600
8	0,2650	0,1500	0,1600
9	0,2650	0,1500	0,1500

10	0,2350	0,1500	0,1500
11	0,2500	0,0750	0,1600

MAKROELEMENT 3 - LINES

Number	Joint at the beg.	Joint at the end		Number	Joint at the beg.	Joint at the end
1	1	2		9	4	8
2	2	3		10	8	7
3	3	4		11	5	9
4	4	5		12	9	8
5	5	1		13	1	10
6	3	7		14	10	9
7	7	6		15	6	10
8	6	2				

MAKROELEMENT 3 - SURFACES

Number	List of boundary lines
1	1-5
2	2,6-8
3	3,6,9-10
4	4,9,11-12
5	5,11,13-14
6	1,8,13,15
7	7,10,12,14-15

MACROELEMENT 3 - PROPERTIES

Type of macroelement standard, azimuth = 0,00°, zenith = 180,00°

CS	Used	Material		
1	Yes	Ident	Material	Ratio [%]
Basic	Steel			

Punching test of 200 mm slab

MACROELEMENT 1

MACROELEMENT 1 - JOINTS

Number	X [m]	Y [m]	Z [m]
1	0,0000	0,0000	0,0000
2	1,3000	0,0000	0,0000
3	1,3000	1,3000	0,0000
4	0,0000	1,3000	0,0000
5	0,0000	0,0000	0,2000
6	1,3000	0,0000	0,2000
7	1,3000	1,3000	0,2000
8	0,0000	1,3000	0,2000

MAKROELEMENT 1 - LINES

Number	Joint at the beg.	Joint at the end		Number	Joint at the beg.	Joint at the end
1	1	2		7	7	6

2	2	6		8	3	4
3	6	5		9	4	8
4	5	1		10	8	7
5	2	3		11	4	1
6	3	7		12	5	8

MAKROELEMENT 1 - SURFACES

Number	List of boundary lines
1	1-4
2	2,5-7
3	6,8-10
4	4,9,11-12
5	1,5,8,11
6	3,7,10,12

MACROELEMENT 1 - PROPERTIES

Type of macroelement standard, azimuth = 0,00°, zenith = 0,00°

CS	Used	Material			
1	Yes	Ident	Material	Ratio [%]	
Basic	SFRC				

MACROELEMENT 2

MACROELEMENT 2 - JOINTS

Number	X [m]	Y [m]	Z [m]
1	0,0000	0,0000	-0,0500
2	0,1000	0,0000	-0,0500
3	0,1000	0,1000	-0,0500
4	0,0000	0,1000	-0,0500
5	0,0000	0,0000	0,0000
6	0,1000	0,0000	0,0000
7	0,1000	0,1000	0,0000
8	0,0000	0,1000	0,0000

MAKROELEMENT 2 - LINES

Number	Joint at the beg.	Joint at the end		Number	Joint at the beg.	Joint at the end
1	1	2		7	7	6
2	2	6		8	3	4
3	6	5		9	4	8
4	5	1		10	8	7
5	2	3		11	4	1
6	3	7		12	5	8

MAKROELEMENT 2 - SURFACES

Number	List of boundary lines
1	1-4
2	2,5-7
3	6,8-10
4	4,9,11-12

5	1,5,8,11
6	3,7,10,12

MACROELEMENT 2 - PROPERTIES

Type of macroelement standard, azimuth = 0,00°, zenith = 0,00°

CS	Used	Material			
1	Yes	Ident	Material	Ratio [%]	
Basic	Steel				

MACROELEMENT 3

MACROELEMENT 3 - JOINTS

Number	X [m]	Y [m]	Z [m]
1	0,6670	0,6670	0,2000
2	0,7470	0,6670	0,2000
3	0,7470	0,7470	0,2000
4	0,6670	0,7470	0,2000
5	0,6670	0,6670	0,2100
6	0,7470	0,6670	0,2100
7	0,7470	0,7470	0,2100
8	0,6670	0,7470	0,2100
9	0,7070	0,7070	0,2100

MAKROELEMENT 3 - LINES

Number	Joint at the beg.	Joint at the end		Number	Joint at the beg.	Joint at the end
1	1	2		7	7	6
2	2	6		8	3	4
3	6	5		9	4	8
4	5	1		10	8	7
5	2	3		11	4	1
6	3	7		12	5	8

MAKROELEMENT 3 - SURFACES

Number	List of boundary lines
1	1-4
2	2,5-7
3	6,8-10
4	4,9,11-12
5	1,5,8,11
6	3,7,10,12

MACROELEMENT 3 - PROPERTIES

Type of macroelement standard, azimuth = 0,00°, zenith = 0,00°

CS	Used	Material			
1	Yes	Ident	Material	Ratio [%]	
Basic	Steel				

MACROELEMENT 4

MACROELEMENT 4 - JOINTS

Number	X [m]	Y [m]	Z [m]

1	0,9260	0,2190	0,2000
2	1,0060	0,2190	0,2000
3	1,0060	0,2990	0,2000
4	0,9260	0,2990	0,2000
5	0,9260	0,2190	0,2100
6	1,0060	0,2190	0,2100
7	1,0060	0,2990	0,2100
8	0,9260	0,2990	0,2100
9	0,9660	0,2590	0,2100

MAKROELEMENT 4 - LINES

Number	Joint at the beg.	Joint at the end		Number	Joint at the beg.	Joint at the end
1	1	2		7	7	6
2	2	6		8	3	4
3	6	5		9	4	8
4	5	1		10	8	7
5	2	3		11	4	1
6	3	7		12	5	8

MAKROELEMENT 4 - SURFACES

Number	List of boundary lines
1	1-4
2	2,5-7
3	6,8-10
4	4,9,11-12
5	1,5,8,11
6	3,7,10,12

MACROELEMENT 4 - PROPERTIES

Type of macroelement standard, azimuth = 0,00°, zenith = 0,00°

CS	Used	Material		
1	Yes	Ident	Material	Ratio [%]
Basic	Steel			

MACROELEMENT 5

MACROELEMENT 5 - JOINTS

Number	X [m]	Y [m]	Z [m]
1	0,2190	0,9260	0,2000
2	0,2990	0,9260	0,2000
3	0,2990	1,0060	0,2000
4	0,2190	1,0060	0,2000
5	0,2190	0,9260	0,2100
6	0,2990	0,9260	0,2100
7	0,2990	1,0060	0,2100
8	0,2190	1,0060	0,2100
9	0,2590	0,9660	0,2100

MAKROELEMENT 5 - LINES

Number	Joint at the beg.	Joint at the end		Number	Joint at the beg.	Joint at the end
1	1	2		7	7	6
2	2	6		8	3	4
3	6	5		9	4	8
4	5	1		10	8	7
5	2	3		11	4	1
6	3	7		12	5	8

MAKROELEMENT 5 - SURFACES

Number	List of boundary lines
1	1-4
2	2,5-7
3	6,8-10
4	4,9,11-12
5	1,5,8,11
6	3,7,10,12

MACROELEMENT 5 - PROPERTIES

Type of macroelement standard, azimuth = 0,00°, zenith = 0,00°

CS	Used	Material			
1	Yes	Ident	Material	Ratio [%]	
Basic	Steel				

Punching test of 150 mm slab

MACROELEMENT 1

MACROELEMENT 1 - JOINTS

Number	X [m]	Y [m]	Z [m]
1	0,0000	0,0000	0,0000
2	1,3000	0,0000	0,0000
3	1,3000	1,3000	0,0000
4	0,0000	1,3000	0,0000
5	0,0000	0,0000	0,1500
6	1,3000	0,0000	0,1500
7	1,3000	1,3000	0,1500
8	0,0000	1,3000	0,1500

MAKROELEMENT 1 - LINES

Number	Joint at the beg.	Joint at the end		Number	Joint at the beg.	Joint at the end
1	1	2		7	7	6
2	2	6		8	3	4
3	6	5		9	4	8
4	5	1		10	8	7
5	2	3		11	4	1
6	3	7		12	5	8

MAKROELEMENT 1 - SURFACES

Number	List of boundary lines
1	1-4
2	2,5-7
3	6,8-10
4	4,9,11-12
5	1,5,8,11
6	3,7,10,12

MACROELEMENT 1 - PROPERTIES

Type of macroelement standard, azimuth = 0,00°, zenith = 0,00°

CS	Used	Material			
1	Yes	Ident	Material	Ratio [%]	Direction
		Basic			

MACROELEMENT 2

MACROELEMENT 2 - JOINTS

Number	X [m]	Y [m]	Z [m]
1	0,0000	0,0000	-0,0500
2	0,1000	0,0000	-0,0500
3	0,1000	0,1000	-0,0500
4	0,0000	0,1000	-0,0500
5	0,0000	0,0000	0,0000
6	0,1000	0,0000	0,0000
7	0,1000	0,1000	0,0000
8	0,0000	0,1000	0,0000

MAKROELEMENT 2 - LINES

Number	Joint at the beg.	Joint at the end		Number	Joint at the beg.	Joint at the end
1	1	2		7	7	6
2	2	6		8	3	4
3	6	5		9	4	8
4	5	1		10	8	7
5	2	3		11	4	1
6	3	7		12	5	8

MAKROELEMENT 2 - SURFACES

Number	List of boundary lines
1	1-4
2	2,5-7
3	6,8-10
4	4,9,11-12
5	1,5,8,11
6	3,7,10,12

MACROELEMENT 2 - PROPERTIES

Type of macroelement standard, azimuth = 0,00°, zenith = 0,00°

CS	Used	Material

1	Yes	Ident	Material	Ratio [%]	Direction
		Basic	Steel		

MACROELEMENT 3

MACROELEMENT 3 - JOINTS

Number	X [m]	Y [m]	Z [m]
1	0,6670	0,6670	0,1500
2	0,7470	0,6670	0,1500
3	0,7470	0,7470	0,1500
4	0,6670	0,7470	0,1500
5	0,6670	0,6670	0,1600
6	0,7470	0,6670	0,1600
7	0,7470	0,7470	0,1600
8	0,6670	0,7470	0,1600
9	0,7070	0,7070	0,1600

MAKROELEMENT 3 - LINES

Number	Joint at the beg.	Joint at the end	Number	Joint at the beg.	Joint at the end
1	1	2	7	7	6
2	2	6	8	3	4
3	6	5	9	4	8
4	5	1	10	8	7
5	2	3	11	4	1
6	3	7	12	5	8

MAKROELEMENT 3 - SURFACES

Number	List of boundary lines
1	1-4
2	2,5-7
3	6,8-10
4	4,9,11-12
5	1,5,8,11
6	3,7,10,12

MACROELEMENT 3 - PROPERTIES

Type of macroelement standard, azimuth = 0,00°, zenith = 0,00°

CS	Used	Material			
1	Yes	Ident	Material	Ratio [%]	Direction
		Basic	Steel		

MACROELEMENT 4

MACROELEMENT 4 - JOINTS

Number	X [m]	Y [m]	Z [m]
1	0,9260	0,2190	0,1500
2	1,0060	0,2190	0,1500
3	1,0060	0,2990	0,1500

4	0,9260	0,2990	0,1500
5	0,9260	0,2190	0,1600
6	1,0060	0,2190	0,1600
7	1,0060	0,2990	0,1600
8	0,9260	0,2990	0,1600
9	0,9660	0,2590	0,1600

MAKROELEMENT 4 - LINES

Number	Joint at the beg.	Joint at the end	Number	Joint at the beg.	Joint at the end
1	1	2	7	7	6
2	2	6	8	3	4
3	6	5	9	4	8
4	5	1	10	8	7
5	2	3	11	4	1
6	3	7	12	5	8

MAKROELEMENT 4 - SURFACES

Number	List of boundary lines
1	1-4
2	2,5-7
3	6,8-10
4	4,9,11-12
5	1,5,8,11
6	3,7,10,12

MACROELEMENT 4 - PROPERTIES

Type of macroelement standard, azimuth = 0,00°, zenith = 0,00°

CS	Used	Material			
1	Yes	Ident	Material	Ratio [%]	Direction
		Basic	Steel		

MACROELEMENT 5

MACROELEMENT 5 - JOINTS

Number	X [m]	Y [m]	Z [m]
1	0,2190	0,9260	0,1500
2	0,2990	0,9260	0,1500
3	0,2990	1,0060	0,1500
4	0,2190	1,0060	0,1500
5	0,2190	0,9260	0,1600
6	0,2990	0,9260	0,1600
7	0,2990	1,0060	0,1600
8	0,2190	1,0060	0,1600
9	0,2590	0,9660	0,1600

MAKROELEMENT 5 - LINES

Number	Joint at the beg.	Joint at the end	Number	Joint at the beg.	Joint at the end
1	1	2	7	7	6

2	2	6	8	3	4
3	6	5	9	4	8
4	5	1	10	8	7
5	2	3	11	4	1
6	3	7	12	5	8

MAKROELEMENT 5 - SURFACES

Number	List of boundary lines
1	1-4
2	2,5-7
3	6,8-10
4	4,9,11-12
5	1,5,8,11
6	3,7,10,12

MACROELEMENT 5 - PROPERTIES

Type of macroelement standard, azimuth = 0,00°, zenith = 0,00°

CS	Used	Material			
1	Yes	**Ident**	**Material**	**Ratio [%]**	**Direction**
		Basic	Steel		

Appendix 4 Mathcad calculations

Input variables

Fibre dosage

$\rho_{fibre} :=$ 0 kg/m3 | 20 kg/m3 | 40 kg/m3 | **70 kg/m3**

Reinforcement diameter [mm]

$D_r :=$ No reinforcement | 6 | 8 | 10 | **12** | 16 | 20 | 25

Reinforcement spacing [m]

$k_r :=$ 0.100 | **0.150** | 0.200

$$A_{sl} := \pi \cdot \left(\frac{D_r}{2}\right)^2 \cdot \frac{1}{k_r} = 753.98$$

Reinforcement area [mm²/m]

$\sigma_{cp} := 0$ Compression force [MPa]

$b := 200$ Rektangular column width [mm]

$c_{cover} := 30$ Concrete cover

Parameters

$$f_{ct0.L2} := \begin{cases} 0 & \text{if } \rho_{fibre} = 0 \\ 0.3158 & \text{if } \rho_{fibre} = 20 \\ 0.4590 & \text{if } \rho_{fibre} = 40 \\ 0.7629 & \text{if } \rho_{fibre} = 70 \end{cases}$$

Residual tensile strength (DAfStb)

$f_{ct0.L2} = 0.76$

$$R_{e.3} := \begin{cases} 0 & \text{if } \rho_{fibre} = 0 \\ 0.5746 & \text{if } \rho_{fibre} = 20 \\ 0.9188 & \text{if } \rho_{fibre} = 40 \\ 1.2569 & \text{if } \rho_{fibre} = 70 \end{cases}$$

Equivalent flexural strength ratio (TR34)

$R_{e.3} = 1.26$

$$R_{20.50} := \begin{cases} 0 & \text{if } \rho_{fibre} = 0 \\ 0.45 & \text{if } \rho_{fibre} = 20 \\ 0.71 & \text{if } \rho_{fibre} = 40 \\ 1.1 & \text{if } \rho_{fibre} = 70 \end{cases}$$

Jäännöslujuuskerroin (BY 56)

$R_{20.50} = 1.1$

(20 and 70 are interpolated)

$f_{ck} := 45$ Concrete compression strength [MPa]

$f_{ctm} := 0.3 \cdot f_{ck}^{\frac{2}{3}} = 3.8$ Concrete mean axial tensile strength [MPa]

$f_{ctk} := 0.7 \cdot f_{ctm} = 2.66$ Concrete tensile strength [MPa]

$$f_{ctk.fl}(d) := \begin{cases} 2 \cdot f_{ctk} & \text{if } \left[1 + \left(\frac{200}{d}\right)^{\frac{1}{2}}\right] \cdot f_{ctk} > 2 f_{ctk} \\ \left[1 + \left(\frac{200}{d}\right)^{\frac{1}{2}}\right] \cdot f_{ctk} & \text{otherwise} \end{cases}$$

Concrete flexural strength [MPa] (TR34 eqn 9.1)

$$f_{ctm.fl}(d) := \max\left[\left(1.6 - \frac{d}{1000}\right) \cdot f_{ctm}, f_{ctm}\right]$$

Concrete mean flexural tensile strength [MPa] (EC2 (3.23))

$$k(d) := \begin{cases} 2 & \text{if } d < 200 \\ 1 + \sqrt{\frac{200}{d}} & \text{otherwise} \end{cases}$$

Thickness dependent factor (EC2 (6.2.b))

$$\rho(d) := \begin{cases} \frac{A_{sl}}{1000 \cdot d} & \text{if } \frac{A_{sl}}{1000 \cdot d} < 0.02 \\ 0.02 & \text{otherwise} \end{cases}$$

Reinforcement ratio (EC2 (6.2.b))

$$u_{2d}(d) := 4 \cdot b + 4 \cdot d \cdot \pi$$

Control perimeter at distance 2d, rectangular column

$$u_{0.5d}(d) := 4 \cdot b + \pi \cdot d$$

Control perimeter at distance 0.5d, rectangular column

Residual flexural strengths in CMOD1...CMOD4
(F.i values from graphs below):

$$F_1 := \begin{cases} 0 & \text{if } \rho_{fibre} = 0 \\ 17500 & \text{if } \rho_{fibre} = 20 \\ 28500 & \text{if } \rho_{fibre} = 40 \\ 45800 & \text{if } \rho_{fibre} = 70 \end{cases}$$

$$f_{r1} := \frac{3 \cdot F_1 \cdot 600}{2 \cdot 150 \cdot 150^2} = 12.21$$

$$F_2 := \begin{cases} 0 & \text{if } \rho_{fibre} = 0 \\ 17700 & \text{if } \rho_{fibre} = 20 \\ 27500 & \text{if } \rho_{fibre} = 40 \\ 50000 & \text{if } \rho_{fibre} = 70 \end{cases}$$

$$f_{r2} := \frac{3 \cdot F_2 \cdot 600}{2 \cdot 150 \cdot 150^2} = 13.33$$

$$F_3 := \begin{cases} 0 & \text{if } \rho_{fibre} = 0 \\ 16700 & \text{if } \rho_{fibre} = 20 \\ 24900 & \text{if } \rho_{fibre} = 40 \\ 44800 & \text{if } \rho_{fibre} = 70 \end{cases}$$

$$f_{r3} := \frac{3 \cdot F_3 \cdot 600}{2 \cdot 150 \cdot 150^2} = 11.95$$

$$F_4 := \begin{cases} 0 & \text{if } \rho_{fibre} = 0 \\ 14900 & \text{if } \rho_{fibre} = 20 \\ 21000 & \text{if } \rho_{fibre} = 40 \\ 37300 & \text{if } \rho_{fibre} = 70 \end{cases}$$

$$f_{r4} := \frac{3 \cdot F_4 \cdot 600}{2 \cdot 150 \cdot 150^2} = 9.95$$

Table 1 – Relationship between *CMOD* and *δ*

CMOD (mm)	*δ* (mm)
0,05	0,08
0,1	0,13
0,2	0,21
0,5	0,47
1,5	1,32
2,5	2,17
3,5	3,02
4,0	3,44

Fibre 20 kg/m³:

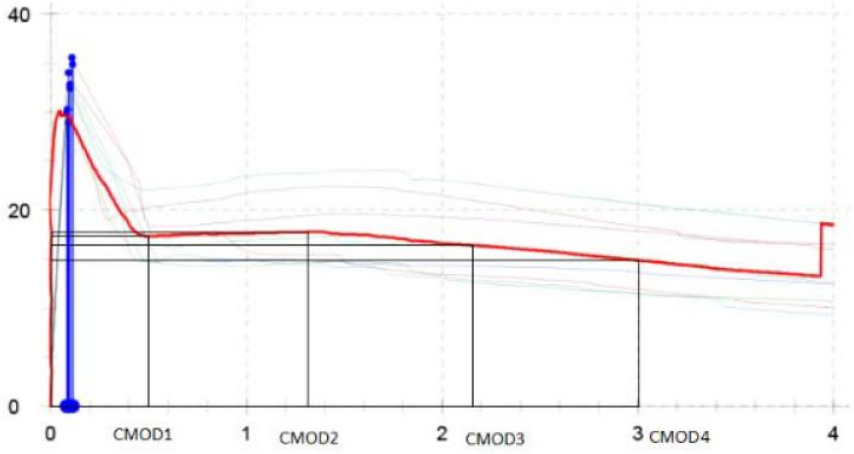

Fibre 40 kg/m³:

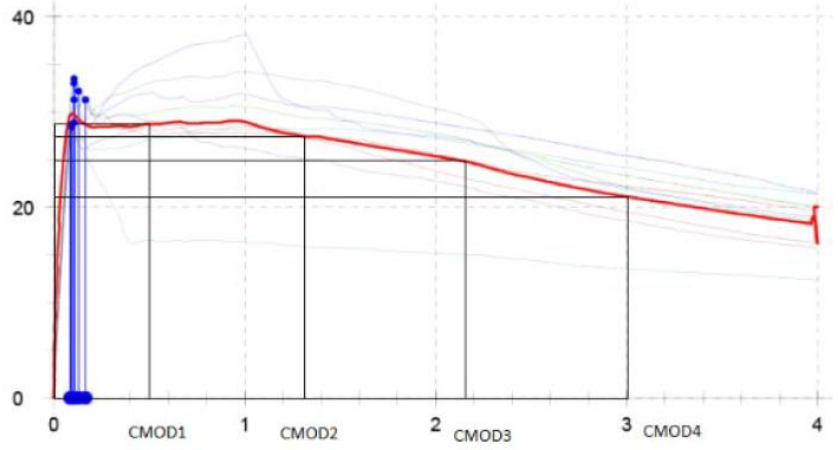

Fibre 70 kg/m³:

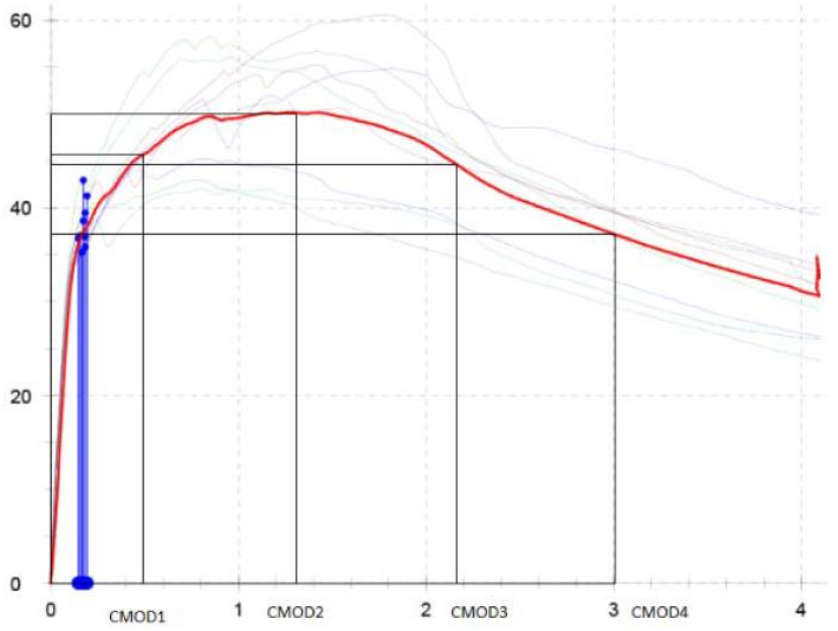

Formulas

EC2 - Punching and shear resistance for reinforced concrete according to EC2 (6.47)

Parameters

$\gamma_c := 1.5$ Concrete partial safety factor

$C_{Rd.c} := \frac{0.18}{\gamma_c} = 0.12$ (6.2.b)

$k_1 := 0.15$ (6.2.b)

$c_{cover} := \begin{cases} 0 & \text{if } A_{sl} = 0 \\ c_{cover} & \text{otherwise} \end{cases}$ Concrete cover

$d_{eff}(d) := d - c_{cover} - D_r$ Effective depth

$d_{eff}(150) = 108$

$d_{eff}(200) = 158$

Design shear resistance [MPa]

$V_{Rd.c}(d) := C_{Rd.c} \cdot k(d) \cdot \left(100 \cdot \rho(d) \cdot f_{ck}\right)^{\frac{1}{3}} + k_1 \cdot \sigma_{cp}$

$V_{Rd.c}(150) = 0.68$

$V_{Rd.c}(200) = 0.62$

Minimum shear resistance [MPa]

$V_{min}(d) := 0.035 \cdot k(d)^{\frac{3}{2}} \cdot \sqrt{f_{ck}}$

$V_{min}(150) = 0.66$

$V_{min}(200) = 0.66$

Design punching resistance (6.47) [kN]

$V_{Rd.c.p}(d) := \frac{\left[C_{Rd.c} \cdot k(d) \cdot \left(100 \cdot \rho(d) \cdot f_{ck}\right)^{\frac{1}{3}} + 0.1 \cdot \sigma_{cp}\right] \cdot u_{2d}(d) \cdot d}{1000}$

$V_{Rd.c.p}\left(d_{eff}(150)\right) = 176.43$

$V_{Rd.c.p}\left(d_{eff}(200)\right) = 293.59$

Minimum punching resistance (6.3N) [kN]

$V_{min.p}(d) := \frac{V_{min}(d) \cdot u_{2d}(d) \cdot d}{1000}$

$V_{min.p}(150) = 267.45$

$V_{min.p}(200) = 440.05$

Punching resistance (6.47) [kN]

$$V_{Rd.c.p.EC2}(d) := \begin{cases} V_{min.p}(d) & \text{if } A_{sl} = 0 \quad \text{no bending reinforcement} \\ \max\left(V_{Rd.c.p}\left(d_{eff}(d)\right), V_{min.p}(d)\right) & \text{otherwise} \end{cases}$$

$V_{Rd.c.p.EC2}(150) = 267.45$

$V_{Rd.c.p.EC2}(200) = 440.05$

FIN - BY 56

Parameters

Increase in punching resistance due to fibres

$\tau_{fd}(d) := 0.12 \cdot R_{20.50} \cdot f_{ctk.fl}(d)$

$k_1 := 0.15$

$k_f := 1$

$v_{fd}(d) := 0.7 \cdot k_f \cdot k(d) \cdot \tau_{fd}(d)$

Fibre contribution to punching [kN]

$$V_{Rd.f.p.FIN}(d) := \frac{\left(v_{fd}(d)\right) \cdot u_{2d}(d) \cdot d}{1000}$$

$V_{Rd.f.p.FIN}(150) = 395.48$

$V_{Rd.f.p.FIN}(200) = 650.7$

Punching resistance [kN]

$V_{Rd.cf.p.FIN}(d) := V_{Rd.c.p.EC2}(d) + V_{Rd.f.p.FIN}(d)$

$V_{Rd.cf.p.FIN}(150) = 662.93$

$V_{Rd.cf.p.FIN}(200) = 1090.75$

UK - TR34, 3th edition

Parameters

Fibre contribution [kN]

$$V_{Rd.f.UK.3}(d) := \frac{\left(0.12 \cdot R_{e.3} \cdot f_{ctk.fl}(d)\right) \cdot u_{2d}(d) \cdot d}{1000}$$

$V_{Rd.f.UK.3}(150) = 322.78$

$V_{Rd.f.UK.3}(200) = 531.08$

Punching resistance for unreinforced slabs [kN]

$$V_{Rd.cf.p.UK.3.no.reinforcement}(d) := \frac{\left(0.035\,k(d)^{\frac{3}{2}} \cdot f_{ck}^{\frac{1}{2}} + 0.12 \cdot R_{e.3} \cdot f_{ctk.fl}(d)\right) \cdot 0.75 \cdot d \cdot u_{2d}(0.75d)}{1000}$$

$V_{Rd.cf.p.UK.3.no.reinforcement}(150) = 364.98$

$V_{Rd.cf.p.UK.3.no.reinforcement}(200) = 590.23$

Punching resistance for reinforced slabs [kN]

$$V_{Rd.cf.p.UK.3.reinforcement}(d) := V_{Rd.c.p.EC2}(d) + \frac{0.12 \cdot R_{e.3} \cdot f_{ctk.fl}(d) \cdot 0.75d \cdot u_{2d}(0.75d)}{1000}$$

$V_{Rd.cf.p.UK.3.reinforcement}(150) = 467.05$

$V_{Rd.cf.p.UK.3.reinforcement}(200) = 762.83$

Punching resistance [kN]

$$V_{Rd.cf.p.UK.3}(d) := \begin{cases} V_{Rd.cf.p.UK.3.no.reinforcement}(d) & \text{if } A_{sl} = 0 \quad \text{no bending reinforcement} \\ \max\left(V_{Rd.cf.p.UK.3.reinforcement}(d), V_{Rd.cf.p.UK.3.no.reinforcement}(d)\right) & \text{otherwise} \end{cases}$$

$V_{Rd.cf.p.UK.3}(150) = 467.05$

$V_{Rd.cf.p.UK.3}(200) = 762.83$

UK - TR34, 4th edition

Parameters

Fibre contribution [kN]

$$V_{Rd.f.UK.4}(d) := \frac{0.015\left(f_{r1} + f_{r2} + f_{r3} + f_{r4}\right) \cdot u_{2d}(d) \cdot d}{1000}$$

$V_{Rd.f.UK.4}(150) = 286.59$

$V_{Rd.f.UK.4}(200) = 471.55$

Punching resistance [kN]

$$V_{Rd.cf.p.UK.4}(d) := \begin{cases} V_{Rd.c.p.EC2}(0.75d) + V_{Rd.f.UK.4}(0.75d) & \text{if } A_{sl} = 0 \quad \text{no bending reinforcement} \\ V_{Rd.c.p.EC2}(d) + V_{Rd.f.UK.4}(0.75d) & \text{otherwise} \end{cases}$$

$V_{Rd.cf.p.UK.4}(150) = 444.67$

$V_{Rd.cf.p.UK.4}(200) = 726.65$

GER - DAfStb

Parameters

$$f_{ct0.u} := \begin{cases} 0 & \text{if } f_{ct0.L2} = 0 \\ 0.45 & \text{if } f_{ct0.L2} = 0.3158 \\ 0.67 & \text{if } f_{ct0.L2} = 0.4590 \\ 1.11 & \text{if } f_{ct0.L2} = 0.7629 \end{cases}$$

Basic value of residual tensile strength

$f_{ct0.u} = 1.11$

$\alpha_{cf} := 0.85$

Reduction factor

$a(d) := 2 \cdot d$

$$A_{ct.p}(d) := \frac{0.9\, u_{2d}(d) \cdot d}{1000000}$$

Tension zone in punching [m^2]

$K_F := 1$

Fibre orientation factor

$$K_{G.p}(d) := \begin{cases} 1 + A_{ct.p}(d) \cdot 0.5 & \text{if } 1 + A_{ct.p}(d) \cdot 0.5 \le 1.7 \\ 1.7 & \text{otherwise} \end{cases}$$

Member size factor

$f_{ctR.u.p}(d) := K_F \cdot K_{G.p}(d) \cdot f_{ct0.u}$

Calculated value of residual tensile strength

$\gamma_{ct} := 1.25$

Fibre concrete partial safety factor

Fibre contribution [kN]

$$V_{Rd.f.p.GER}(d) := \frac{0.85 \cdot \frac{\alpha_{cf} \cdot f_{ctR.u.p}(d) \cdot u_{2d}(d) \cdot d}{\gamma_{ct}}}{1000}$$

$V_{Rd.f.p.GER}(150) = 305.22$

$V_{Rd.f.p.GER}(200) = 551.92$

Punching resistance [kN]

$$V_{Rd.cf.p.GER}(d) := 2 \cdot \frac{d}{a(d)} \cdot V_{Rd.c.p.EC2}(d) + V_{Rd.f.p.GER}(d)$$

$V_{Rd.cf.p.GER}(150) = 572.67$

$V_{Rd.cf.p.GER}(200) = 991.98$

SWE - SS 812310:2014

Parameters

$f_{ft.R3} := f_{r3} \cdot 0.37 = 4.42$ Characteristic residual tensile strength [MPa]

$\gamma_f := 1.5$ Partial safety factor for fibre concrete

$C := 0.45$ Coefficient

Punching resistance for reinforced slabs [kN] (6.3):

$$V_{Rd.cf.p.with.reinforcement}(d) := \frac{\left[\frac{0.18}{\gamma_c} \cdot k(d) \cdot \left[100\,\rho(d) \cdot \left(1 + 7.5 \cdot \frac{f_{ft.R3}}{f_{ctk}}\right) \cdot f_{ck}\right]^{\frac{1}{3}} + 0.15 \cdot \sigma_{cp}\right] \cdot u_{2d}(d) \cdot d}{1000}$$

$V_{Rd.cf.p.with.reinforcement}(d_{eff}(150)) = 419.87$

$V_{Rd.cf.p.with.reinforcement}(d_{eff}(200)) = 698.69$

Punching resistance for unreinforced slabs [kN] (6.4):

$$V_{Rd.cf.p.no.reinforcement}(d) := \frac{\left[\left(\frac{k(d)}{2}\right) \cdot C \cdot \frac{f_{r3}}{\gamma_f}\right] \cdot u_{0.5d}(d) \cdot d}{1000}$$

$V_{Rd.cf.p.no.reinforcement}(150) = 683.42$

$V_{Rd.cf.p.no.reinforcement}(200) = 1023.82$

Punching resistance [kN]

$$V_{Rd.cf.p.SWE}(d) := \begin{cases} \max\left(V_{Rd.cf.p.no.reinforcement}(d), V_{min.p}(d)\right) & \text{if } A_{sl} = 0 \quad \text{no bending reinforcement} \\ \max\left(V_{Rd.cf.p.with.reinforcement}\left(d_{eff}(d)\right), V_{min.p}(d), V_{Rd.cf.p.no.reinforcement}(d)\right) & \text{otl} \end{cases}$$

$V_{Rd.cf.p.SWE}(150) = 683.42$

$V_{Rd.cf.p.SWE}(200) = 1023.82$

MC2010

Level of approximation: I

Parameters

$L_x := 2$ Span [m]

$r_{s.x} := 0.22 \cdot L_x = 0.44$ Distance where radial moment is zero

$\kappa_e := 0.9$ Eccentricity coefficient

$f_{yd} := 550$ Reinforcement yield strength

$E_s := 200000$ Reinforcement modulus of elasticity

$$\psi_x(d) := 1.5 \cdot \frac{r_{s.x}}{\frac{d}{1000}} \cdot \frac{f_{yd}}{E_s} \rightarrow \frac{1.815}{d}$$ Slab rotation at failure

$k_{dg} := 1$ Aggregate size factor

$$k_\psi(d) := \frac{1}{1.5 + 0.9 \cdot k_{dg} \cdot \psi_x(d) \cdot d}$$ Slab rotation factor

Concrete contribution to punching

$$V_{Rd.c.p.MC2010}(d) := \begin{cases} 0 & \text{if } A_{sl} = 0 \quad \text{no bending reinforcement} \\ \frac{k_\psi(d) \cdot \frac{\sqrt{f_{ck}}}{\gamma_c} \cdot \kappa_e \cdot u_{0.5d}(d) \cdot d}{1000} & \text{otherwise} \end{cases}$$

$V_{Rd.c.p.MC2010}(150) = 244.93$

$V_{Rd.c.p.MC2010}(200) = 366.93$

$CMOD3 := 2.5$ Value at CMOD3 [mm]

$f_{Fts} := 0.45 \cdot f_{r1}$ Serviceability residual strength [MPa]

$w_u := 1.5$ Maximum crack opening accepted in structural design [mm]

$\gamma_F := 1.5$ Partial safety factor for FRC

$$f_{Ftuk} := \frac{f_{Fts} - \frac{w_u}{CMOD3} \cdot \left(f_{Fts} - 0.5 f_{r3} + 0.2 f_{r1}\right)}{1000}$$ Ultimate residual strength

Fibre contribution [kN]

$$V_{Rd.f.p.MC2010}(d) := \frac{f_{Ftuk}}{\gamma_F} \cdot u_{0.5d}(d) \cdot d$$

$V_{Rd.f.p.MC2010}(150) = 548.77$

Punching resistance [kN]

$$V_{Rd.cf.p.MC2010}(d) := \begin{cases} V_{Rd.c.p.MC2010}(d) + V_{Rd.f.p.MC2010}(d) & \text{if } A_{sl} = 0 \quad \text{no bending reinforcement} \\ V_{Rd.c.p.MC2010}\left(d_{eff}(d)\right) + V_{Rd.f.p.MC2010}(d) & \text{otherwise} \end{cases}$$

$V_{Rd.cf.p.MC2010}(150) = 706.82$

$V_{Rd.cf.p.MC2010}(200) = 1085.2$

Karv1

Parameters

$C_{Rd.c} := 0.2$

Concrete contribution [kN]

$$V_{Rk.c.p.Karv}(d) := \frac{\left[C_{Rd.c} \cdot k(d) \cdot \left(100 \cdot \rho(d) \cdot f_{ck}\right)^{\frac{1}{3}} + 0.1 \cdot \sigma_{cp}\right] \cdot u_{2d}(d) \cdot d}{1000}$$

$V_{Rk.c.p.Karv}\left(d_{eff}(150)\right) = 294.05$

$V_{Rk.c.p.Karv}\left(d_{eff}(200)\right) = 489.32$

Minimum concrete contribution [kN]

$$V_{min.p}(d) := \frac{V_{min}(d) \cdot u_{2d}(d) \cdot d}{1000}$$

$V_{min.p}(0.75 \times 150) = 165.38$

$V_{min.p}(0.75 \times 200) = 267.45$

Fibre contribution [kN]

$$V_{Rk.f.p.Karv}(d) := \frac{\alpha_{cf} \cdot f_{ctR.u.p}(d) \cdot u_{2d}(d) \cdot d}{1000}$$

$V_{Rk.f.p.Karv}(150) = 448.86$

$V_{Rk.f.p.Karv}(200) = 811.65$

Punching resistance [kN]

$$V_{Rk.c.p.Karv}(d) := \begin{cases} V_{min.p}(0.75d) & \text{if } A_{sl} = 0 \quad \text{no bending reinforcement} \\ \max\left(V_{Rk.c.p.Karv}\left(d_{eff}(d)\right), V_{min.p}(0.75d)\right) & \text{otherwise} \end{cases}$$

$V_{Rk.cf.p.Karv1}(d) := V_{Rk.c.p.Karv}(d) + V_{Rk.f.p.Karv}(d)$

$V_{Rk.cf.p.Karv1}(150) = 742.9$

$V_{Rk.cf.p.Karv1}(200) = 1300.97$

Karv2

Punching resistance [kN]

$V_{Rk.cf.p.Karv2}(d) := V_{Rk.c.p.Karv}(d) + V_{Rd.f.UK.3}(d)$

$V_{Rk.cf.p.Karv2}(150) = 616.82$

$V_{Rk.cf.p.Karv2}(200) = 1020.4$

Summary

Punching resistance d=150 [kN]:

$V_{Rd.c.p.EC2}(150) = 267.45$

$V_{Rd.cf.p.FIN}(150) = 662.93$

$V_{Rd.cf.p.GER}(150) = 572.67$

$V_{Rd.cf.p.UK.3}(150) = 467.05$

$V_{Rd.cf.p.UK.4}(150) = 444.67$

$V_{Rd.cf.p.SWE}(150) = 683.42$

$V_{Rd.cf.p.MC2010}(150) = 706.82$

$V_{Rk.cf.p.Karv1}(150) = 742.9$

$V_{Rk.cf.p.Karv1}(200) = 1300.97$

Punching resistance d=200 [kN]:

$V_{Rd.c.p.EC2}(200) = 440.05$

$V_{Rd.cf.p.FIN}(200) = 1090.75$

$V_{Rd.cf.p.GER}(200) = 991.98$

$V_{Rd.cf.p.UK.3}(200) = 762.83$

$V_{Rd.cf.p.UK.4}(200) = 726.65$

$V_{Rd.cf.p.SWE}(200) = 1023.82$

$V_{Rd.cf.p.MC2010}(200) = 1085.2$

$V_{Rk.cf.p.Karv2}(150) = 616.82$

$V_{Rk.cf.p.Karv2}(200) = 1020.4$

Graph

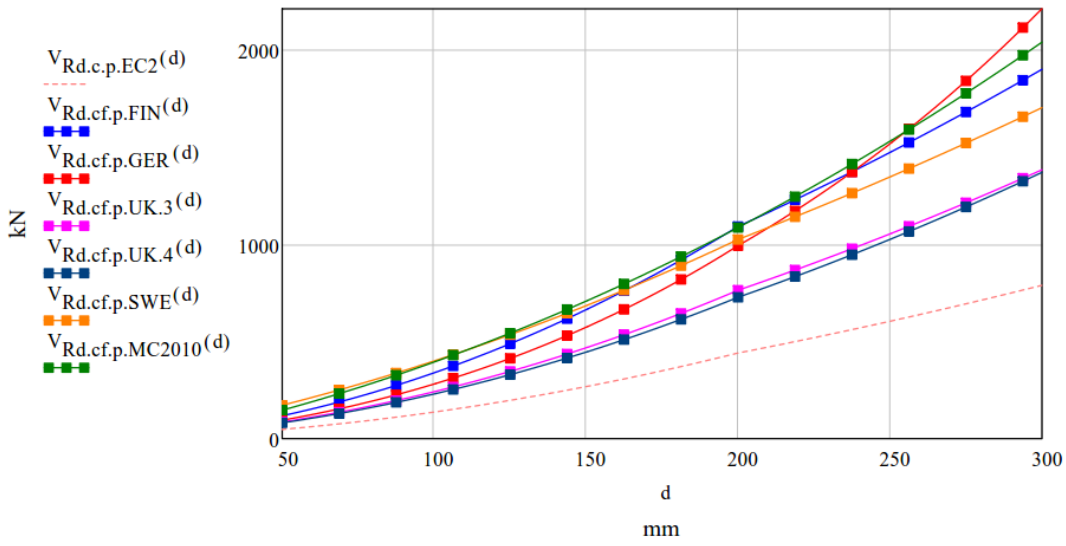

Appendix 5 Graphs illustrating punching capacity as a function of slab thickness

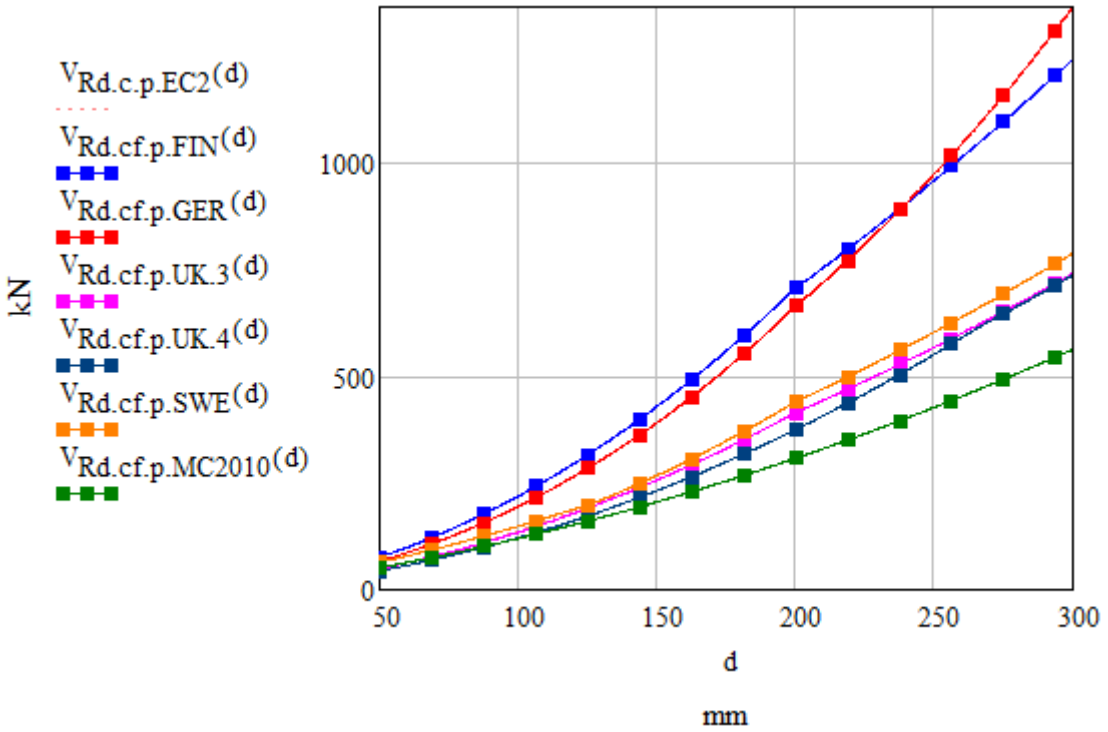

Figure 0.1. Punching capacity for SFRC20 with no bending reinforcement.

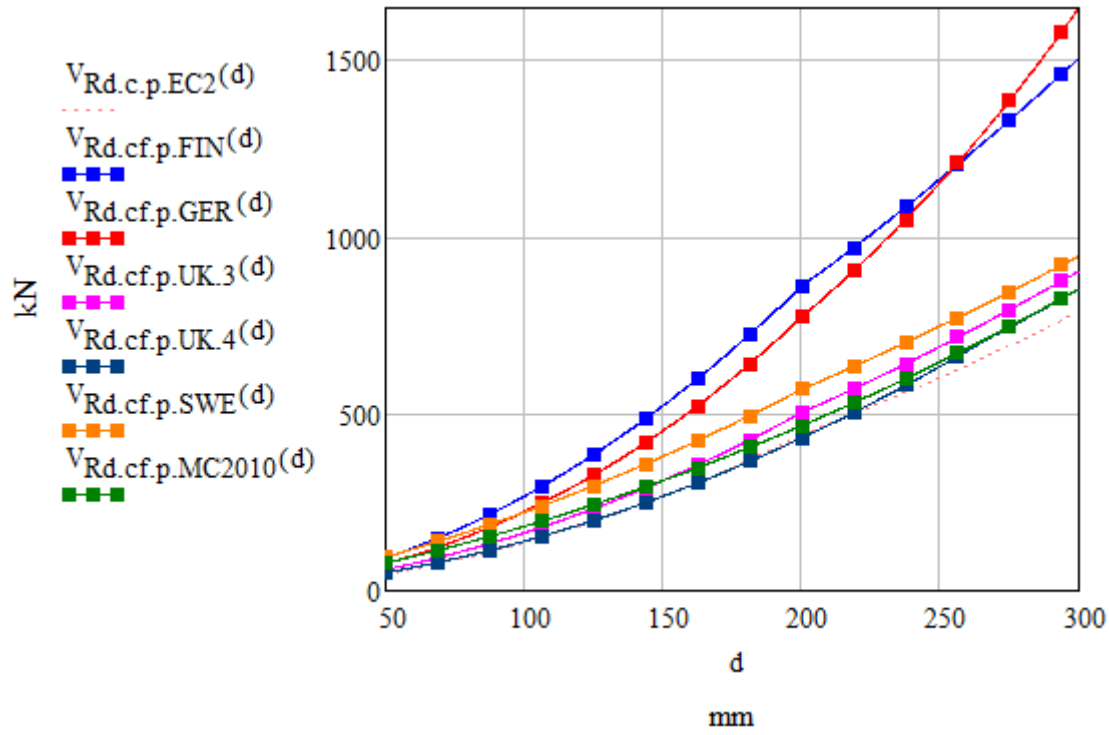

Figure 0.2. Punching capacity for SFRC40 with no bending reinforcement.

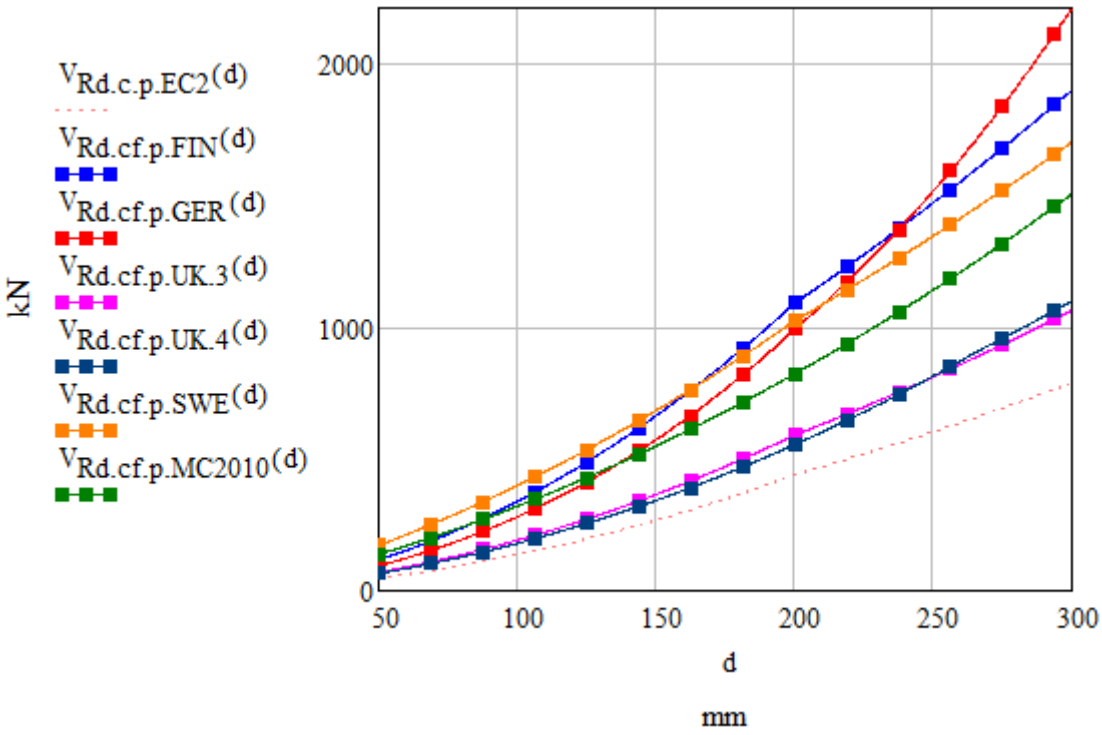

Figure 0.3. Punching capacity for SFRC70 with no bending reinforcement.

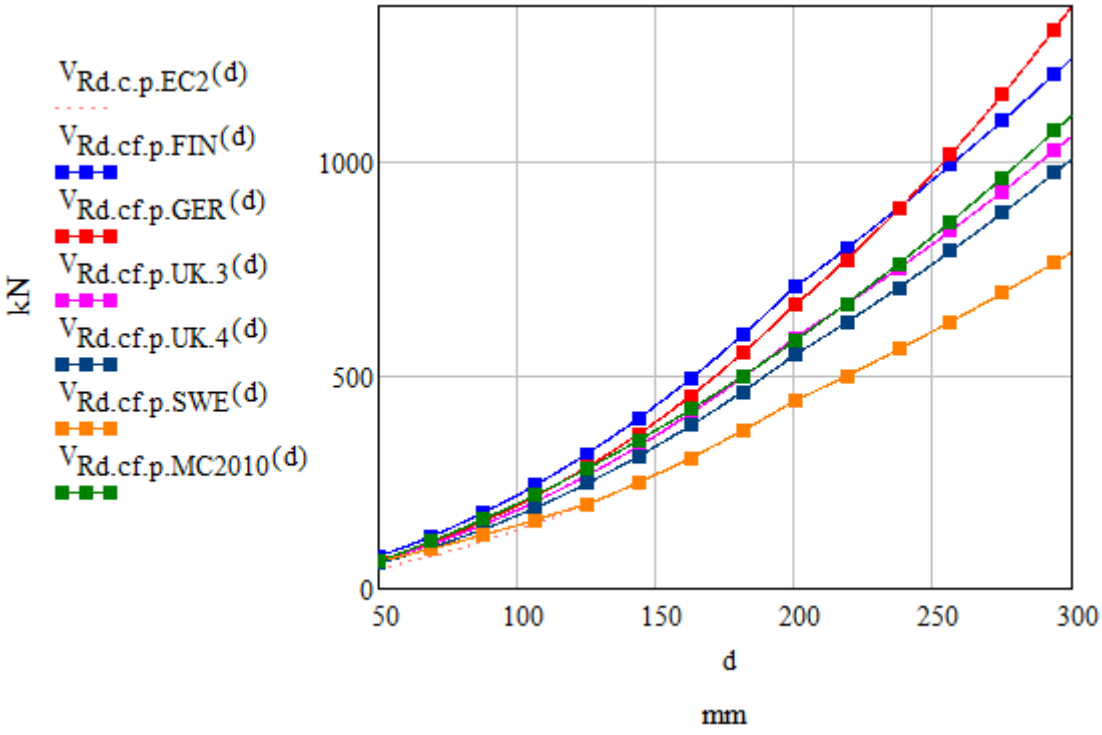

Figure 0.4. Punching capacity for SFRC20 ⌀8 c/c 150.

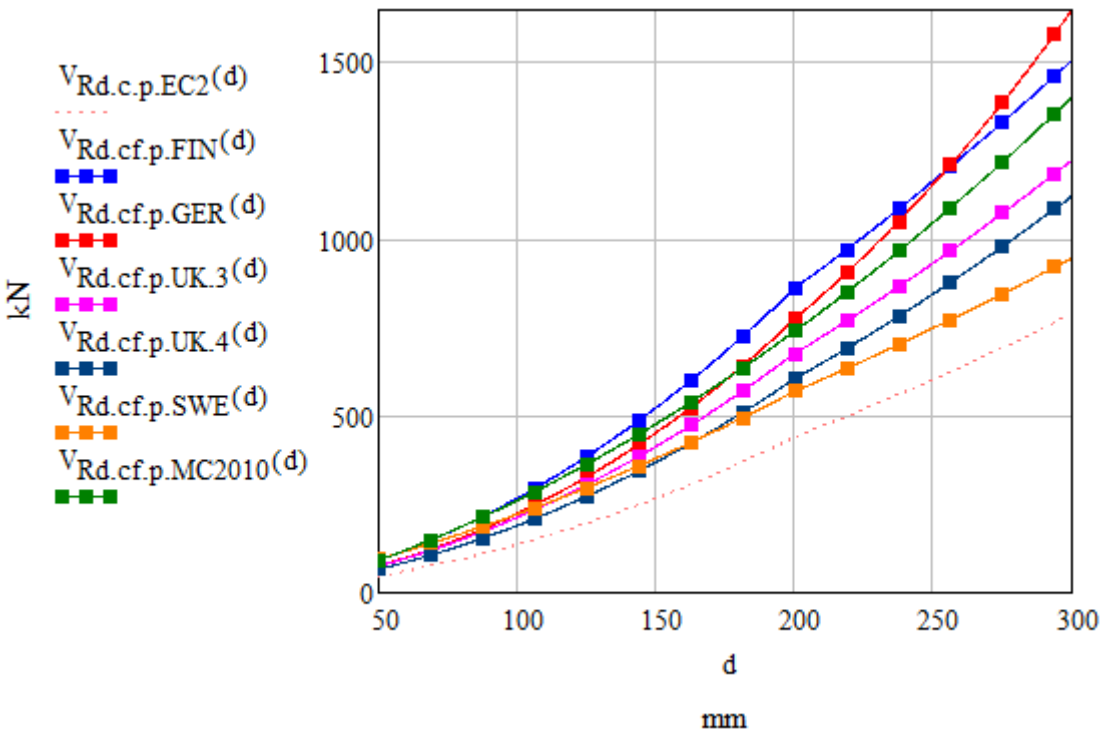

Figure 0.5. Punching capacity for SFRC40 ⌀8 c/c 150.

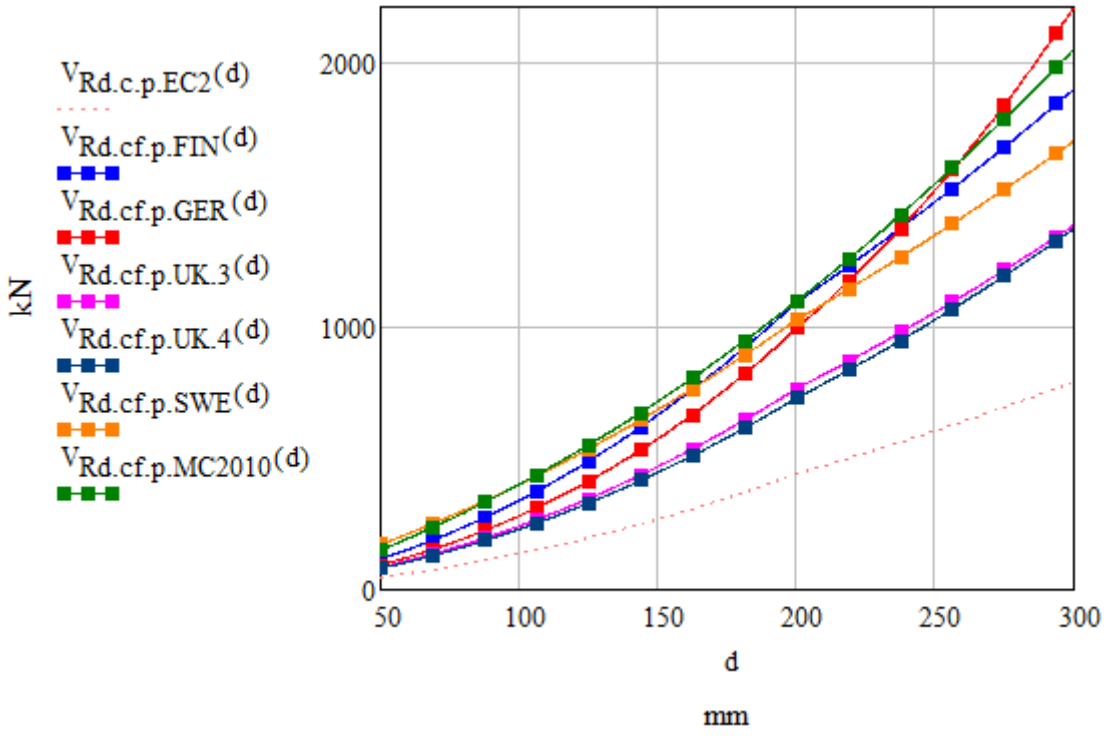

Figure 0.6. Punching capacity for SFRC70 ⌀8 c/c 150.

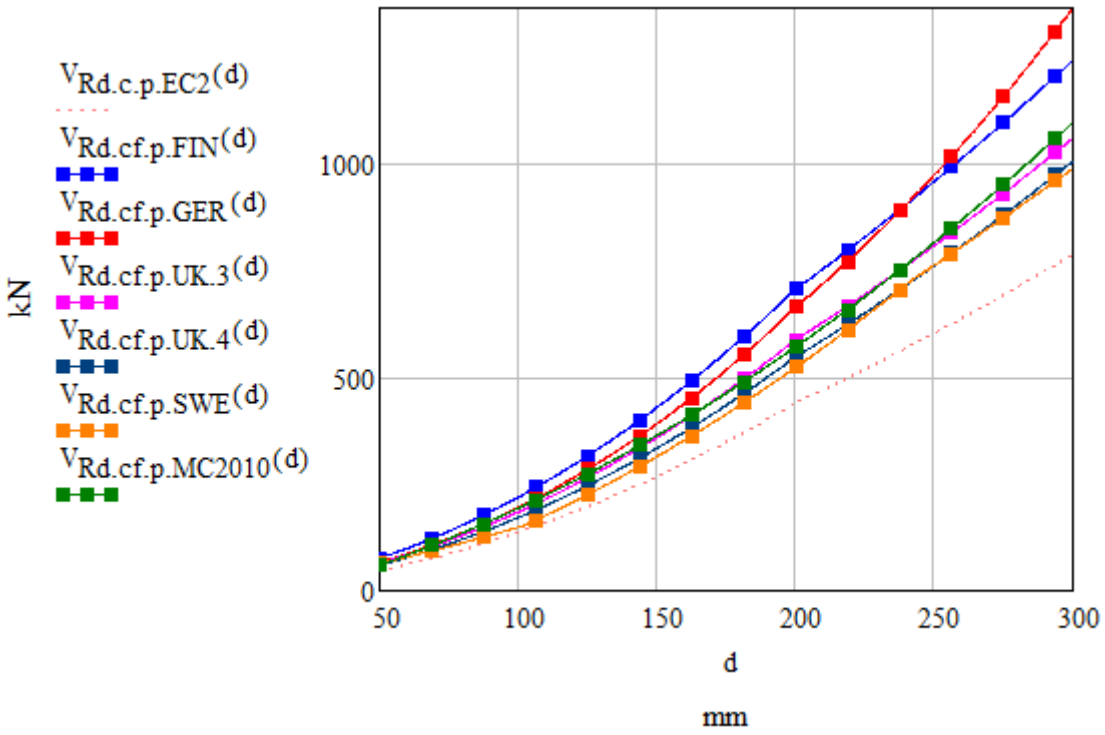

Figure 0.7. Punching capacity for SFRC20 ⌀12 c/c 150.

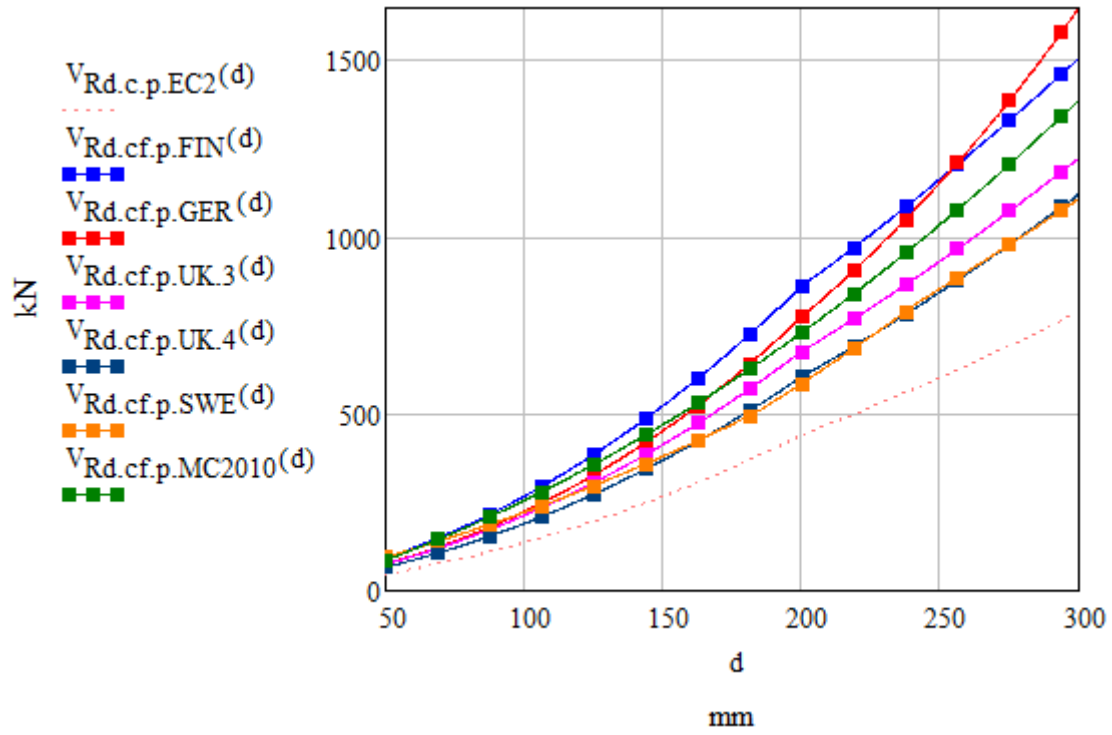

Figure 0.8. Punching capacity for SFRC40 ⌀12 c/c 150.

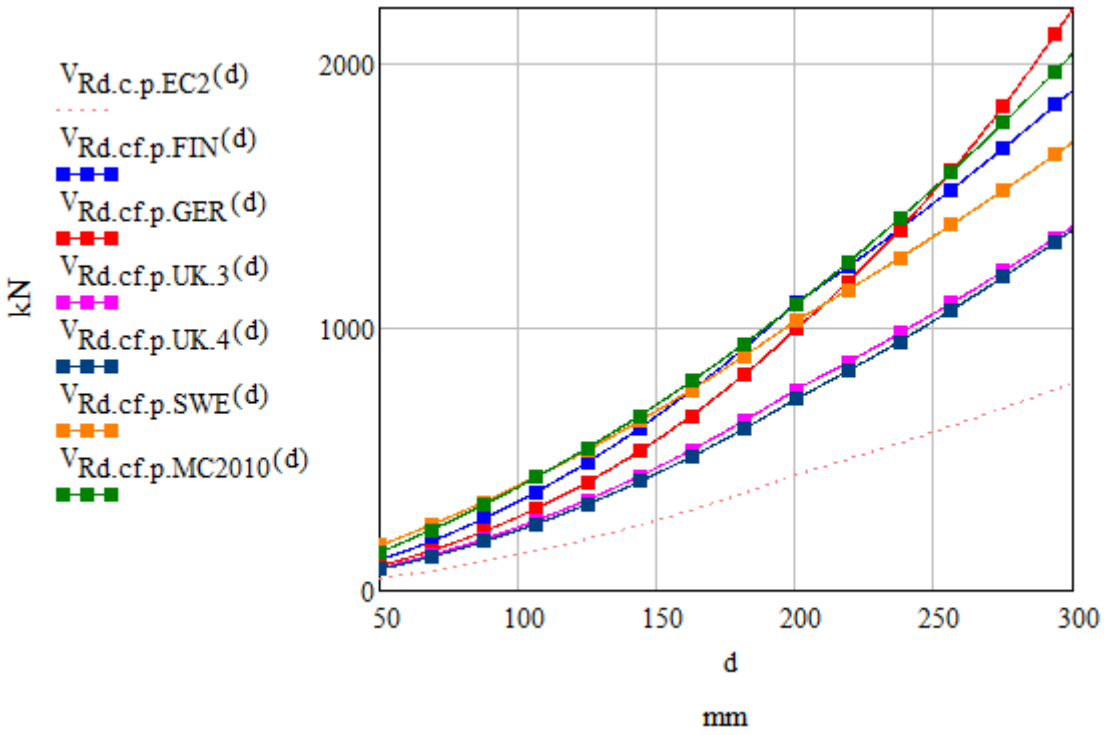

Figure 0.9. Punching capacity for SFRC70 ⌀12 c/c 150.